comptes rendus O a le V O le

2025 • 24 • 14



DIRECTEURS DE LA PUBLICATION / PUBLICATION DIRECTORS:

Gilles Bloch, Président du Muséum national d'Histoire naturelle

Étienne Ghys, Secrétaire perpétuel de l'Académie des sciences

RÉDACTEURS EN CHEF / EDITORS-IN-CHIEF: Michel Laurin (CNRS), Philippe Taquet (Académie des sciences)

Assistante de rédaction / Assistant Editor: Adenise Lopes (Académie des sciences; cr-palevol@academie-sciences.fr)

MISE EN PAGE / PAGE LAYOUT: Pénélope Laurin (Muséum national d'Histoire naturelle; audrina.neveu@mnhn.fr), Pénélope Laurin

RÉVISIONS LINGUISTIQUES DES TEXTES ANGLAIS / ENGLISH LANGUAGE REVISIONS: Kevin Padian (University of California at Berkeley)

RÉDACTEURS ASSOCIÉS / ASSOCIATE EDITORS (*, took charge of the editorial process of the article/a pris en charge le suivi éditorial de l'article):

Micropaléontologie/Micropalaeontology

Lorenzo Consorti (Institute of Marine Sciences, Italian National Research Council, Trieste)

Paléobotanique/Palaeobotany

Cyrille Prestianni (Royal Belgian Institute of Natural Sciences, Brussels)

Anaïs Boura (Sorbonne Université, Paris)

Métazoaires/Metazoa

Annalisa Ferretti (Università di Modena e Reggio Emilia, Modena)

Paléoichthyologie/Palaeoichthyology

Philippe Janvier (Muséum national d'Histoire naturelle, Académie des sciences, Paris)

Amniotes du Mésozoïque/Mesozoic amniotes

Hans-Dieter Sues (Smithsonian National Museum of Natural History, Washington)

Tortues/Turtles

Walter Joyce (Universität Freiburg, Switzerland)

Lépidosauromorphes/Lepidosauromorphs

Hussam Zaher (Universidade de São Paulo)

Oiseaux/Birds

Jingmai O'Connor (Field Museum, Chicago)

Paléomammalogie (mammifères de moyenne et grande taille)/Palaeomammalogy (large and mid-sized mammals)

Grégoire Métais* (CNRS, Muséum national d'Histoire naturelle, Sorbonne Université, Paris)

Paléomammalogie (petits mammifères sauf Euarchontoglires)/Palaeomammalogy (small mammals except for Euarchontoglires)
Robert Asher (Cambridge University, Cambridge)

Paléomammalogie (Euarchontoglires)/Palaeomammalogy (Euarchontoglires)

K. Christopher Beard (University of Kansas, Lawrence)

Paléoanthropologie/Palaeoanthropology

Aurélien Mounier (CNRS/Muséum national d'Histoire naturelle, Paris)

Archéologie préhistorique (Paléolithique et Mésolithique)/Prehistoric archaeology (Palaeolithic and Mesolithic)

Nicolas Teyssandier (CNRS/Université de Toulouse, Toulouse)

Archéologie préhistorique (Néolithique et âge du bronze)/Prehistoric archaeology (Neolithic and Bronze Age)

Marc Vander Linden (Bournemouth University, Bournemouth)

 $R\'{e}r\'{e}r\'{e}s \ / \ Reviewers: https://sciencepress.mnhn.fr/fr/periodiques/comptes-rendus-palevol/referes-du-journal and the state of the state$

COUVERTURE / COVER:

Ursus arctos taubachensis (upper), Ursus deningeri hercynicus (bellow). Credits: W. Gornig.

Comptes Rendus Palevol est indexé dans / Comptes Rendus Palevol is indexed by:

- Cambridge Scientific Abstracts
- Current Contents® Physical
- Chemical, and Earth Sciences®
- ISI Alerting Services®
- Geoabstracts, Geobase, Georef, Inspec, Pascal
- Science Citation Index®, Science Citation Index Expanded®
- Scopus®.

Les articles ainsi que les nouveautés nomenclaturales publiés dans Comptes Rendus Palevol sont référencés par / Articles and nomenclatural novelties published in Comptes Rendus Palevol are registered on:

 $-\,ZooBank^{\tiny{\circledR}}\,\,(http://zoobank.org)$

Comptes Rendus Palevol est une revue en flux continu publiée par les Publications scientifiques du Muséum, Paris et l'Académie des sciences, Paris Comptes Rendus Palevol is a fast track journal published by the Museum Science Press, Paris and the Académie des sciences, Paris

Les Publications scientifiques du Muséum publient aussi / The Museum Science Press also publish:

Adansonia, Geodiversitas, Zoosystema, Anthropozoologica, European Journal of Taxonomy, Naturae, Cryptogamie sous-sections Algologie, Bryologie, Mycologie. L'Académie des sciences publie aussi / The Académie des sciences also publishes:

Comptes Rendus Mathématique, Comptes Rendus Physique, Comptes Rendus Mécanique, Comptes Rendus Chimie, Comptes Rendus Géoscience, Comptes Rendus Biologies.

Diffusion – Publications scientifiques Muséum national d'Histoire naturelle CP 41 – 57 rue Cuvier F-75231 Paris cedex 05 (France) Tél.: 33 (0)1 40 79 48 05 / Fax: 33 (0)1 40 79 38 40

diff.pub@mnhn.fr / https://sciencepress.mnhn.fr

Académie des sciences, Institut de France, 23 quai de Conti, 75006 Paris.

© This article is licensed under the Creative Commons Attribution 4.0 International License (https://creativecommons.org/licenses/by/4.0/) ISSN (imprimé / print): 1631-0683/ ISSN (électronique / electronic): 1777-571X

Ursidae (Carnivora, Mammalia) from Tunel Wielki Cave (southern Poland)

Adrian MARCISZAK

Department of Palaeozoology, University of Wrocław, Sienkiewicza 21, 50-335 Wrocław (Poland) adrian.marciszak@uwr.edu.pl (corresponding author)

Małgorzata KOT

Faculty of Archaeology, University of Warsaw, Krakowskie Przedmieście 26/28, 00-927 Warszawa (Poland) m.kot@uw.edu.pl

Katarzyna ZARZECKA-SZUBIŃSKA

Department of Palaeozoology, University of Wrocław, Sienkiewicza 21, 50-335 Wrocław (Poland) katarzyna.zarzecka-szubinska@uwr.edu.pl

Grzegorz LIPECKI

Institute of Systematics and Evolution of Animals, Polish Academy of Sciences, Sławkowska 17, 31-016 Kraków (Poland) lipecki@isez.pan.krakow.pl

Submitted on 13 September 2024 | Accepted on 16 January 2025 | Published on 21 May 2025

urn:lsid:zoobank.org:pub:3F227405-93A0-4B1F-926C-46C2B5CE2817

Marciszak A., Kot M., Zarzecka-Szubińska K. & Lipecki G. 2025. — Ursidae (Carnivora, Mammalia) from Tunel Wielki Cave (southern Poland). Comptes Rendus Palevol 24 (14): 241-302. https://doi.org/10.5852/cr-palevol2025v24a14

ABSTRACT

The presence of two ursids, *Ursus deningeri hercynicus* Rode, 1935 and *Ursus arctos taubachensis* Rode, 1935, was documented from the Tunel Wielki Cave. Of them, *Ursus deningeri hercynicus* is represented by almost all skeletal elements, with the predominance of isolated teeth, metapodials and phalanges. The analysis performed shows that the remains of this bear subspecies from Tunel Wielki have intermediate morphological features and metric values between individuals recorded in the materials from the early-mid (MIS 19-13) and late Middle Pleistocene (MIS 12-9) localities. A set of features suggests a more recent geological age than MIS 19-13. Most of these characters were found in the dental material, while postcranial bones have a rather limited biochronological and taxonomical value. The material of *Ursus arctos taubachensis* is represented by five bones. Together with the German site Bad Frankenhausen, Tunel Wielki Cave probably documented the first appearance of the species of Asian origin and related to the Mammoth Fauna in Europe.

KEY WORDS Biostratigraphy, ursids, Ursus deningeri, Ursus arctos, morphotypes.

RÉSUMÉ

Ursidae (Carnivora, Mammalia) de la grotte de Tunel Wielki (Sud de la Pologne).

La présence de deux ursidés, *Ursus deningeri hercynicus* Rode, 1935 et *Ursus arctos taubachensis* Rode, 1935, a été documentée dans la grotte de Tunel Wielki. Parmi eux, *Ursus deningeri hercynicus* est représenté par presque tous les éléments du squelette, avec la prédominance de dents isolées, de métapodes et de phalanges. L'analyse effectuée montre que les restes de cette sous-espèce d'ours du Tunel Wielki présentent des caractéristiques morphologiques et des valeurs métriques intermédiaires entre les individus enregistrés dans les matériaux des localités du Pléistocène précoce-moyen (MIS 19-13) et du Pléistocène moyen tardif (MIS 12-9). Un ensemble de caractéristiques suggère un âge géologique plus récent que le MIS 19-13. La plupart de ces caractères ont été trouvés dans le matériel dentaire, tandis que les os postcrâniens ont une valeur biochronologique et taxonomique plutôt limitée. Le matériel d'*Ursus arctos taubachensis* est représenté par cinq os. Avec le site allemand de Bad Frankenhausen, la grotte de Tunel Wielki a probablement documenté la première apparition de l'espèce d'origine asiatique liée à la faune des mammouths en Europe.

MOTS CLÉS Biostratigraphie, ursidés, Ursus deningeri, Ursus arctos, morphotypes.

INTRODUCTION

Despite the rich fossil record, the timing of the separation of the two most important ursid lineages, the arctoid and the spelaeoid ones, is still a subject of intensive debates. These ursids evolved from Ursus etruscus Cuvier, 1823 between 1.6 and 1.4 mya (Torres Pérez-Hidalgo 1992; Koufos et al. 2018; Gimranov et al. 2023). It was a time when both lineages started to evolve independently, leading to omnivory and opportunism in arctoid bears and herbivory and specialisation in spelaeoid bears. The earliest specimens are still very similar, and it is not easy to distinguish them correctly. Some authors assigned bears from sites dated at 1.4-1.1 mya as Ursus arctos Linnaeus, 1758 (Rustioni & Mazza 1993; Musil 2001; Olive 2006) or Ursus arctos suessenbornensis Soergel, 1926 (Rabeder et al. 2010; Marciszak & Lipecki 2020a, b). The others include them to the evolutionary lineage of spelaeoid ursids (García & Arsuaga 2001; Wagner 2006, 2010; Baryshnikov 2007; Argant 2009). The oldest remains of Ursus deningeri von Reichenau, 1904 are dated at 1.1-1.0 mya (Moullé 1992; Erbaeva et al. 2001; Wagner 2006, 2010; Baryshnikov 2007; Wagner & Sabol 2007; Argant 2009; Madurell-Malapeira et al. 2009).

The fossil record of the latest Early and early to mid Middle Pleistocene Eurasian ursids of Poland was previously regarded as relatively more poorly studied than that of neighborhood countries, like the Czech Republic and Germany. Among relevant Polish fossil records of this age, only those from Kozi Grzbiet (MIS 17) (Głazek et al. 1976a, 1977a-d; Wiszniowska 1989; Wagner & Čermák 2012) and Jasna Strzegowska Cave (MIS 19-17) (Marciszak & Lipecki 2020a) were previously decribed in detail. Fossil remains from other sites like Przymiłowice C (MIS 19-17), Zamkowa Dolna Cave (fauna C, MIS 19-17), Południowa Cave (MIS 19-17), Sitkówka (MIS 15-13), Draby (MIS 11) and layers 19ad-19 of the Biśnik Cave were only mentioned or at the most briefly described (Głazek et al. 1976b, 1977e; Marciszak et al. 2011, 2016, 2020, 2023; Woroncowa-Marcinowska et al. 2017; Marciszak & Lipecki 2020b).

However, the ursid material from the Tunel Wielki Cave (further abbreviated as TW in the text) has never been analysed in the context of possible occurrence of *U. deningeri*. Apart the scarce material of *Pliomys coronensis* Méhely, 1914, considered as re-deposited (Bartolomei *et al.* 1975; Nadachowski 1982; Chmielewski *et al.* 1988) or related to the Late Biharian (Nadachowski 1989), this site was never dated to the Middle Pleistocene. In the previous papers, the sequence of deposits from this locality was usually considered to be of Late Pleistocene-Holocene age (Bartolomei *et al.* 1975; Nadachowski 1982, 1988, 1989; Chmielewski *et al.* 1988).

The aim of this paper is to describe the remains of ursids from the Tunel Wielki Cave, especially those of *Ursus deningeri*, which is the most abundant species in the collection from this site, in order to re-evaluate the evolutionary model of spelaeoid bears. It was tried to find a link between the early and mid Middle Pleistocene and advanced, highly evolved late Middle Pleistocene bear populations. Abundant and well-preserved fossil material allows refining the set of diagnostic characters and patterns of their variation and phylogenetic meaning. The present paper is intended to define a morphometric characteristic of the TW bear palaeopopulation and critically evaluate its taxonomic status within the Eurasian records of *U. deningeri*. In addition, we evaluate the occurrence of *U. arctos* and discuss the early appearance of its special ecomoph.

SITE

Tunel Wielki Cave (TW) is located on the eastern slope of the Sąspów Valley in the southern part of Kraków-Częstochowa Upland (50°13'21"N, 19°47'40"E, 410 m a.s.l.) (Fig. 1). The site is a horizontal 24 m long cave with two chambers connected by a narrowing corridor. The cave has the form of a 24 m long tunnel with two openings heading the north-west and south. It consists of two chambers connected by 8 m long narrow corridor. The spacious southern chamber has a high ceiling, but recently a huge boulder almost entirely covered its opening. The northern chamber of much smaller size has a

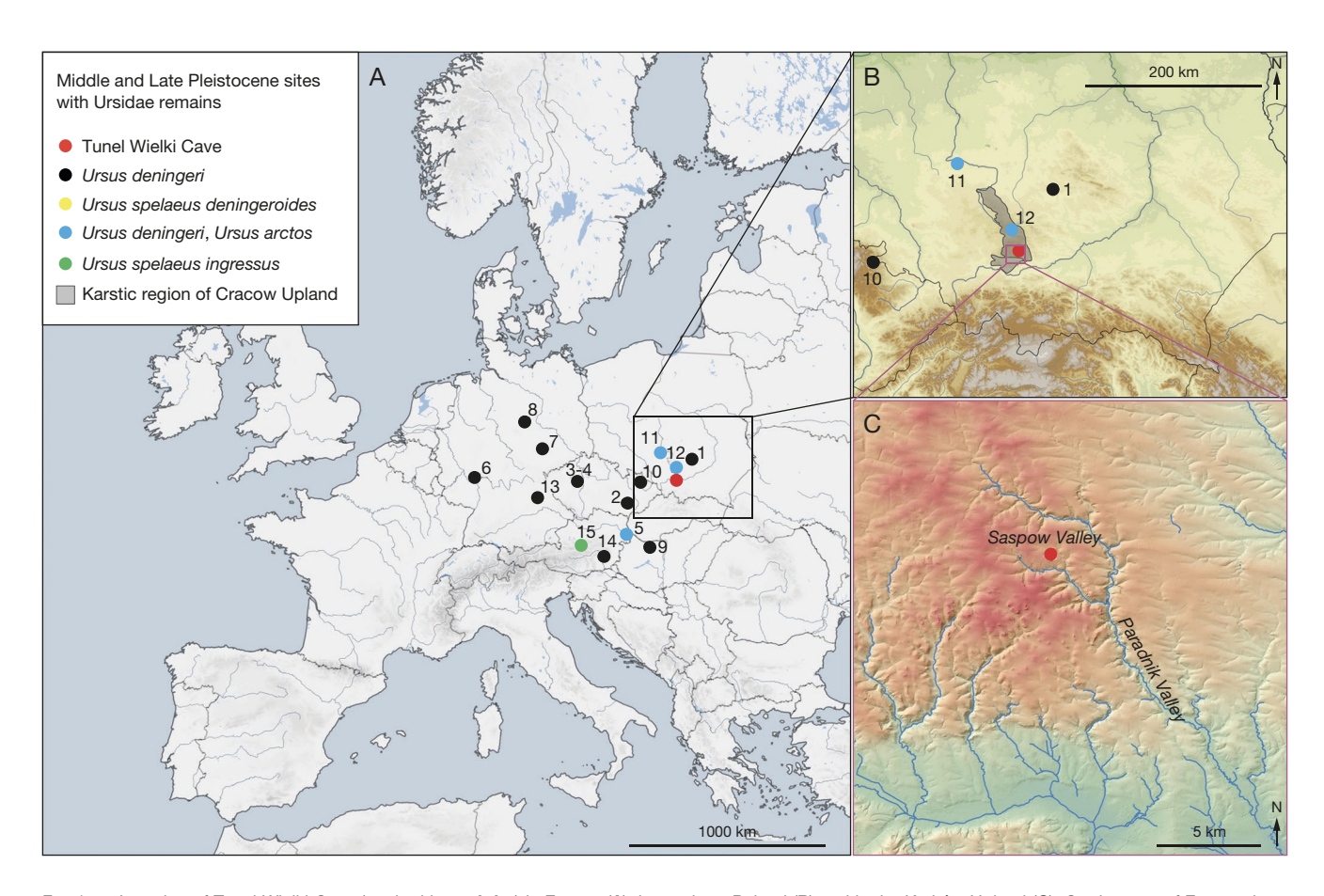


Fig. 1. — Location of Tunel Wielki Cave (marked by red dot) in Europe (A), in southern Poland (B) and in the Kraków Upland (C). On the map of Europe there are showed also other sites, from which ursid remains were used for comparative analyses. Ursus deningeri von Reichenau, 1904: 1, Kozi Grzbiet; 2, Stránská Skála; 3, 4, Koněprusy C 718; 5, Hundsheim; 6, Mosbach 2; 7, Urdhöhle; 8, Einhornhöhle; 9, Vértesszőlős 2; 10, Za Hájovnou Cave; 11, Draby; 12, Biśnik Cave; layers 19ad-19; 13, Hunas. Ursus spelaeus deningeroides Mottl, 1964: 14, Repolusthöhle. Ursus spelaeus ingressus (Rabeder, Hofreiter, Nagel & Withalm, 2004): 15, Gamssulzenhöhle. Ursus arctos Linnaeus, 1758: 5, Hundsheim; 12, Biśnik Cave; layers 19ad-19.

large entrance of 6×1.5 m. The southern entrance overlooks a steep slope, whereas a flat terrace is in front of the northern one (Berto et al. 2021; Kot et al. 2022).

The first description of the fossils remains from this cave was made by Cietak in 1935, who called this site Tunel Przechodni 2 in Koziarnia valley (Kowalski 1951). The cave was excavated in 1967-1968 by W. Chmielewski, who opened four trenches placed both in the northern and the southern chambers (Fig. 2) (Chmielewski et al. 1988). Chmielewski uncovered a 4.5 m deep sequence, subdividing it into 15 lithostratigraphic units including Pleistocene loams covered with a c. 1 m thick loess layer and a 1 m thick Holocene humic strata (Madeyska 1988; Krajcarz et al. 2016). The southern chamber was revisited in 2016. Both excavations revealed the presence of up to 1.5 m thick Upper Pleistocene-Holocene deposits (Wojenka et al. 2017).

In 2018, the northern chamber was excavated again in order to collect geological, paleoenvironmental and chronostratigraphic data. Fieldworks enabled to verify the previously described stratigraphy and resulted in the collecting of a large palaeontological and archaeological collections. The 4 m profile in the northern chamber begins on the top with Holocene, black c. 1.5 m thick humus with limestone rubbles (layers A2, B1, B2 and B3). Below is located a c. 1 m

thick loess layer C, which covers another loess layer D with limestones. Erosional layers with mixed silty loams and a large limestone rubble (layers E, K1, L1 and L2) are located below. A 1.5 m series of clay layers with clasts of manganese and limestone rubble (layers F, G, H, I, J1, J2, M1, M2, N, and O) lies further below. The lowermost strata are represented by thin, silty and sandy loams without limestone (layer P1-P3). Current analysis revealed the presence of ursid remains within the loamy layers F to O, as well as in the erosional layers E, K1, L1, and L2 (Fig. 2; Berto et al. 2021; Kot et al. 2022).

The remains of *Pliomys coronensis* Méhely, 1914 were found in the lower loam layers and interpreted as a possible secondary re-deposition of Middle Pleistocene materials within the site (Bartolomei et al. 1975; Nadachowski 1982, 1988). Archaeological artefacts found in the upper part of the series of loamy strata were therefore identified as representing the late Middle Palaeolithic (Madeyska 1988). All bird remains were attributed to the Holocene (Bocheński 1974, 1988). Ursids were classified as representing *U. spelaeus* and *U. arctos* (Nadachowski 1988). While the remains of small mammals were well studied, and the results of this study were published (Bartolomei et al. 1975; Nadachowski 1982, 1988, 1990; Chmielewski et al. 1988), the remains of large mammals from TW remained in fact so far undescribed.

The re-study of old collection and investigation of the new material obtained in 2018 allows clarifying the chronology of this complex stratigraphy. The revision of the entire TW fauna showed that the Middle Pleistocene fauna consists of 52 species of mammals, including three insectivores, 11 bats, one lagomorph, 17 rodents, 14 carnivores, two perissodactyls, and four artiodactyls. The Late Pleistocene and Holocene faunal lists count a total of 58 species: 22 gastropods, five birds, two insectivores, three lagomorphs, 13 rodents, six carnivores, one perissodactyl, and six artiodactyls (Bocheński 1974, 1988; Bartolomei *et al.* 1975; Nadachowski 1982, 1988, 1989; Chmielewski *et al.* 1988; Marciszak *et al.* 2019b, 2020, 2021, 2023; Berto *et al.* 2021; Marciszak & Lipecki 2020a, b; Kot *et al.* 2022).

MATERIAL AND METHODS

All the original material analysed in this paper was examined by the authors. The old TW collection, recovered during the Chmielewski' campaigns in the 1960s, is stored in the Institute of Systematics and Evolution of Animals, Polish Academy of Sciences (ISEA PAN) in Kraków, Poland. The remains found during the 2018 campaign are currently stored in the Faculty of Archaeology, University of Warsaw (FA UW). The detailed list of the studied material is presented in the Appendix 1. It should be noticed that MF inventory numbers refer to the old collection, whereas TWB and TW inventory numbers refer to the 2018 collection.

Measurements of the fossils were taken point to point, with an electronic calliper, to the nearest 0.01 mm. Osteological and dental terminology follows Rabeder (1999). A standard scheme for teeth measurements was applied and modified from Rode (1935) and Baryshnikov (2007), and it is shown in Appendices 2; 3. A standard scheme for postcranial skeleton measurements was applied and modified from Hilpert (2006) and Argant (2010), and it is shown in Appendices 4; 5. The definition and subdivisions of the Quaternary follow Gibbard (2015) and Gibbard & Cohen (2019). The definition and subdivisions of mammal zones and their correlation with the chronostratigraphic scale as well as with MN zones follow Kahlke et al. (2011). The nomenclatural codification follows the current (fourth) edition of the International Code of Zoological Nomenclature (ICZN, 1999). Capital and lowercase letters, e.g. C/c (canines), I/i (incisors), P/p (premolars), and M/m (molars), refer to the upper and lower teeth, respectively. The measurements of bones from Gamssulzenhöhle were used as a basis for the standardisation of measurement values and for morphodynamic indices according to Rabeder (1983, 1989, 1992, 1995a, 1999) and shown in Appendices 6-37. The measurements and indices for metapodial analysis follow Withalm (2001).

For comparison, we used ursid fossils from 14 Middle and Late Pleistocene European sites, ranging between 800 and 30 kya. The occurrence timespan of *U. deningeri* was divied into two main groups. The group 1 (MIS 19-13) including Kozi Grzbiet (Poland, MIS 17; *U. deningeri*, *U. arctos*), Stránská

Skála (Czech Republic, MIS 19-17; U. deningeri), Koněprusy C 718 Cave (Czech Republic, MIS 19-17; U. deningeri), Hundsheim (Austria, MIS 15-13; *U. deningeri*, *U. arctos*), Mosbach 2 (Germany, MIS 15-13; *U. deningeri*), and Urdhöhle (Germany, MIS 15-13; *U. deningeri*). The group 2 (MIS 11-8) includes Einhornhöhle (Germany, MIS 11-10; *U. deningeri*), Vértesszőlős 2 (Hungary, MIS 11; *U. deningeri*), Za Hájovnou Cave (Czech Republic, MIS 11; U. deningeri), Draby (Poland, MIS 11; *U. deningeri*, *U. arctos*), and Biśnik Cave, layers 19ad-19 (Poland, MIS 10-8; U. deningeri, U. arctos). In addition, we analysed the material of *Ursus spelaeus denin*geroides Mottl, 1964 from Repolusthöhle (Austria, MIS 8-7) and Ursus spelaeus ingressus (Rabeder, Hofreiter, Nagel & Withalm, 2004) from Gamssulzenhöhle (Austria, MIS 3). The remains of *U. deningeri* from Hunas (Germany, MIS 7; but see also Hilpert 2006) were also included in the analysis. Morphometric analysis is based on measurements taken by one of the authors (A.M.), and data set is taken from the literature (Schütt 1968; Feustel et al. 1971; Musil 1972, 2005; Rabeder 1983, 1989, 1995a, b, 1999; Jánossy 1990; Wagner 2005a, 2014; Hilpert 2006; Wagner & Čermák 2012).

ABBREVIATIONS

B bucco-lingual breadth;
Ba mesial breadth;
Bp distal breadth;
B ta talonid breadth;
B tr trigonid breadth;

ISEA PAN Institute of Systematics and Evolution of Animals,

Polish Academy of Sciences;

L mesio-distal length; L ta talonid m1 length; L tr trigonid m1 length;

M mean;

max maximal value;
min minimal value;
mm millimetre;
mya million years ago;
N number in sample;
TW Tunel Wielki Cave;

WA UW Faculty of Archaeology, University of Warsaw.

SYSTEMATIC PALEONTOLOGY

Class MAMMALIA Linnaeus, 1758 Order CARNIVORA Bowdich, 1821 Family URSIDAE Batsch, 1788 Subfamily URSINAE Batsch, 1788 Genus *Ursus* Linnaeus, 1758 *Ursus deningeri* von Reichenau, 1904

Ursus deningeri hercynicus Rode, 1935

REFERRED MATERIAL. — The material of *U. deningeri*, the most abundant carnivore species from TW is represented by almost all skeletal elements (NISP 641, MNI 26; left/right bones are given in brackets): 4 cranium fr., 5 maxilla fr. (4/1), 15 mandibles (8/7), 19 I1 (10/9), 26 I2 (8/18), 30 I3 (14/16), 19 C1 (11/8), P1 (0/1), 15 P4 (9/6), 30 M1 (17/13), 44 M2 (22/22), 15 i1 (7/8), 26 i2 (15/11), 15 i3 (6/9), 25 c1 (12/13), 3 p1 (3/0), 13 p4 (5/8), 43 m1

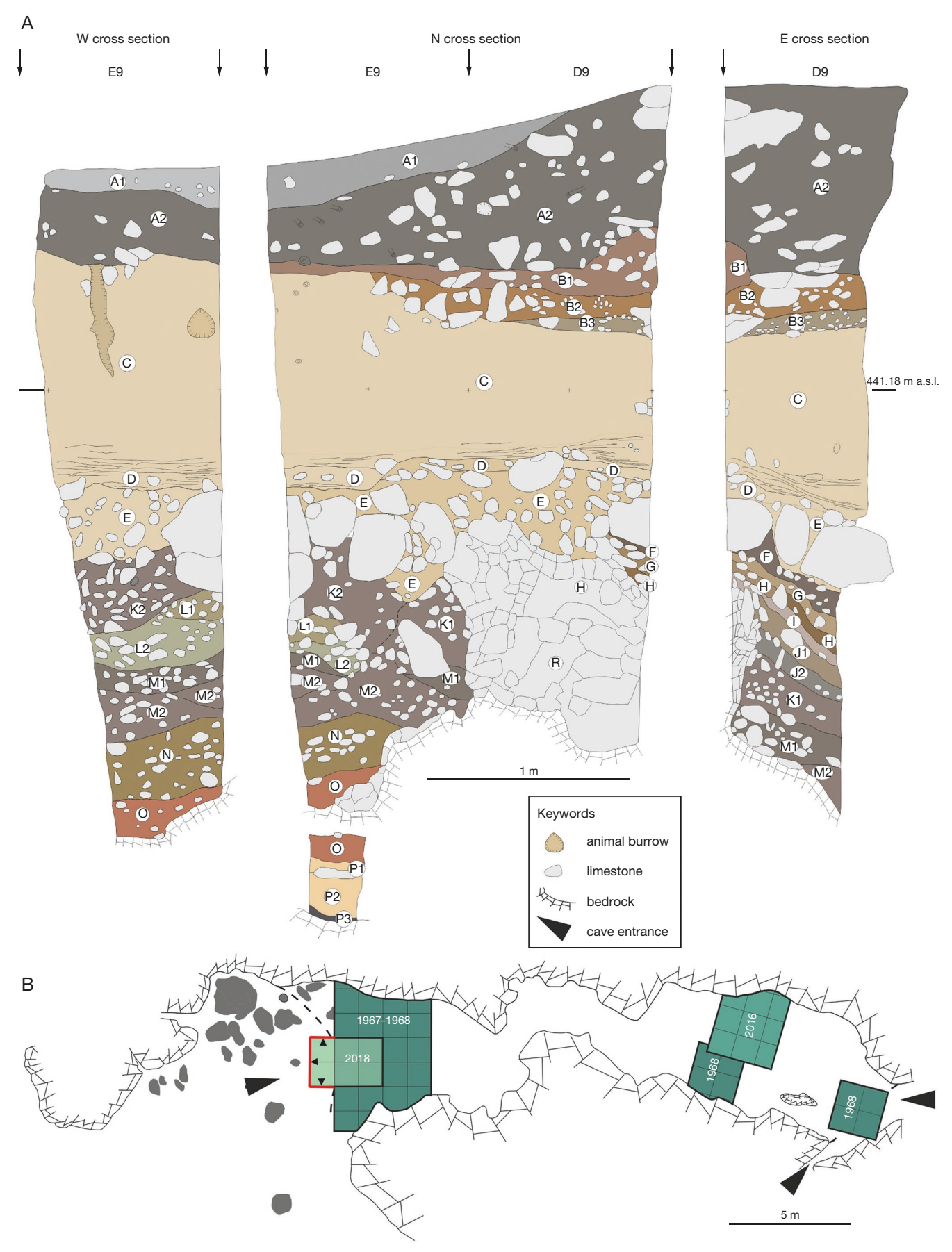


Fig. 2. - Tunel Wielki Cave: A, stratigraphy of the 2018 trench (squares D9 and E9); B, plan with the excavation areas; in green the area investigated in 2018.

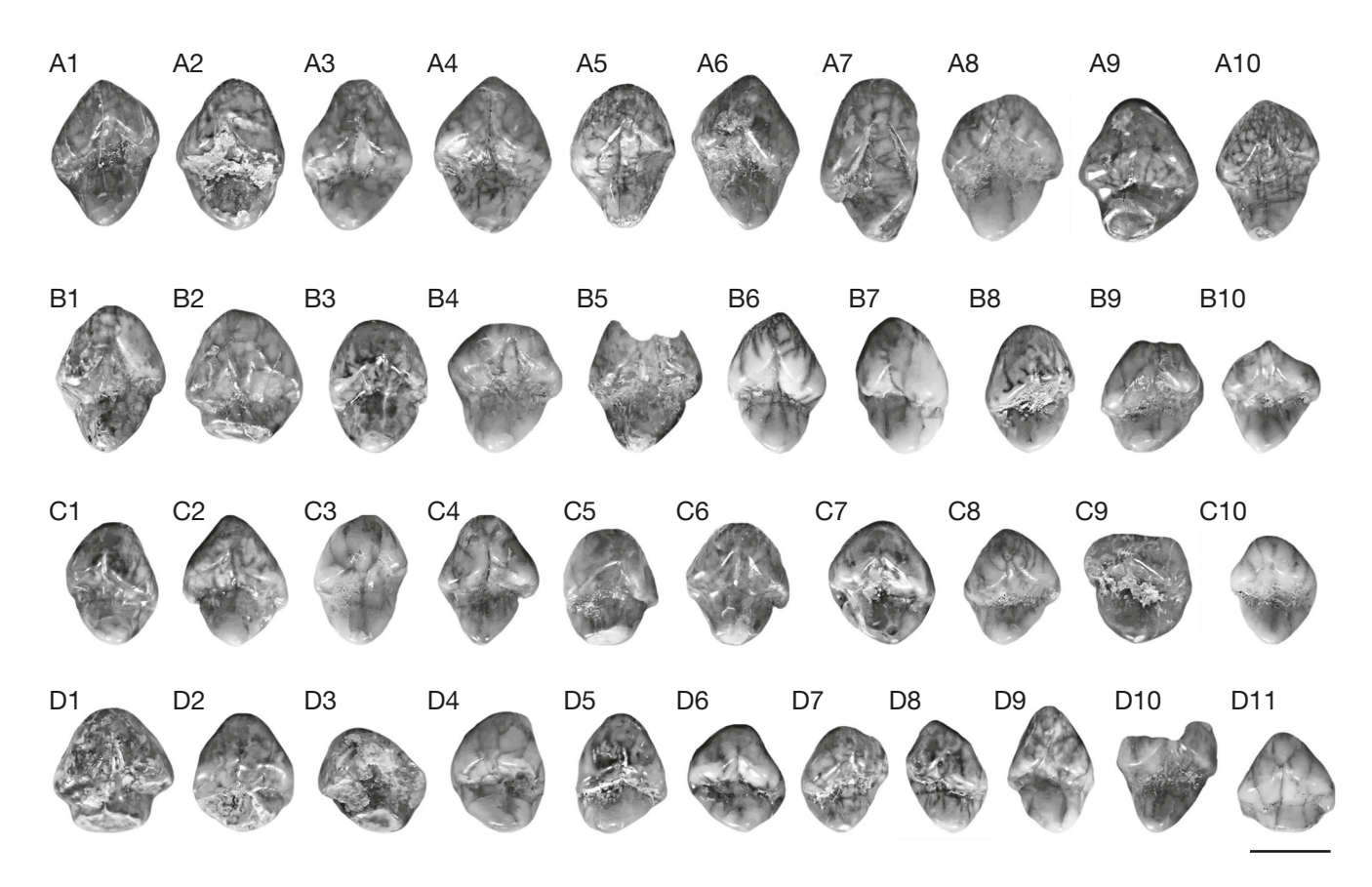


Fig. 3. — Mesial view of I1-I2 of *Ursus deningeri hercynicus* Rode, 1935 from Tunel Wielki Cave: **A1**, TWB 198; **A2**, TWB 142; **A3**, TWB 104; **A4**, TWB 169; **A5**, MF/7319; **A6**, MF/7317; **A7**, TWB 958; **A8**, TWB 61; **A9**, TWB 457; **A10**, TWB 382; **B1**, MF/7324; **B2**, MF/7335; **B3**, TWB 718; **B4**, TWB 327; **B5**, TWB 165; **B6**, MF/7328; **B7**, MF/7329; **B9**, TWB 228; **B10**, MF/7337; **C1**, MF/7316; **C2**, MF/7325; **C3**, MF/7332; **C4**, MF/7326; **C5**, MF/7320; **C6**, MF/7331; **C7**, TWB 192; **C8**, MF/7333; **C9**, TWB 319; **C10**, MF/7330; **D1**, TWB 481; **D2**, TWB 673; **D3**, TWB 247; **D4**, TWB 332; **D5**, TWB 278; **D6**, TWB 1241; **D7**, MF/7334; **D8**, MF/7338; **D9**, MF/7321; **D10**, MF/7336; **D11**, MF/7322. Scale bar: 10 mm.

(17/26), 34 m2 (16/18), 27 m3 (15/12), scapula (1/0), humerus (0/1), 7 radii (3/4), 5 ulnae (3/2), 6 tibiae (3/3), 2 fibulae (2/0), sternum (1), 4 patellae (2/2), 4 naviculares (4/0), 6 calcanei (0/6), 4 tali (0/4), 2 capitatums (1/1), 2 cuboides (0/2), 3 ectocuneiformes (1/2), 4 pisiformes (3/1), 2 scapholunares (0/2), 3 mc 1 (1/2), 6 mc 2 (1/5), 9 mc 3 (3/6), 7 mc 4 (3/4), 9 mc 5 (6/3), 7 mt 1 (5/2), 5 mt 2 (3/2), 6 mt 3 (3/3), 13 mt 4 (5/8), 7 mt 5 (5/2), 2 mtpd, 5 atlas (5), 8 thoracic (8), cervical (1), lumbar (1), 2 caudale (2), 44 ph 1, 17 ph 2, 20 ph 3, and 2 sesamoides (Appendix 1). Some bones hold the traces of chewing, gnawing and biting, and documented the interaction with other carnivores. The main factors responsible for the accumulation of bear remains on the site were probably carnivores, accidental falls, and water transport.

EMENDED DIAGNOSIS. — Smaller than the nominotypical subspecies *Ursus deningeri deningeri* (von Reichenau, 1904), often present P3, I3 with a calyx, i1 and i2 with larger and broader crowns and enlarged distoconid, P4 and p4 with morphologically more complicated crowns, M1 with a stronger developed parastyle and lingual cingulum, M2 with a narrower talon, m1 with a longer talonid and triple entoconid, m2 with a broader and longer talonid, and m3 with a shorter trigonid (Rode 1935; Schütt 1968; Baryshnikov 2007).

DESCRIPTION

Upper incisors

Among 39 I2s from TW, 29 teeth belong to the most ancestral morphotype d with an asymmetrical, narrow crown without a lingual edge nor fossa lunaris (Fig. 3). The other 10 I1-I2s

represent the more advanced morphotype d/p,which is broader, with a weakly developed lingual part, but still without any cusplets on the mesial cingulum. The morphotype d predominates in the sites dated on MIS 19-13; it is characteristic for all I2s from Kozi Grzbiet, Mosbach 2, and Stránska skálá (Table 1). The I2 from TW is metrically comparable to those from the sites dated on MIS 19-15, but with more robust crowns (Fig. 3). The B/L index for TW is 81.5 (75.6-85.6, n = 10), and it is higher than MIS 19-15 group of *U. deningeri* (B/L = 77.9, 77.1-78.7, n = 9) (Table 1). The bear crowns of younger populations (MIS 11-9) are larger and broader (B/L = 82.7, 77.8-91.9, n = 15), the ratio of the morphotypes p to the d is higher, and the calyx size increasing (Table 1).

All I3s from the group 1 (MIS 19-13) represent the most ancestral morphotype 0, without calyx (Table 1). Only 2 I3s from Hundsheim hold a very delicate structure resembling a minute calyx. Among 26 I3s from TW, seven specimens represent the more evolved morphotype 1, with a minute to small calyx located on the buccal side, above the apex (Fig. 4). The rest 21 specimens of I3 from TW were assigned to the morphotype 0 (Fig. 4). The I3 from TW has a developed lingual edge and fossa lunaris that occurs as a clearly visible pit on the mesial side of the tooth. The cingulum is weak and even absent in some of the specimens (Fig. 4). In all I3s from TW, the mesial and distal edges delimit a somewhat

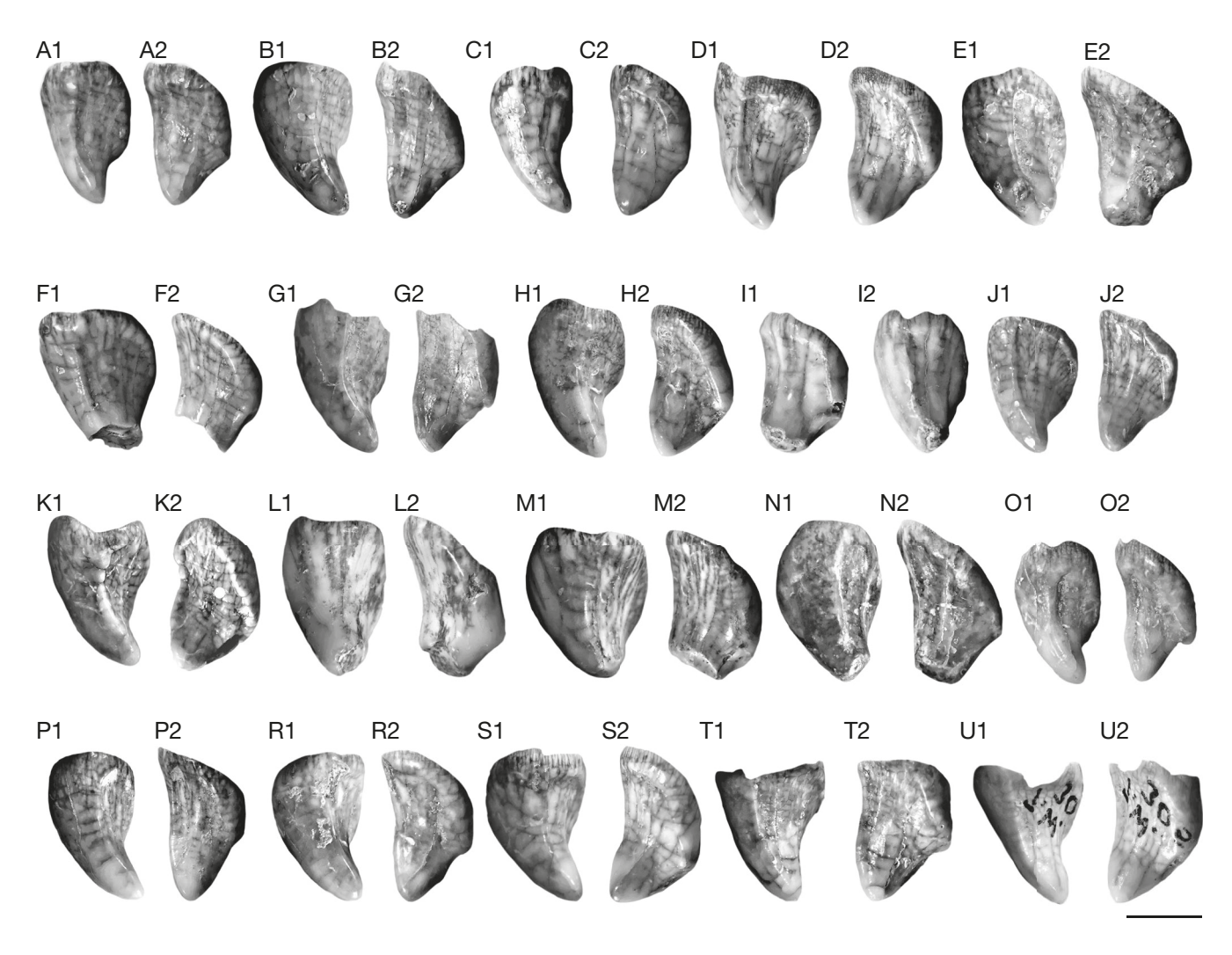


Fig. 4. — The I3 of *Ursus deningeri hercynicus* von Reichenau, 1904 from Tunel Wielki Cave: **A**, TWB 690; **B**, MF/7281; **C**, TWB 807; **D**, MF/7277; **E**, MF/7276; **F**, MF/7271; **G**, MF/7270; **H**, MF/7278; **I**, MF/7269; **J**, TWB 632; **K**, MF/7284; **L**, MF/7282; **M**, MF/7486; **N**, MF/7283; **O**, TWB 90; **P**, MF/7485; **R**, MF/7273; S, MF/7280; T, MF/7279; U, MF/7274. All teeth are figured as left specimens (C, D, G-K, M, S-U, are mirrored). 1, buccal view; 2, mesial view. Scale bar: 10 mm.

Table 1. — Measurements and morphological indices of the upper incisors of Ursus deningeri Richenau, 1904, Ursus spelaeus deningeroides Mottl, 1964, and Ursus spelaeus ingressus (Rabeder, Hofreiter, Nagel & Withalm, 2004) from Gamssulzenhöhle (GS) as a standard. Abbreviations: JB, Biśnik Cave; KZ, Kozi Grzbiet; RP, Repolusthöhle; SS, Stránska skálá; TW, Tunel Wielki Cave; V2, Vértesszőlős 2.

		I1-	12 L			I1-I2 B		Fossa lunaris/cingulum cusp index
	MIS	M	Min-Max	N	M	Min-Max	N	M
KZ	17	8.9	7.3-11.2	16	8.3	6.5-9.6	16	3.2/4.3
SS	19-17	9.1	7.9-11.6	9	8.6	7.6-9.3	9	11.1/11.1
TW	13-12	9.5	8.4-12.4	39	8.9	6.9-10.9	39	12.8/20.5
JB	10-8	9.7	7.9-12.3	43	10.1	8.5-11.5	43	16.3/26.7
RP	8-7	8.8	7.1-10.5	74	10.1	8.8-12.3	74	19.7/36.4
GS-S	3	10.0	8.2-12.3	59	11.4	9.5-13.6	59	150.9/168.8
		13	3 L			13 B		
	MIS	М	Min-Max	N	М	Min-Max	N	Calyx index
KZ	17	12.6	10.9-13.9	6	9.9	8.9-10.3	6	0
SS	19-17	13.1	12.2-15.3	17	11.7	11.2-12.7	17	14.7
TW	13-12	13.3	10.7-14.6	26	11.1	9.9-12.2	26	30.8
V2	11	13.2	11.5-15.3	9	11.4	10.3-12.5	9	38.9
JB	10-8	13.7	11.8-16.5	24	12.0	10.5-14.3	24	43.4
RP	8-7	13.6	_	30	_	_	_	50.0
GS-S	3	13.9	_	46	_	_	_	100.0

Table 2. — Measurements and morphological indices of the lower incisors of *Ursus deningeri* von Reichenau, 1904, *Ursus spelaeus deningeroid*es Mottl, 1964, and *Ursus spelaeus ingressus* (Rabeder, Hofreiter, Nagel & Withalm, 2004) from Gamssulzenhöhle (**GS**) as a standard. Abbreviations: **JB**, Biśnik Cave; **KZ**, Kozi Grzbiet; **RP**, Repolusthöhle; **SS**, Stránska skálá; **TW**, Tunel Wielki Cave.

			i1 L			i1 B		Morphotypes index
	MIS	М	Min-Max	N	М	Min-Max	N	М
KZ	17	5.9	5.1-6.9	7	7.9	6.8-9.2	7	14.3
SS	19-17	5.9	5.1-6.3	5	7.9	6.8-8.3	5	20.0
TW	13-12	6.1	5.3-6.6	13	8.4	7.6-9.2	13	35.7
JB	10-8	5.7	5.5-7.4	26	8.3	6.6-9.9	26	38.5
RP	8-7	5.8	5.2-7.0	30	8.3	7.6-10.8	30	48.0
GS	3	6.6	5.3-7.2	40	8.8	7.9-9.7	40	80.7
			i2 L			i2 B		Morphotypes index
	MIS	М	Min-Max	N	М	Min-Max	N	M
KZ	17	8.0	7.3-8.5	6	9.9	9.4-10.9	6	8.3
SS	19-17	8.2	7.2-9.6	5	10.6	9.6-11.5	5	20.0
TW	13-12	8.6	7.4-10.1	25	10.3	8.9-11.7	25	34.0
JB	10-8	9.3	8.3-10.7	23	10.8	9.8-12.4	23	39.1
RP	8-7	9.1	_	_	10.3	_	40	41.4
GS	3	9.7	-	-	10.9	-	33	100.0
			i3 L			i3 B		Morphotypes index
	MIS	М	Min-Max	N	М	Min-Max	N	М
KZ	17	10.5	9.6-11.8	6	10.1	9.3-11.1	6	58.3
SS	19-17	10.0	7.5-11.6	16	9.4	7.9-11.9	16	68.8
TW	13-12	10.8	10.1-12.1	14	11.4	9.6-13.5	14	125.0
JB	10-8	11.8	10.1-13.6	16	12.1	10.8-14.4	16	128.1
RP	8-7	11.6	_	30	11.2	_	30	130.5
GS	3	13.2	_	60	12.5	_	60	256.6

recessed field with the lingual cingulum. The I3s from TW are larger than those from MIS 19-13, but smaller than I3s from MIS 11-9. A general tendency to increasing in size and broadening of all three upper incisors is observed (Table 1).

Lower incisors (i1-i3) and canines (C1/c1)

Among 14 i1s from TW, eight specimens represent the most ancestral morph. A, simply build and small, while five others were assigned to the morph. C (Table 2). The latter have larger and broader crowns, with an enlarged distoconid, and thickened mesial and mesio-buccal margins. The moph. A is the only occurring in the group 1 (MIS 19-13). The i1 from TW is large and robust, and its size exceeds the dimensions of the i1 from most of the sites the material from which was used for comparison (Table 2). The relatively large crown of the i2 is divided into two (in most specimens) or three (in a few teeth) parts, and its apex is oriented vertically and slightly distally, being oval-shaped in occlusal view (Fig. 5; Table 2).

Among 25 i2s from TW, 10 represent the most ancestral morph. d, with a simply build crown, divided into two parts (Table 2). The other 10 i2s from TW belong to the morph. d/s, with a weakly developed mesioconid, smooth distal surface, and without any cusplets. Finally, two specimens were assigned to the tricuspid morph. s, with a large mesioconid and a double distoconid (Fig. 5; Table 2). The i2 from TW represents a higher evolutionary level as compared to the group 1 (MIS 19-13). Among six i2s from Kozi Grzbiet, five specimens represent the morph. d, while only a single – d/s. In Hundsheim (n = 5) and Stránska skálá (n = 4), the morph. d/s is represented only by a single tooth. The

i2 from the group 1 (MIS 19-13) is also slightly smaller than that from TW, which in turn is smaller than i2 from the group 2 (MIS 11-9). In the group 2, the number of more evolved morphotypes (d/s and s) is higher than that in TW (Table 2). Among 15 specimens of i3 from TW, nine were assigned to the morph. B, a double-crowned, well-developed distoconid distinct from the protoconid, and a well-developed sulcus medialis, while six others belong to B/C (Fig. 6). The i3 from the group 1 (MIS 19-13) is smaller and evolutionarily more ancestral, although a high variability is inherent to this group (Table 2).

Among 37 canines from TW, majority of the specimens is more or less worn, and therefore it is not possible to take their precise measurements. Among them, large and robust male canines are easily distinguishable from the smaller and narrower female canines. In addition, the lower canines are moderately curved distally and weakly flattened bucco-lingually, while the upper canines are straighter. All canines are characterised by an elongated and massive root, oval-shaped in cross-section. The crown is quite short (as compared to the root), blunt, with a poorly developed, very thin inner enamel crest running through its entire length.

P4

Among 15 P4s from TW, eight specimens represent the ancestral morph. A, with a simple morphology, without any cusplets such as protoloph and metaconule (Fig. 7; Table 3). Seven other P4s from TW are more evolved, with a distinct metaloph or a small metaconule (Fig. 7; Table 3). Comparison of P4s from TW with those from

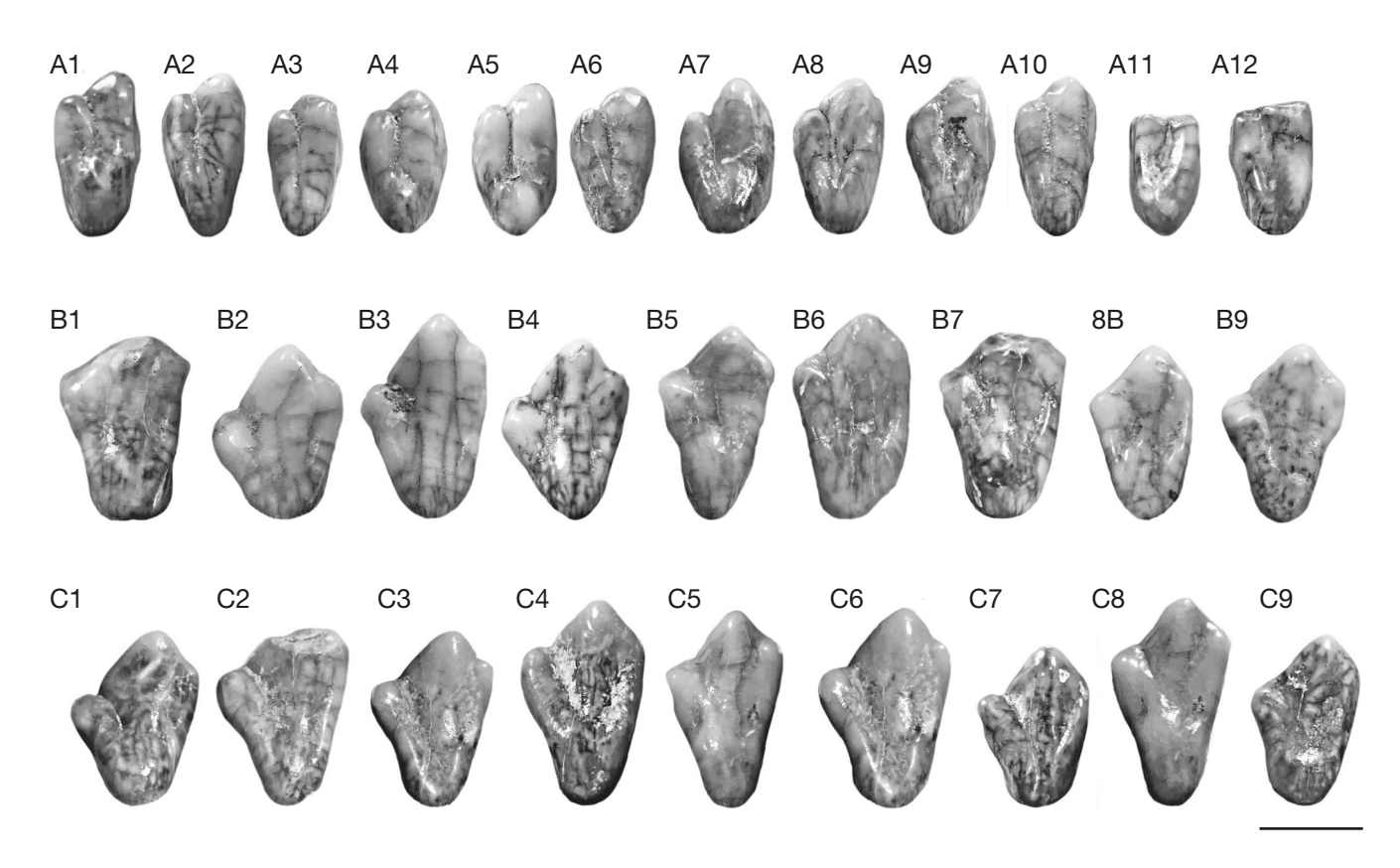


Fig. 5. — Mesial view of i1-i2 of *Ursus deningeri hercynicus* Rode, 1935 from Tunel Wielki Cave. The i1: **A1**, TWB 230; **A2**, TWB 283; **A3**, TWB 78; **A4**, TWB 220; A5, MF/7311; A6, MF/7313; A7, MF/7315; A8, MF/7314; A9, MF/7567; A10, MF/7312; A11, MF/7569; A12, MF/7568. The i2: B1, MF/7344; B2, MF/7349; B3, MF/7342; B4, MF/7341; B5, MF/7348; B6, MF/7343; B7, MF/7347; B8, MF/7339; B9, MF/7350; C1, TWB 769; C2, TWB 299; C3, TWB 288; C4, TWB 180; C9, MF/7570. All teeth are figured as left specimens (1, 2, 5, 6, 8-12, 15, 17-19, 21-24, 27, 28, 30, are mirrored). Scale bar: 10 mm.

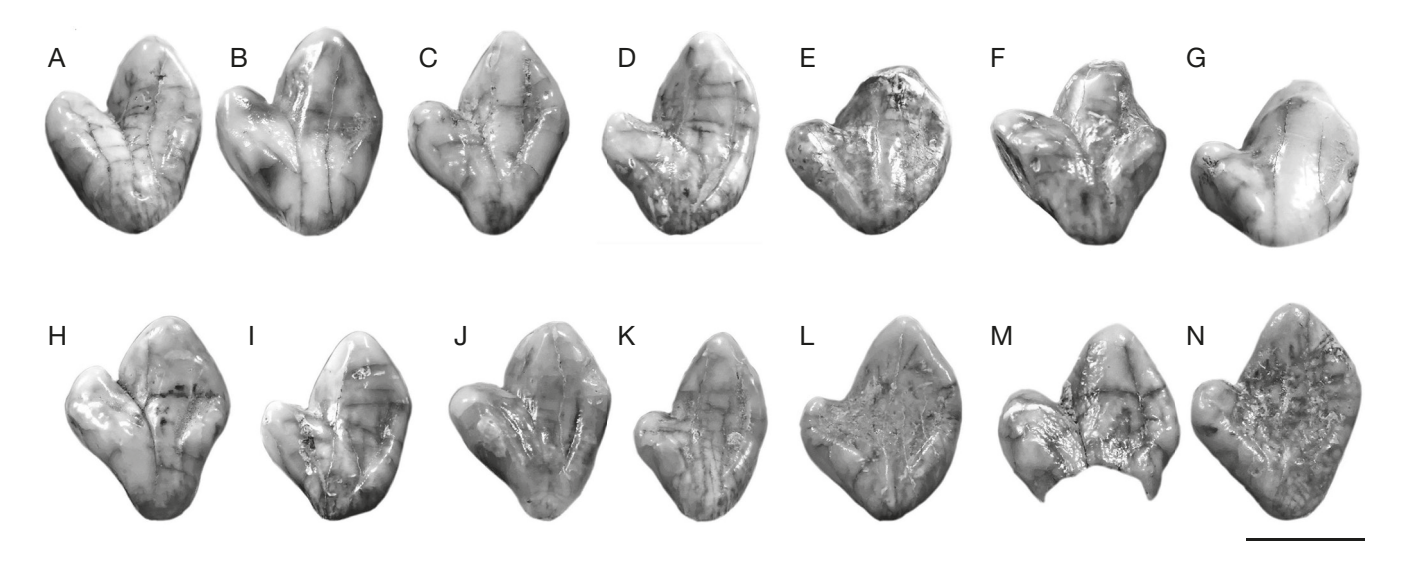


Fig. 6. — Mesial view of i3 of Ursus deningeri hercynicus Rode, 1935 from Tunel Wielki Cave: A, MF/7579; B, MF/7268; C, MF/7265; D, MF/7263; E, MF/7267; F, MF/7261; G, MF/7262; H, MF/7264; I, MF/7266; J, TWB 800; K, TWB 78; L, TWB 108; M, TWB 872; N, TWB 327. All teeth are figured as left specimens (A2, A3, A6, A8-A10, B1-B2, are mirrored). Scale bar: 10 mm.

other Middle Pleistocene bear palaeopopulations showed that they do not differ metrically (Table 3), but the TW material represents a slightly higher evolutionary level. Among the P4s from the group 1 (MIS 19-13), teeth with a small metaloph or metaconule can be found, but the morph. A predominates in the sample. Among nine P4 specimens from Kozi Grzbiet, only a single tooth represents A/B, while the others – A (Table 3).

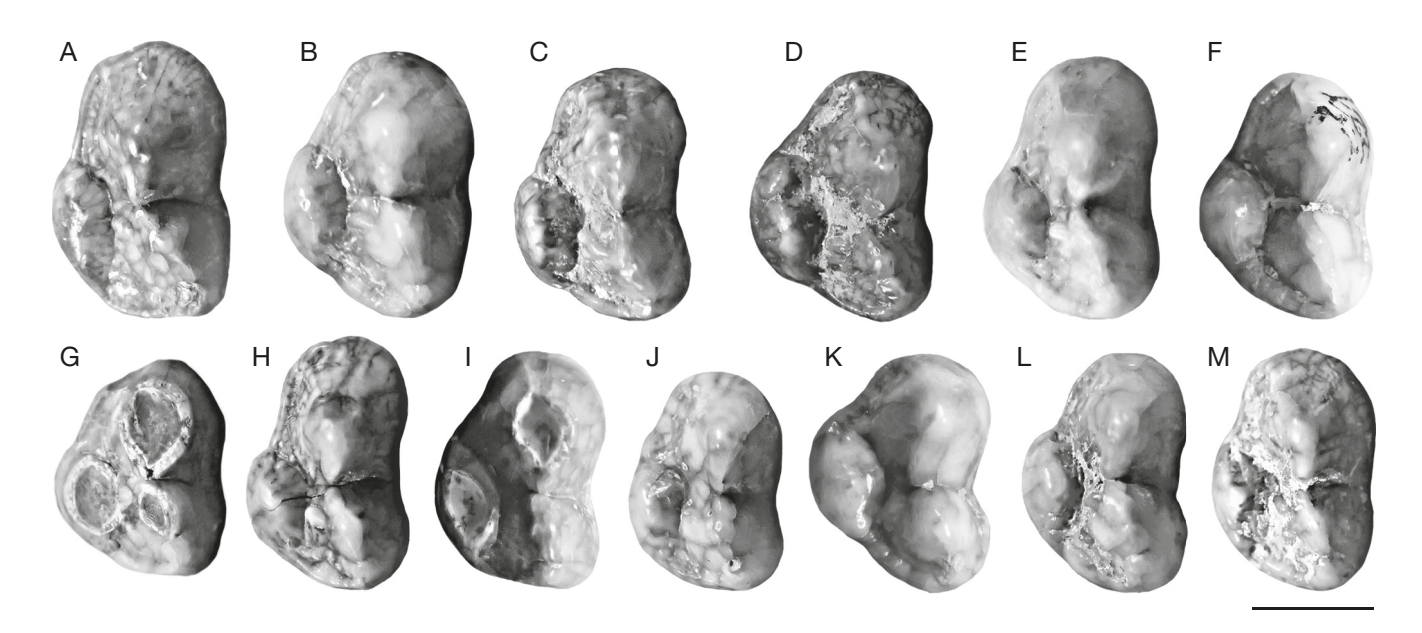


Fig. 7. — Occlusal view of P4 of *Ursus deningeri hercynicus* Rode, 1935 from Tunel Wielki Cave: **A**, MF/7150; **B**, MF/7146; **C**, TWB 131; **D**, TWB 110; **E**, MF/7151; **F**, MF/7144; **G**, MF/7148; **H**, MF/7147; **I**, MF/7145; **J**, MF/7149; **K**, MF/7143; **L**, TWB 245; **M**, TWB 96. All teeth are figured as left specimens (B, E, L, are mirrored). Scale bar: 10 mm.

Table 3. — Measurements and morphological indices of P4 of *Ursus deningeri* von Reichenau, 1904, *Ursus spelaeus deningeroid*es Mottl, 1964, and *Ursus spelaeus ingressus* (Rabeder, Hofreiter, Nagel & Withalm, 2004) from Gamssulzenhöhle (**GS**) as a standard. Abbreviations: **HU**, Hunas; **JB**, Biśnik Cave; **KZ**, Kozi Grzbiet; **M2**, Mosbach 2; **RP**, Repolusthöhle; **SS**, Stránska skálá; **TW**, Tunel Wielki Cave; **V2**, Vértesszőlős 2.

	Age		P4 L		P4 Bp		Bp/L	Index	Sta	nd.
	MIS	M	Min-Max	M	Min-Max	M	Min-Max	М	М	N
KZ	17	18.3	16.5-19.8	12.4	11.1-13.7	67.6	63.1-73.2	5.6	2.2	9
SS	17	18.9	16.7-20.8	13.8	12.3-15.5	72.1	65.1-75.5	14.3	5.6	7
M2	15-13	18.6	16.3-21.2	13.9	12.4-16.9	74.2	65.3-83.9	19.2	7.5	13
TW	13-12	18.3	15.5-19.9	13.0	11.2-14.2	71.3	65.2-80.7	23.3	9.1	15
V2	11	18.4	16.5-20.5	12.9	11.2-14.2	70.3	66.6-75.9	31.8	12.4	11
JB	10-8	18.4	15.9-20.2	12.8	10.7-14.2	70.7	63.8-77.8	31.3	12.3	40
RP	8-7	_	_	_	_	_	_	32.4	12.7	105
HU	7	_	_	_	_	_	_	39.9	15.6	56
GS	3	_	_	_	_	_	_	255.7	100.0	123

p4

The morphology of p4 from TW is highly variable, and metrically most of them are quite small (Fig. 8; Table 4). Four specimens from TW belong to the ovoid morphotype B2, with a prominent protoconid, moderate metaconid edge running distally, conical paraconid located mesio-lingually and a small but distinct hypoconid shifted disto-lingually. Two other p4s from TW represent the morphotype D2, with a well-developed paraconid and metaconid of variable size, and a small cusplet between them. One specimen was recognised as representing the morphotype D3, with a small entoconid (Fig. 8; Table 4). Two p4s from TW belong to C2, similar to B2, but with a small metaconid and a strong hypoconid shifted mesio-lingually. Three others were assigned to C3, with a small entoconid located between the paraconid and the hypoconid (Fig. 8; Table 4).

Ancestral morphotypes of p4 (B1 and C1) are the most common in the group 1 (MIS 19-13), where also a very ancestral p4 is recorded (Table 4). These single-cusped teeth without

para- and metaconid closely resemble the morph. b1, typical for arctoid bears. Metrically, p4s from TW do not differ from those in bear palaeopopulations of both groups, also the width to the length ratio (B/L) does not show any particular differences. Only the material from Biśnik Cave shows slightly higher dimensions (Table 4). The p4 from TW is already not so ancestral as those from the group 1 (MIS 19-13), but it cannot by any means be considered to be advanced. The morphodynamic index of P4/p4 shows that the TW material is grouped alightly above the populations from the group 1 (MIS 19-13) (Fig. 9). Simultaneously, the TW index is clearly lower than that of the group 2 (MIS 11-9) and *U. deningeri* from TW holds an intermediate position between both groups (Fig. 9).

MI

Morphologically, the M1 from TW shows the predominance of ancestral features, closely resembling those from the group 1 (MIS 19-13), although with a number of more progressive characteristics (Fig. 10; Table 5). Among 21 M1s from TW,

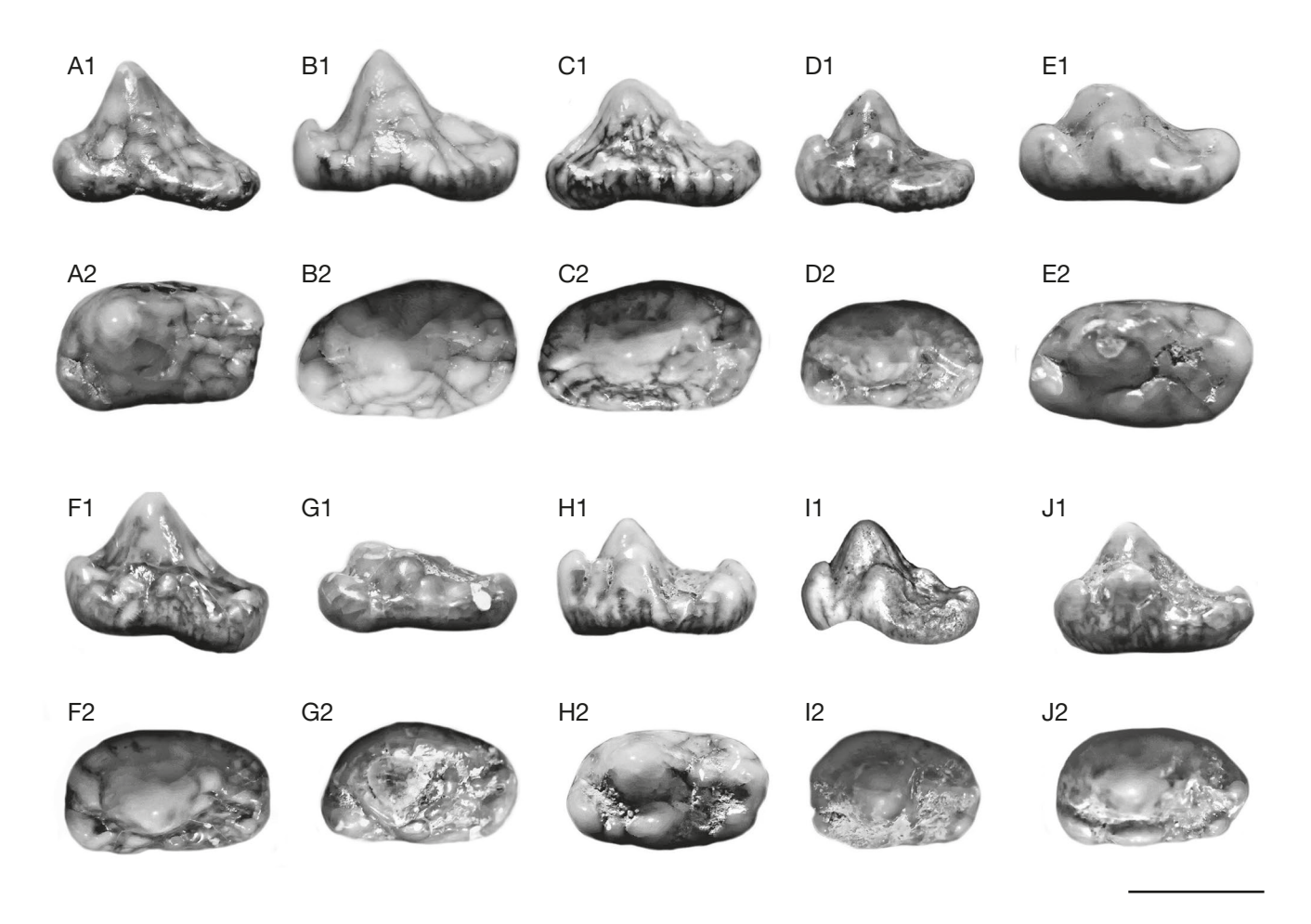


Fig. 8. - The p4 of Ursus deningeri hercynicus Rode, 1935 from Tunel Wielki Cave: A, MF/7139; B, MF/7153; C, MF/7142; D, MF/7141; E, TWB 249; F, MF/7140; G, TWB 328; H, TWB 202; I, TWB 302; J, TWB 161. All teeth are figured as left specimens (E is mirrored). 1, lingual view; 2, occlusal view. Scale bar: 10 mm.

Table 4. — Measurements and morphological indices of the p4 of Ursus deningeri von Reichenau, 1904, Ursus spelaeus deningeroides Mottl, 1964, and Ursus spelaeus ingressus (Rabeder, Hofreiter, Nagel & Withalm, 2004) from Gamssulzenhöhle (GS) as a standard. Abbreviations: HU, Hunas; JB, Biśnik Cave; KZ, Kozi Grzbiet; RP, Repolusthöhle; SS, Stránska skálá; TW, Tunel Wielki Cave; V2, Vértesszőlős 2

	Age	L			В		B/L	Index	Stan	d.	P4/p4 stand.	
	MIS	М	Min-Max	М	Min-Max	М	Min-Max	М	М	N	М	
KZ	17	14.4	13.3-15.7	9.2	8.4-9.9	64.3	59.3-69.8	10.6	5.4	9	_	
SS	17	14.7	13.4-16.7	7.7	6.5-8.2	63.7	46.4-69.1	18.9	9.5	5	_	
M2	15-13	14.9	12.4-17.1	10.2	8.1-12.5	68.6	53.6-83.3	21.9	11.1	31	_	
TW	13-12	14.1	12.3-16.3	8.8	7.4-10.1	62.6	57.1-69.3	22.9	11.6	12	20.8	
V2	11	14.3	12.2-16.6	8.9	7.9-11.2	63.7	57.9-70.5	45.9	23.2	8	_	
JB	10-8	14.5	11.8-17.9	9.5	8.1-11.6	66.1	56.9-76.9	62.1	31.3	44	_	
RP	8-7	_	_	_	_	_	_	64.1	32.3	71	20.2	
HU	7	_	_	_	_	_	_	74.4	37.5	45	24.2	
GS	3	-	_	_	-	-	_	198.2	100.0	97	100.0	

nine teeth have a smooth internal slope of the paracone, (morph. 0), while the next 12 specimens have a moderately thick edge running from the paracone apex to its base, and accompanying with one or two smaller thin pillars reaching the half of its height (morph. 1) (Table 5). Internal slope of the metacone is smooth in 10 of 24 teeth (morph. 0), while 14 others represent the morph. 1 (Fig. 10; Table 5). The small metastyle is shallow and elongated, without any distal

edge and is strongly associated with the distal cingulum. The mesocone is undivided. The shallow and small metastyle is weakly developed, with a smooth internal surface. The protocone is a low rectangular cusp, on the internal wall of which there are a few thin and sharp pillars and ribs. In a few M1s from TW, these pillars and ribs occur also on the boundary between the protocone and the mesocone, and in one tooth they are present even on the internal slope of the mesocone.

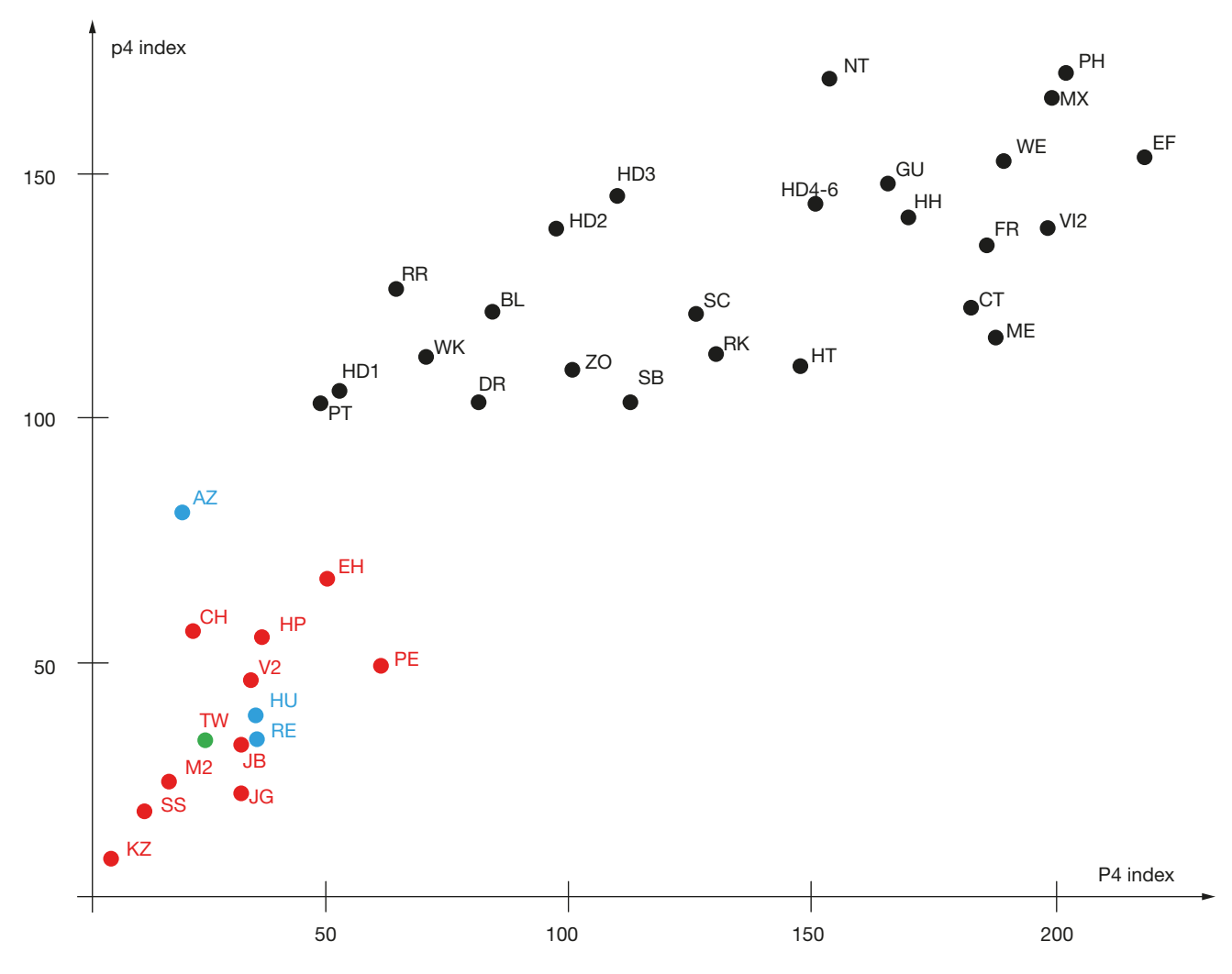


Fig. 9. — The use of morphodynamic indices of the P4 and p4 to determine the degree of evolution of bears from Tunel Wielki Cave compared to other European sites (modified from Rabeder 1999). *Ursus deningeri* von Reichenau, 1904 (**red**; TW marked by **green**): **CH**, Château; **EH**, Einhornhöhle; **HP**, Heppenloch; **HU**, Hunas; **JB**, Biśnik Cave; layer 19ad-19; **JG**, Jagsthausen; **KZ**, Kozi Grzbiet; **M2**, Mosbach 2; **PE**, Petralona; **SS**, Stránská skála; **TW**, Tunel Wielki Cave; **V2**, Vértesszóllós 2. *Ursus spelaeus deningeroides* Mottl, 1964 (**blue**): **AZ**, Azé 1-3; **RE**, Repolusthöhle. *Ursus spelaeus ingressus* (Rabeder, Hofreiter, Nagel & Withalm, 2004) (**black**): **BL**, Brieglhöhle; **CT**, Čertova díra; **DR**, Drachenloch; **EF**, Erpfingen; **FR**, Frauenloch; **GU**, Guloloch; **HT**, Hartlesgrabenhöhle; **HD**, Herdengelhöhle; **HH**, Hohlestein; **ME**, Merkensteinhöhle; **MX**, Mixnitz; **NT**, Nietoperzowa Cave; **PT**, Petersbuch; **PH**, Pod hradem Cave; **RK**, Rameschknochenhöhle; **RR**, Romain-la-Roche; **SB**, Sibyllenhöhle; **SC**, Schusterlucke; **VI**, Vindija; **WE**, Weinberghöhlen; **WK**, Wildkirchli; **ZO**, Zoolithenhöhle.

In this respect, they represent various morph. B (2 B1, 9 B2, 6 B3) and one specimen morph. C1. One to three small cusplets, accompanying with the delicate and thin enamel, are mostly situated on the talon surface. Most of them represent the morph. B (19 among 23), while the talon field in four specimens is almost smooth, with a few weak pillars. The talon field is also separated from the weakly developed distal cingulum. Cingulum crest around the crown is almost absent. The lingual cingulum in nine M1s represents the morphotype 1.5, and is situated mostly on the lingual slope of the protocone. In the other nine specimens representing the morph. 2, the lingual cingulum collared the lingual slope of the protocone and terminated in the indentation between the mesocone and hypocone (Fig. 10; Table 5).

Metrically, the M1s from TW are moderately large, being slightly larger than those from the group 1 (MIS 19-13) (Table 5). They are morphologically similar, although the features mentioned above are stronger developed. Among

others, the parastyle in most M1s from TW is larger and more strongly separated from the paracone. The lingual cingulum is more strongly developed. In half of the M1s from TW, the lingual cingulum collared the entire protocone (morph. 1.5), while in the other half it starts from the mesial wall of the protocone and reaches the bounduary between the mesocone and the hypocone. In the M1s from the group 1 (MIS 19-13), the lingual cingulum is weaker, and represents morph. 1, more strongly developed only on the mesocone and protocone base. Morphotypes 1.5 and 2 also occur, but they are much rarer than in the TW material (Table 5).

M2

The mesial ridge of the M2 paracone in eight of 29 teeth is in contact with the mesial ridge of the protocone, forming a smooth junction (A3). The next 11 teeth represent the morph. B (5 B1, 5 B2, 1 B3), with an additional branch running on the mesio-lingual slope of the parastyle and mesial

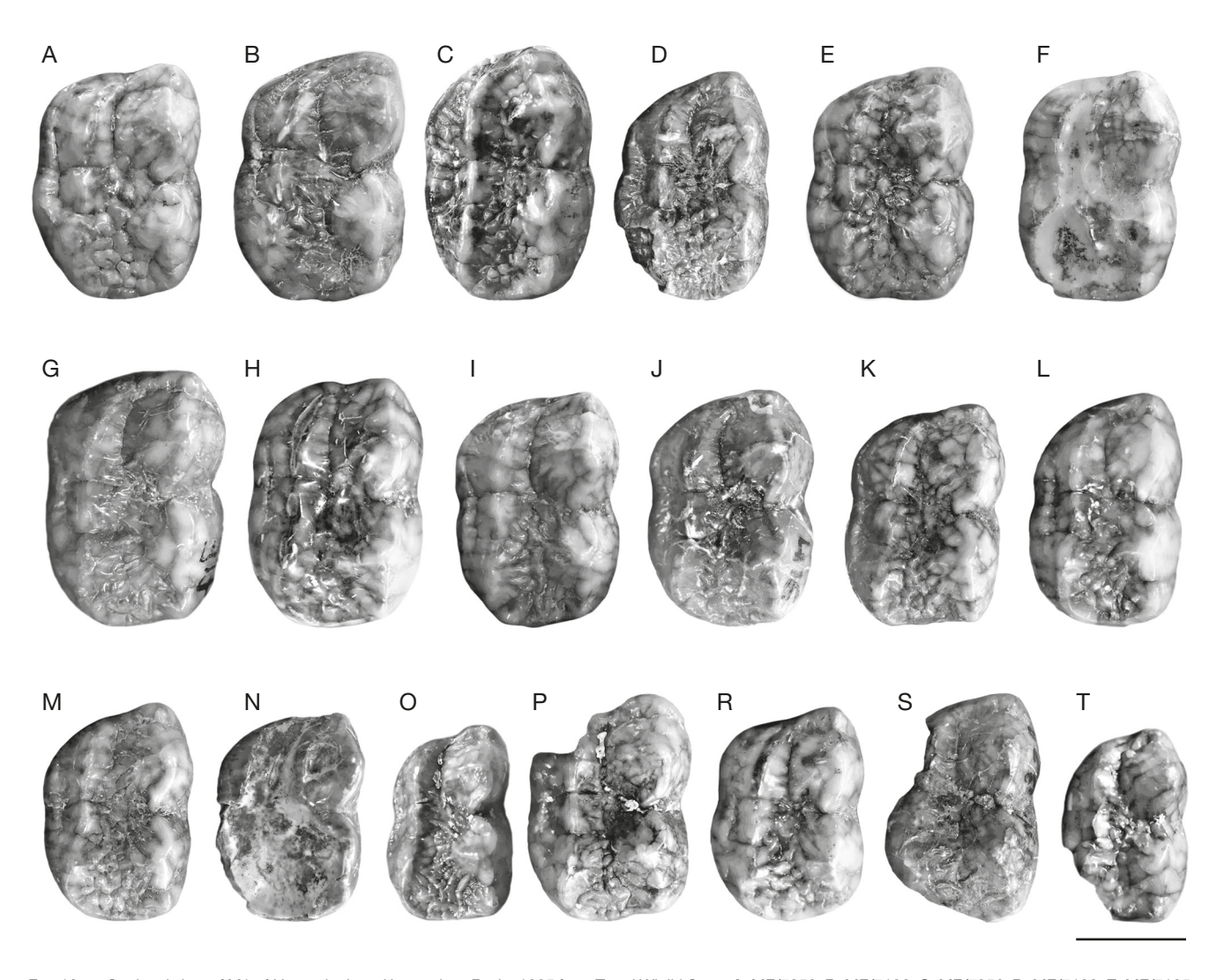


Fig. 10. — Occlusal view of M1 of Ursus deningeri hercynicus Rode, 1935 from Tunel Wielki Cave: A, MF/7252; B, MF/7196; C, MF/7256; D, MF/7193; E, MF/7195; F. MF/7191: G. MF/7255: H. MF/7190: I. MF/7257: J. MF/7254: K. MF/7251: L. MF/7194: M. MF/7192: N. MF/7200: O. TWB 811: P. MF/7199: R. MF/7253: S, MF/7201; T, TWB 847. All teeth are figured as left specimens (A, B, E-G, I, O, are mirrored). Scale bar: 10 mm.

ridge of the parastyle, that formed a group of 4-5 cusplets like structures that collared the mesial wall of the trigon (Fig. 11; Table 6). The 26 from 28 M2s yield two or three pillars on the internal wall of the paracone, which started from the base and reaching the half of its height (B). In two M2 specimens, the internal wall of the paracone is smooth, without any pillars and ribs (Fig. 11; Table 6). Among 27 M2s from TW, 13 specimens represent the morphotype A (2 A, 7 A1 and 4 A2), where the mesostyle complex forms a double arch (Fig. 11; Table 6). The next 13 teeth belong to the morphotype B (8 B, 4 B1, B2), with the distal arm of the paracone curved considerably centrally, where it loses connection with the mesial arm of the metacone and forms a separate arch. The metaloph complex is less variable (single A/B), the 26 other specimens belong to B. Among them, there are seven teeth representing the morphotype B2, with a few (5-7) small cusplets in disordered forms located between the protocone and the metacone, and the metaloph complex is pushed more distally. The next four specimens represent B1, where a few (5-7) cusplets running in quite order from

the metacone to the hypocone. Finally, five teeth belong to the morphotype B3, where the metaloph complex is located between the metacone and the protocone.

All M2s (n = 29) have the posteroloph complex uniform in shape (morph. 1), where between the metastyle and hypocone, there are a few (4-6) small cusplets, which do not form any regular structure. The talon field is moderately developed, with 15 M2s from TW representing A/B, where the surface is partially smooth and partially covered by a few (5-8) small cusplets. The next 16 teeth belong to B, where the entire talon field is covered with numerous small cusplets. The talon field is collared by a thick wall of the distal cingulum, which forms numerous small cusplets, and, except one tooth, all the M2s from TW represent B. Among 25 M2s from TW, metastyle and posthypocone in 23 are present but weakly developed into a small and low cusp. The metastyle and posthypocone are absent in three other specimens. Most of M2s from TW (n = 23) have the internal wall of the protocone with a few, usually 3-4, pillars and ribs starting from the internal base of the protocone but not reaching the apex.

Table 5. — Measurements and morphological indices of M1 of *Ursus deningeri* von Reichenau, 1904. Abbreviations: **C 718**, Koněprusy C 178; **HH**, Hundsheim; **JB**, Biśnik Cave; **KZ**, Kozi Grzbiet; **M2**, Mosbach 2; **SS**, Stránská Skála; **TW**, Tunel Wielki Cave; **ZH**, Za Hájovnou Cave.

	Age		1			2			3			4			6	
	MIS	М	Min-Max	N	М	Min-Max	N	М	Min-Max	N	М	Min-Max	N	М	Min-Max	N
KZ	17	25.3	22.7-27.8	9	11.8	10.5-13.0	9	12.5	9.8-13.6	10	10.3	9.9-10.7	2	17.8	15.80-18.9	9
C 718	19-17	25.3	22.1-28.7	22	12.1	10.8-13.1	14	12.7	11.0-15.2	19	10.2	9.1-12.3	6	17.7	15.7-19.8	23
SS	19-17	25.4	22.5-27.5	8	12.2	10.6-12.9	8	12.9	10.6-14.9	8	10.4	9.4-11.9	8	18.4	17.4-20.1	8
M2	15-13	25.0	22.3-27.8	23	11.9	10.5-13.1	23	12.1	10.2-14.1	24	10.0	8.6-11.5	18	17.2	14.9-19.6	23
HH	15-13	26.2	24.5-29.3	9	12.2	10.4-14.5	10	12.5	11.2-14.9	11	10.0	9.3-10.9	3	17.7	16.7-20.0	12
TW	13-12	26.3	23.5-29.2	22	13.8	12.5-15.3	22	13.2	11.5-14.7	25	11.1	9.8-14.9	20	18.3	15.9-20.9	23
ZH	11	26.8	23.0-30.0	20	12.8	11.1-13.8	22	12.8	11.2-13.8	22	10.3	9.3-11.3	10	18.0	16.5-20.1	20
ZH	9	26.0	23.7-28.3	11	12.3	11.4-13.6	11	12.2	10.0-13.7	11	10.1	9.6-10.9	5	17.3	15.8-19.9	10
JB	10-8	26.8	23.6-30.5	36	13.6	12.2-14.6	36	12.8	11.5-13.9	36	11.1	9.7-15.6	36	18.6	16.3-21.4	36
	Age		7			2/3			6/1			7/1			7/6	
	MIS	М	Min-Max	N	M	Min-Max	N	M	Min-Max	N	М	Min-Max	N	М	Min-Max	N
KZ	17	18.5	16.2-19.8	11	102.8	97.8-110.8	9	70.2	65.2-73.9	8	72.5	66.4-78.6	9	103.0	94.1-109.0	9
C 718	17	18.4	15.9-21.2	19	106.3	97.9-119.2	18	69.4	65.1-75.5	15	72.0	67.9-77.4	15	103.5	96.7-108.9	17
SS	19-17	18.8	17.2-20.7	8	104.1	96.9-118.4	8	70.1	66.2-74.1	8	72.1	66.1-77.9	8	103.6	95.6-104.9	8
M2	15-13	17.6	15.8-20.5	24	107.9	94.3-139.0	23	68.7	62.3-75.6	22	70.0	64.2-74.4	22	101.8	93.2-106.0	23
HH	15-13	18.1	16.5-20.5	12	106.9	93.1-115.4	12	68.3	66.6-71.3	9	70.1	66.5-73.3	9	102.3	96.3-108.6	12
TW	13-12	18.9	17.3-20.8	22	105.1	98.6-113.2	22	68.2	64.5-72.3	22	70.5	66.4-74.1	22	103.5	98.9-112.7	23
	11	18.8	17.0-21.5	22	109.1	93.5-123.3	22	68.0	62.2-71.9	18	70.5	67.3-75.8	19	104.4	99.0-112.3	19
ZH								~~ ~	F7 0 70 0	40	70.0	040 740	_	4044	1010100	_
ZH ZH	10-9	18.2	16.2-20.5	9	109.5	102.2-118.5	10	66.6	57.2-70.6	10	70.6	64.0-74.2	9	104.4	101.2-110.0	9

Table 6. — Measurements and morphological indices of M2 of *Ursus deningeri* von Reichenau, 1904. Abbreviations: **C 718**, Koněprusy C 178; **HH**, Hundsheim; **JB**, Biśnik Cave; **KZ**, Kozi Grzbiet; **M2**, Mosbach 2; **SS**, Stránská Skála; **TW**, Tunel Wielki Cave; **ZH**, Za Hájovnou Cave.

	Age		1			2			3			4			5	
	MIS	М	Min-Max	N												
KZ	17	39.6	38.5-41.1	5	12.2	11.6-12.8	5	7.4	5.8-8.8	7	21.2	19.4-23.3	6	20.7	19.8-22.0	5
C 718	19-17	40.7	34.9-45.8	23	12.1	9.9-14.1	22	7.6	6.3-9.8	17	20.7	17.1-24.2	24	20.7	17.2-23.3	24
M2	15-13	39.9	33.8-44.4	33	12.3	10.2-14.7	27	8.4	5.2-12.4	27	20.2	16.9-24.5	34	19.9	17.8-23.3	33
HH	15-13	42.9	40.4-45.8	5	12.5	11.1-14.3	6	7.9	6.9-9.5	7	21.1	19.7-22.5	9	20.7	18.9-22.7	10
TW	13-12	41.5	38.1-44.3	21	12.3	11.0-14.7	29	8.4	7.6-11.4	28	20.5	18.0-23.0	27	20.3	17.5-21.8	28
ZH	11	42.1	38.3-47.3	23	12.8	10.9-15.4	24	7.3	4.7-9.5	23	21.5	18.0-23.8	26	20.4	17.8-23.0	27
ZH	9	42.5	41.0-44.5	6	13.4	11.7-14.7	10	7.9	5.9-10.9	9	21.4	20.4-23.3	9	20.4	18.8-21.9	10
JB	10-8	40.9	33.9-44.5	25	12.9	11.6-13.7	25	8.9	6.8-11.7	25	20.3	17.8-22.2	25	18.2	15.6-19.2	25
	Age		2/1			3/2			4/1			5/1			5/4	
	MIS	М	Min-Max	N												
KZ	17	28.7	27.9-29.3	6	68.7	58.4-75.8	5	54.6	47.2-54.6	4	51.4	50.0-56.0	4	96.6	93.8-98.2	6
C 718	19-17	29.7	28.4-30.8	22	62.8	63.6-69.5	17	50.7	47.2-59.5	22	50.8	47.0-63.6	22	97.1	94.5-97.9	22
M2	15-13	29.8	28.0-31.1	26	68.3	51.0-84.4	27	50.3	44.0-58.0	33	49.9	45.8-53.6	32	95.2	93.5-99.5	27
HH	15-13	29.5	26.4-31.4	6	63.2	62.2-66.4	6	49.2	46.9-52.7	5	48.9	47.8-51.0	5	94.8	92.7-97.5	6
TW	13-12	30.6	26.7-30.8	21	58.3	54.9-67.5	28	49.4	45.5-53.1	21	48.1	44.7-51.9	21	89.2	87.9-98.3	28
ZH	11	30.4	28.5-32.6	23	57.0	43.1-61.7	23	51.0	46.4-54.0	20	49.0	45.8-52.2	22	91.6	86.8-97.4	20
ZH	9	31.5	28.5-33.1	6	59.0	50.4-74.2	9	50.5	49.2-52.4	6	47.6	45.1-50.0	6	91.4	91.6-95.4	6
JB	10-8	31.7	30.3-34.1	25	59.9	50.6-69.2	25	49.4	46.6-52.6	25	45.4	44.6-48.7	25	84.8	80.8-89.8	25

Only three M2s have a single, similarly developed pillar. The lingual cingulum shows a low evolutionary stage, with most teeth (24 of 32 specimens) representing the morph. 1. It is characterised by the cingulum running through the base of the protocone and terminating between the protocone and the hypocone. In eight other M2 specimens, the lingual cingulum is better developed and ends near the top of the hypocone (1.5) (Fig. 11; Table 6). Metrically, the M2 from TW is moderately large, and in average it is slightly larger than those from Koněprusy C 178 or Mosbach 2, but smaller than M2 from Hundsheim (Table 6). Any particular differences

between populations have not been found. Only the distal to the mesial breadth ratio shows a tendency to decreasing, with the narrowing of the distal part of the crown. In this index, the M2 from TW is closer to the group 2 (MIS 11-9), than those from the group 1 (MIS 19-13) (Table 6).

mI

The main cusps of the m1 from TW are connected to each other by a crest, which follows the outline of the tooth. In occlusal view, the tooth is elongated, and has moderately expanded talonid. The mesial margin of the trigonid is



Fig. 11. — Occlusal view of M2 of Ursus deningeri hercynicus Rode, 1935 from Tunel Wielki Cave: A, MF/7205; B, MF/7352; C, MF/7203; D, MF/7207; E, MF/7209; F, MF/7360; G, MF/7216; H, MF/7214; I, MF/7359; J, MF/7353; K, MF/7210; L, MF/7218; M, MF/7212; N, MF/7206; O, MF/7213; P, MF/7351; R, MF/7215; S, MF/7204. All teeth are figured as left specimens (A, B, H, I, M, R-S, are mirrored). Scale bar: 10 mm.

rounded, the lingual one is straight, while the buccal margin is almost straight, with a gentle concavity at the level of the protoconid. The broader talonid has a straight lingual margin, strongly convex buccal and rounded or blunt distal margins. The trigonid is moderately broad and long and clearly distinguishing from the wide and long talonid. The apex of the triangular and low paraconid inclines slightly mesially. Situated behind, rectangular protoconid is the highest and largest cusp, with almost with the vertical axe of the cusp

almost perpendicular to the tooth occlusal plane. Both main cusps are separated by a wide, V-shaped valley. A relatively high, elongated and rectangular metaconid is situated after the metastylid. The lingual half of the talonid is occupied by entoconid, square-shaped to rectangular and relatively low cusp, with well developed entoconid 2. In TW, 15 of 23 m1 have a single metastylid (1), rather it is double or triple (2, n = 7) (Fig. 12; Table 7). Among 28 m1 from TW, the entoconid is sometimes double (A2, n = 7), and the most

often triple (A3, n = 19), and rarely quadruple (A4, n = 4) (Table 7). On the internal slopes of the entoconids occur a few moderately developed ribs and pillars, reached half of the entoconid height (B in 22 of 23 teeth). Only in one tooth pillars and ribs are thicker and stronger developed (C). The entyphoconid is present in all 23 m1, but in 13 it is weakly developed and not separated from the hypoconid (A/B). In the next 10 m1, well-developed entyphoconid is separated from the hypoconid by a thick ridge (B).

The talonid cusps are closely situated, and in five of 24 m1 from TW its distal margin is very compact and narrow, like that in *U. arctos arctos*, without any entyphoconid or hypoconulid. However, a slightly broader morphotype 2, with entyphoconid and small hypoconulid dominated (n = 19) (Fig. 12; Table 7). Metrically, the m1 from TW does not differ from the group 1 (MIS 19-13). Slow increasing in size is observed since MIS 11 (Table 7). There are no particular differences in breadth proportion between different populations. The m1 from TW has proportionally slightly longer talonid, and the L ta/L tr index is closer to the group 2 (MIS 11-9) than to the group 1 (MIS 19-13). The trend to shortening trigonid with simultaneous lengthening of the talonid starts to be well visible since MIS 11, and it is well recognised in the m1 from Biśnik Cave (Table 7).

m2

The m2s from TW strongly vary in size, but they are within the range of variation of *U. deningeri* (Fig. 13; Table 8). The mesial and distal margins are gently rounded or blunt, the lingual margin is straight, moderately concave in the middle part, in the transition between the trigonid and the talonid. The buccal margin of the trigonid is slightly rounded, while that of the talonid is moderately expanded and rounded. In some teeth, the lingual margin is almost straight (Fig. 13). Occlusal surface is moderately complicated, less than in *U. spelaeus*, but definitely stronger than in the group 1 (MIS 19-13). Among 25 m2s, nine specimens have a simple metalophid complex developed as a straight, thick edge (morph. A). The dominant is B (n = 16), with the entprotoconid located on the internal slope of the protoconid. The internal field of the trigonid in eight m2 specimens holds only a few weak furrows and pillars (morph. 1). Among them, the dominant is the morphotype 2 (n =17), with one to three small but prominent cusplets and one or two thick furrows and pillars.

Most of the m2s from TW (24 of 26) have the metastylid complicated by the presence of small cusplets. As was showed by Rabeder (1999), the presence of smaller cusplets (usually 3 mesial, 1 paterial and 2 distal) is more ancestral state, and the occurrence of one large cusp is a more derived one. Only in two m2s, the metastylid is double, with two larger cusplets (mesial and distal). The mesolophid complex is moderately developed, still ancestral, with dominant morphotype B (22 of 24 teeth). In two specimens, the mesolophid is developed as a short and moderately thick ridge, not connected with the distal slope of the protoconid (A). The enthypoconid is variably developed, with the dominant morphotype B

(20 among 27), where it is prominent, thick, triple or quadruple, separated from the hypoconid by a wide groove. The four m2 specimens represent the morph. A/B, with the moderately developed enthypoconid not separated from the surrounded hypoconid. The other three teeth represent the morph. B/C, where a very strongly developed enthypoconid is still not divided. In half of the m2 specimens from TW (16 of 30), the hypoconulid is absent, while it is well marked in 14 other teeth, being situated on the internal slope of the hypoconid (Fig. 13; Table 8).

The m2s from TW differ from those of the group 1 (MIS 19-13) in a more complicated occlusal surface, more strongly developed metalophid and mesolophid complexes, and in a broader inner talonid field. Dimensions of m2s and their particular indexes do not differ among bear palaeopopulations recorded from different sites (Table 8). The size of the m2 is quite variable, and the TW palaeopopulation is characterised by a small size of the m2. The mean length of the m2 from Hundsheim (28.66 mm), Koněprusy C 178 (29.56 mm), Kozi Grzbiet (29.27 mm) and Stránska skálá (28.35 mm) is higher than that of TW (27.56 mm), while only that from Mosbach 2 (26.97 mm) has a smaller value. Increasing in size is observed in the specimens which come from the layers 19ad-19 of Biśnik Cave (MIS 10-9) and later. It was also found a tendency to shortening and narrowing the trigonid and elongating and broadening the talonid. In all these ratios, the m2 from TW holds an intermediate position between the group 1 (MIS 19-13) and the group 2 (MIS 11-9) (Table 8).

m3

In outline of the m3 from TW, the morphotype B predominates (20 of 22); it has an irregular shape, broad and expanded trigonid, long and wide talonid, and distinctly marked concavity on the buccal side of the boundary between the trigonid and talonid (Fig. 14; Table 9). Two others represent a more evolved morphotype C, oval-shaped, with less marked buccal concavity and sharper distal margin of the crown. The morphology of the protoconid complex is quite variable, and among 20 m3s from TW the most common are morphotypes B (1 B2, 1 B3, 7 B4, and 6 B5), a strongly developed mesolophid of which is connected with the protoconid. The next four teeth have anmesolophid (A4) extending disto-lingually. Most of the m3s (n = 15) hold one small but prominent cusplet on the internal wall of the metaconid (morph. B). Five other specimens have two small cusplets, and one tooth also has a thin pillar (morph. C). All m3s from TW hold still quite simple, but already present hypoconid, from which running 1-3 (B2, n = 9) or 4-6 thin (B3, n = 10) short ridges and pillars. In most of the m3s (22 of 24), the centrolophid is present as a series of small and low cusplets running disto-buccally from the metaconid base to the buccal slope of this cusp (B) (Table 9). In two m3s, the centrolophid is similarly developed, but additionally it is connected with the mesolophid by a thin and sharp ridge (C). The entoconid is always present, usually (19 of 24) occurring in a series of quite large and low

256

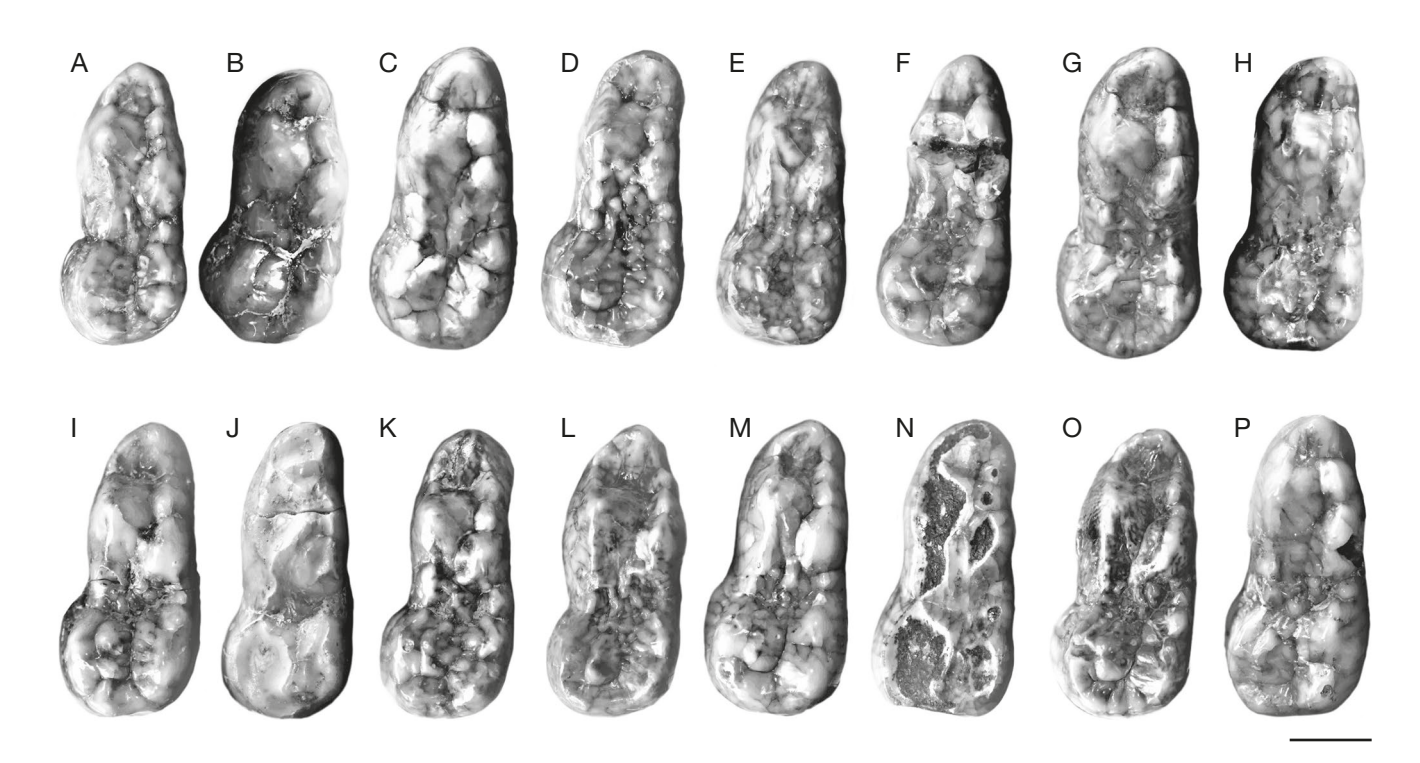


Fig. 12. — Occlusal view of m1 of Ursus deningeri hercynicus Rode, 1935 from Tunel Wielki Cave: A, TWB 301; B, MF/7237; C, MF/7219; D, MF/7222; E, MF/7221; F, MF/7231; G, MF/7225; H, MF/7224; I, MF/7228; J, MF/7234; K, MF/7220; L, MF/7223; M, MF/7227; N, MF/7226; O, MF/7229; P, MF/7230. All teeth are figured as left specimens (A, B, E-G, I-J, L-P, are mirrored). Scale bar: 10 mm.

Table 7. — Measurements and morphological indices of m1 of Ursus deningeri von Reichenau, 1904. Abbreviations: C 718, Koněprusy C 178; HH, Hundsheim; JB, Biśnik Cave; KP, Koněprusy; M2, Mosbach 2; TW, Tunel Wielki Cave; ZH, Za Hájovnou Cave.

	Age		1			2			3			6			7	
	MIS	М	Min-Max	N												
C 718	17	27.8	24.5-31.5	24	17.4	16.4-19.3	23	10.3	8.9-12.0	23	10.2	8.6-11.8	24	12.9	11.5-14.9	25
KP	17	27.0	24.2-31.3	20	17.0	15.2-19.5	21	10.1	8.9-11.7	27	10.0	8.8-11.4	23	12.5	11.3-13.7	26
M2	15-13	27.4	25.3-31.2	19	17.4	16.6-18.8	9	9.9	8.9-10.7	9	10.2	8.6-11.8	24	12.9	11.5-14.9	25
HH	15-13	27.1	24.9-30.1	7	17.7	16.2-19.2	5	10.3	9.4-11.6	7	10.7	9.8-11.4	7	12.8	11.6-14.0	9
TW	13-12	27.5	25.1-30.7	20	17.1	15.2-19.1	21	10.8	8.8-12.0	26	10.9	9.6-12.6	24	13.2	11.9-14.7	29
ZH	11	28.0	25.6-30.9	15	17.4	14.9-19.1	14	10.4	9.2-12.5	18	10.6	9.5-11.5	14	13.3	11.9-15.0	21
JB	10-8	28.4	25.4-32.6	39	16.7	15.6-19.7	39	12.8	10.7-14.8	39	11.5	9.7-13.7	39	13.6	11.6-14.6	39
	Age		2/1			3/2			6/1			7/1			6/7	
	MIS	М	Min-Max	N												
C 718	17	62.5	56.9-66.9	23	59.2	54.3-62.2	23	36.6	33.8-43.4	24	46.6	44.4-52.2	24	85.4	74.7-95.9	24
KP	17	63.0	55.8-67.4	20	59.4	58.6-60.0	21	36.9	33.3-40.1	20	46.4	42.7-49.5	19	84.4	77.9-93.2	23
M2	15-13	62.4	57.1-66.4	19	61.7	58.7-66.9	9	37.7	34.1-40.5	19	48.0	44.8-54.1	18	83.6	81.7-94.6	18
HH	15-13	62.3	55.6-65.3	5	62.5	57.9-65.8	5	38.8	37.2-41.4	6	46.8	44.6-49.5	7	84.9	80.4-93.3	6
TW	13-12	62.1	57.3-64.9	19	64.6	58.8-74.7	19	39.9	36.1-43.9	24	48.3	44.7-50.5	25	82.8	73.1-95.8	24
ZH	11	62.1	58.2-64.6	14	65.1	58.5-72.5	14	37.8	34.7-40.9	13	48.0	45.9-50.7	15	80.0	73.4-85.6	13
JB	10-8	61.6	52.1-68.9	39	69.7	64.7-82.9	39	40.5	37.3-43.9	39	47.8	44.2-51.6	39	84.8	77.8-93.9	39

cusplets (4-7), arranged one behind the other (B). In five others, the entoconid is similarly developed, but 1-2 among these cusplets are enlarged (C). The stage of development of the talon field is variable, and in nine teeth this structure is quite smooth, sometimes the are one or two gentle pillars (B). In most specimens (n = 14), the talonid field holds one to three moderately large cusplets (C), while this structure in a single m3 is more complicated and holds six additional cusplets (D) (Fig. 14; Table 9).

The m3 from TW is moderately large and broad and matches in this respect other Middle Pleistocene populations. No particular differences between the m3 from TW and those from the group 1 (MIS 19-13) and the group 2 (MIS 11-9) have been found (Table 9). A tendency to the lengthening of the talonid is observed in the course of time. In the trigonid length to the total length (L tr/L m3) index, the m3 from TW matches the value of the group 2 (MIS 11-9), and the trigonid is shorter than that in the group 1 (MIS 19-13) (Table 9).

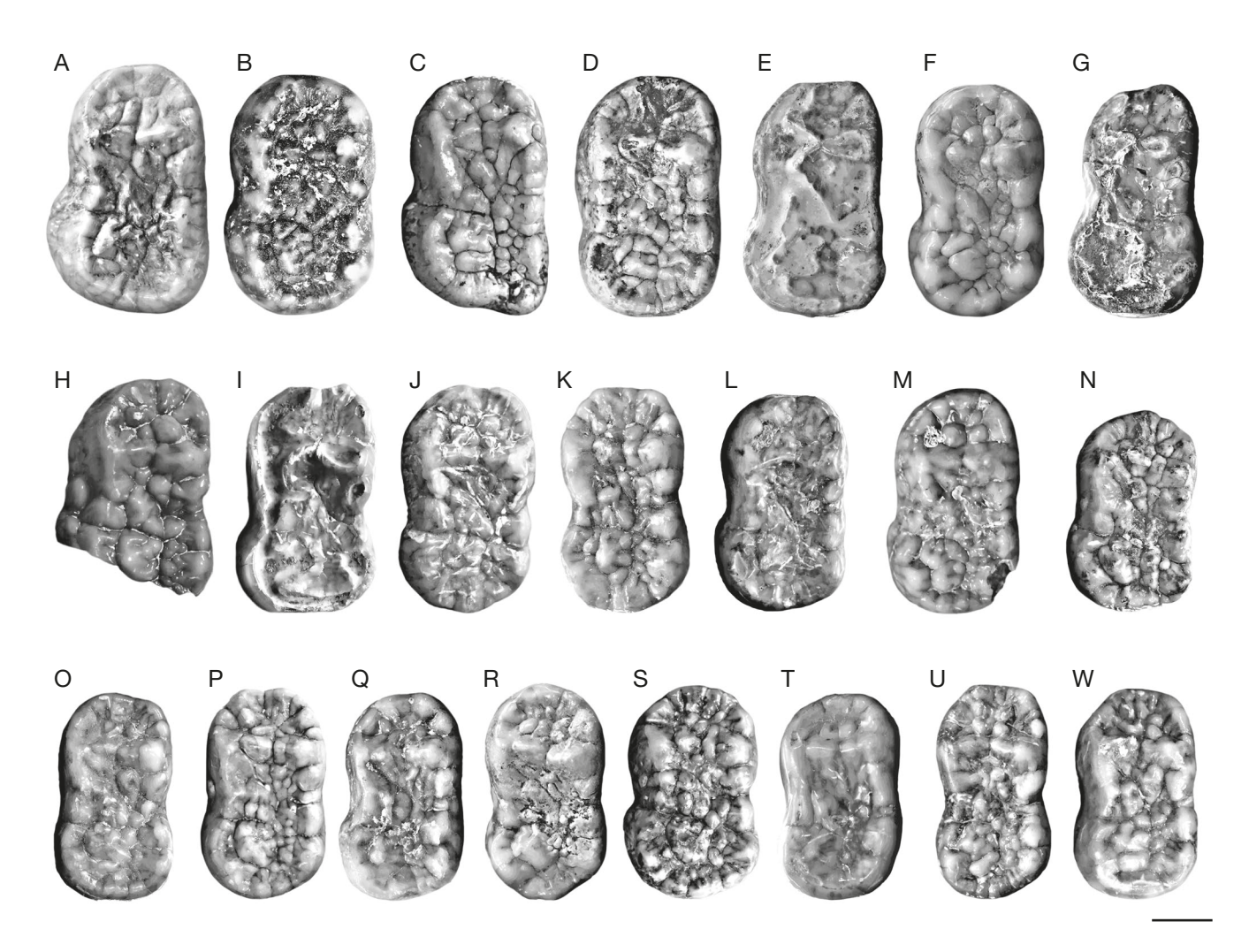


Fig. 13. — Occlusal view of m2 of *Ursus deningeri hercynicus* Rode, 1935 from Tunel Wielki Cave: **A**, MF/7161; **B**, MF/7156; **C**, MF/7154; **D**, MF/7170; **E**, MF/7168; **F**, MF/7157; **G**, MF/7163; **H**, TWB 338; **I**, TWB 610; **J**, MF/7155; **K**, MF/7167; **L**, MF/7159; **M**, MF/7158; **N**, MF/7173; **O**, MF/7169; **P**, MF/7164; **Q**, MF/7175; **R**, MF/7172; **S**, MF/7171; **T**, MF/7166; **U**, MF/7165. All teeth are figured as left specimens (B-E, G, I-L, P-Q, T-W, are mirrored). Scale bar: 10 mm.

Table 8. — Measurements and morphological indices of m2 of *Ursus deningeri* von Reichenau, 1904. Abbreviations: **C 718**, Koněprusy C 178; **HH**, Hundsheim; **JB**, Biśnik Cave; **KP**, Koněprusy; **KZ**, Kozi Grzbiet; **M2**, Mosbach 2; **TW**, Tunel Wielki Cave; **ZH**, Za Hájovnou Cave.

	Age		1			2			3			4			5			6			7	
	MIS	М	Min-Max	N	М	Min-Max	N															
KZ	17	29.2	26.5-31.5	8	15.8	13.9-17.4	8	17.8	15.8-19.5	7	13.2	10.8-15.7	10	11.4	10.1-12.5	9	16.7	15.4-18.4	7	17.3	15.9-19.2	8
C 718	17	28.3	25.4-31.1	16	15.2	12.5-17.5	17	17.4	15.9-20.0	16	13.3	11.9-14.9	16	10.9	9.5-13.0	15	15.5	13.3-17.7	16	17.1	14.8-18.8	16
KP	17	29.5	24.9-32.8	15	15.7	13.5-17.3	15	18.4	15.7-20.7	15	13.8	10.5-15.8	16	11.1	9.1-12.1	17	16.0	14.7-17.9	17	17.2	16.2-18.5	15
M2	15-13	26.9	24.7-30.2	40	15.0	12.7-17.4	15	16.7	15.0-17.8	14	11.8	9.5-14.4	14	10.2	8.8-11.8	14	15.8	13.7-18.1	39	16.7	13.9-19.6	39
HH	15-13	28.6	26.1-32.1	8	15.0	13.3-17.7	9	17.9	15.5-20.0	6	13.4	11.7-15.0	8	10.9	9.5-12.1	6	16.1	14.6-17.7	9	17.2	15.8-18.9	8
TW	13-12	27.5	24.0-31.6	25	15.7	13.5-18.6	28	17.2	14.5-19.4	28	12.9	9.4-14.4	32	10.3	9.7-13.7	35	16.1	13.9-18.8	29	16.7	13.2-19.1	31
ZH	11	27.8	24.7-31.2	19	14.8	12.6-17.0	20	17.2	15.0-19.6	20	13.0	10.5-15.6	19	10.6	9.5-12.3	19	16.4	14.2-19.0	21	16.9	14.6-19.6	20
ZH	9	27.9	26.4-29.8	7	14.7	13.0-17.0	8	17.3	15.6-19.2	7	13.2	12.2-13.7	7	10.7	10.3-11.0	6	16.6	14.3-18.2	9	16.5	15.4-18.0	6
JB	10-8	29.1	26.1-35.5	41	17.0	15.3-19.9	41	17.3	15.5-20.9	41	12.1	10.6-15.6	41	11.9	10.3-14.6	41	17.2	14.2-19.2	43	17.4	14.7-20.3	47
	Age		2/1			4/1			4/2			5/3			6/1			7/1			6/7	
	MIS	М	Min-Max	N	М	Min-Max	N															
KZ	17	58.2	50.2-60.2	8	40.8	39.6-42.4	8	61.9	59.6-73.5	8	60.5	58.5-64.1	8	56.9	51.1-63.9	7	59.3	54.9-66.7	8	97.1	94.4-100.1	8
C 718	17	53.4	48.3-58.5	16	42.1	40.5-47.9	16	62.4	58.6-66.3	16	62.6	59.7-65.1	16	54.7	50.2-62.8	16	60.1	57.2-67.4	15	96.8	91.7-99.8	15
KP	17	53.3	48.4-57.4	15	43.1	41.4-48.8	15	62.8	58.1-67.4	15	60.3	57.9-66.3	15	54.6	51.2-59.1	15	58.6	55.6-62.7	13	96.1	90.9-97.9	13
M2	15-13	56.6	50.6-63.1	14	44.8	40.9-49.8	14	63.9	57.5-69.4	14	61.1	58.7-66.2	14	59.2	53.4-65.5	38	62.4	54.1-69.8	38	96.2	87.5-97.1	38
HH	15-13	53.2	50.8-55.9	8	44.7	40.5-48.8	9	63.2	58.1-68.7	8	60.9	61.3-66.9	6	56.7	54.5-59.2	7	61.0	57.5-64.4	7	96.6	91.9-97.8	7
TW	13-12	56.7	52.1-63.4	25	46.4	36.4-49.7	25	65.2	59.8-69.5	28	64.8	49.8-68.9	28	57.9	51.7-65.4	25	60.2	47.4-68.3	25	93.2	90.9-99.1	29
ZH	11	53.1	48.5-60.2	19	46.9	37.5-45.6	7	66.8	60.6-68.4	7	64.6	57.3-66.1	6	59.3	53.2-62.9	18	60.9	54.7-67.7	18	93.6	90.2-97.7	20
ZH	9	52.3	47.5-58.1	7	47.8	36.9-46.1	7	67.3	62.5-69.1	7	67.8	57.3-66.2	6	58.3	54.2-61.2	7	58.8	55.0-61.9	5	93.9	89.5-95.6	6
JB	10-8	50.5	45.2-55.4	41	49.6	40.5-54.9	41	71.1	65.5-81.0	41	68.6	66.6-69.6	41	58.9	54.0-67.9	41	62.4	55.3-66.9	41	90.7	84.5-94.1	41

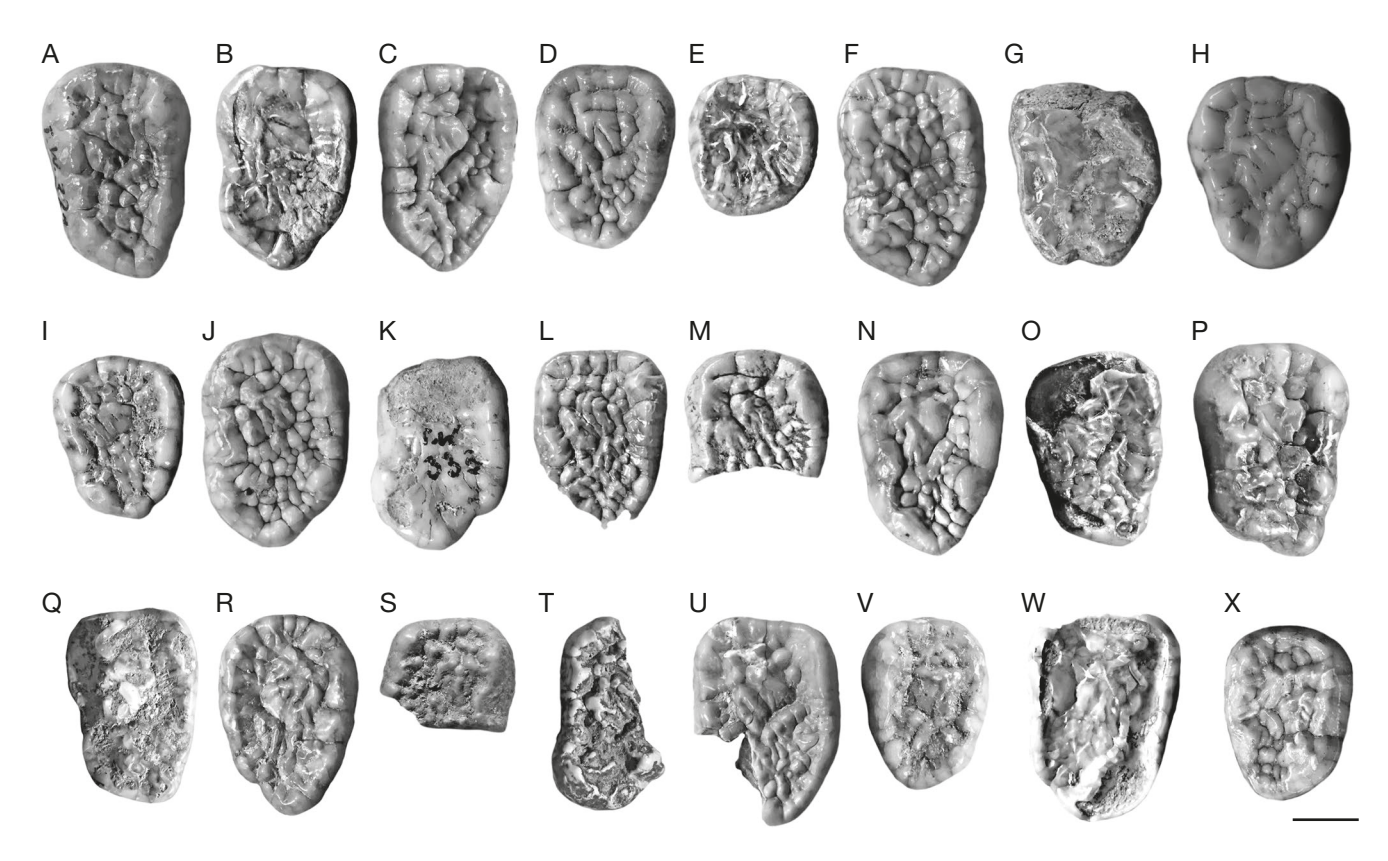


Fig. 14. — Occlusal view of m3 of Ursus deningeri hercynicus Rode, 1935 from Tunel Wielki Cave: A, MF/7177; B, MF/7178; C, MF/7179; D, MF/7186; E, MF/7188; F, MF/7184; G, MF/7584; H, MF/7187; I, MF/7182; J, MF/7183; K, MF/7580; L, MF/7581; M, MF/7580; N, MF/7181; O, MF/7189; P, MF/7185; Q, TWB 61; R, TWB 292; S, TWB 821; T, TWB 114; U, TWB 464; V, TWB 30; W, TWB 613; X, MF/7286. All teeth are figured as left specimens (C, D, N-O, R, U, V, are mir-

Table 9. — Measurements and morphological indices of m3 of Ursus deningeri von Reichenau, 1904. Abbreviations: C 718, Koněprusy C 178; HH, Hundsheim; JB, Biśnik Cave; KP, Koněprusy; KZ, Kozi Grzbiet; M2, Mosbach 2; TW, Tunel Wielki Cave; ZH, Za Hájovnou Cave.

	Age		1			2			3			2/1			3/1	
	MIS	М	Min-Max	N												
KZ	17	24.3	20.0-26.4	7	15.4	13.3-16.3	8	17.9	17.0-19.5	5	63.4	61.7-66.5	7	74.5	68.7-85.0	6
C 718	17	24.2	20.3-26.3	14	14.6	12.9-17.3	13	18.8	15.9-21.4	14	60.3	63.6-65.8	13	74.1	65.9-81.2	13
KP	17	25.1	22.5-28.0	20	15.5	13.5-18.4	20	18.1	16.2-21.7	21	61.8	60.0-65.7	20	71.2	63.8-79.9	20
M2	15-13	23.8	19.8-29.6	6	14.3	11.8-16.4	6	17.5	15.1-20.4	6	60.1	55.4-65.6	6	73.2	62.6-83.9	6
HH	15-13	24.6	23.8-25.7	8	15.2	13.2-16.9	7	18.2	16.6-19.9	6	61.8	55.6-65.8	7	73.6	67.9-83.6	7
TW	13-12	23.8	19.3-26.9	22	15.2	12.9-18.6	26	15.2	12.7-17.3	21	59.6	55.7-64.1	22	73.2	66.3-89.8	21
ZH	11	25.2	22.8-29.4	16	14.9	12.4-18.7	15	18.5	17.0-20.5	17	59.2	54.4-63.6	15	72.7	61.6-88.3	15
ZH	9	24.3	23.2-25.2	4	15.4	13.1-17.4	6	17.6	16.9-18.2	4	59.4	56.5-69.1	4	72.1	70.2-73.7	4
JB	10-8	24.9	21.6-29.9	29	15.1	13.7-17.4	29	18.4	15.8-21.5	29	58.7	56.7-63.4	29	74.4	66.9-79.9	29

POSTCRANIAL MATERIAL

Long bones of *U. deningeri* from TW are numerous but preserved only as fragments and do not give any reliable information. Similarly, differential carpals and tarsals are mostly damaged and represent moderately large and quite robust animals. Among 73 metapodials, only 24 specimens are complete enough to take most of the measurements, including the total length (Table 10). Even more numerous phalanges, with the total of 75 (41 ph 1, 16 ph 2 and 18 ph 3), mostly complete, belong, however, to not fully immature animals, and their biochronological or taxonomical validity is restricted (Table 10). Phalanges of fully adult

specimens, similarly to long bones, also represent large and robust animals. Among elements of the postcranial skeleton, the most valuable information came from metapodials, which were also commonly found in TW.

Metrically, the metapodials from TW resembled those from the group 1 (MIS 19-13) and the group 2 (MIS 11-9). Their size falls within the size variability of equal bones, while K-index and P-index are variable. Sometimes, these indexes for the TW material are higher, smaller or comparable, therefore it is not possible to find one general trend (Table 10). A more in-depth statistical analysis was omitted because of the small number of metapodial bones. Concluding analysis

Table 10. — The means of the total length (L), K-index (KI, counts as the smallest shaft breadth to the total length) and P-index (PI, counts as the breadth of the distal epiphysis to the total length) of metapodials of *Ursus deningeri* von Reichenau, 1904, and *Ursus spelaeus ingressus* (Rabeder, Hofreiter, Nagel & Withalm, 2004) from Gamssulzenhöhle (GS) as a standard. Abbreviations: EH, Einhornhöhle (Athen 2007), JB, Biśnik Cave, layers 19ad-19; HH, Hundsheim; M2, Mosbach 2; TW, Tunel Wielki Cave; UD, Urdhöhle; ZH, Za Hájovnou Cave (Musil 2005).

		TW	НН	EH	M2	UD	ZH	JB	GS
Mc 1	L	61.1 (2)	63.4 (13)	60.2 (40)	59.4 (2)	62.8 (13)	59.1 (9)	58.3 (5)	63.5 (54)
	KI	7.8 (2)	7.4 (11)	8.6 (34)	6.2 (2)	7.7 (13)	8.6 (9)	7.9 (5)	7.4 (54)
	PI	30.7 (2)	28.8 (12)	30.1 (40)	27.0 (2)	28.8 (13)	27.1 (8)	30.2 (5)	30.2 (54)
Mc 2	L KI PI	70.0 (2) 6.1 (2) 31.3 (2)	73.4 (11) 7.2 (9) 31.1 (10)	73.7 (39) 5.5 (30) 31.3 (36)	67.8 (1) 29.0 (1)	73.2 (10) 6.4 (8) 31.3 (8)	72.7 (7) 5.9 (7) 26.3 (7)	74.4 (4) 7.0 (4) 32.9 (4)	73.7 (58) 7.6 (58) 34.2 (58)
Mc 3	L	74.8 (5)	78.9 (9)	74.9 (36)	70.8 (3)	76.8 (9)	76.1 (11)	79.4 (6)	79.8 (64)
	KI	6.8 (4)	7.1 (6)	6.6 (24)	5.5 (2)	6.7 (9)	6.4 (10)	6.8 (6)	8.3 (64)
	PI	30.2 (5)	29.4 (9)	30.3 (29)	28.9 (3)	29.6 (9)	25.2 (11)	32.1 (5)	33.1 (64)
Mc 4	L	75.5 (2)	77.2 (12)	78.5 (35)	73.6 (2)	76.5 (14)	79.4 (2)	77.2 (7)	83.6 (52)
	KI	6.1 (1)	7.2 (9)	7.6 (32)	5.8 (2)	6.9 (13)	7.2 (1)	7.6 (9)	8.9 (52)
	PI	28.6 (2)	30.1 (8)	31.1 (35)	29.9 (2)	31.7 (14)	26.8 (2)	34.1 (9)	33.6 (52)
Mc 5	L	82.1 (2)	77.7 (9)	81.3 (34)	70.6 (4)	78.7 (10)	80.3 (7)	87.0 (7)	82.5 (59)
	KI	12.3 (1)	10.6 (8)	11.7 (30)	8.1 (1)	9.9 (10)	11.2 (8)	11.7 (7)	13.1 (59)
	PI	32.9 (1)	33.8 (5)	33.9 (33)	30.3 (4)	32.9 (10)	31.5 (7)	37.5 (7)	35.5 (59)
Mt 1	L	56.3 (5)	57.7 (8)	57.2 (33)	58.7 (1)	55.8 (6)	63.5 (8)	55.2 (8	53.4 (36)
	KI	10.3 (2)	8.5 (7)	10.7 (32)	8.4 (1)	8.5 (6)	9.3 (8)	12.0 (8)	11.2 (36)
	PI	29.5 (5)	29.2 (8)	30.8 (32)	26.2 (1)	28.2 (6)	24.6 (8)	33.1 (8)	33.3 (36)
Mt 2	L	64.5 (2)	65.6 (10)	65.6 (33)	63.3 (2)	65.3 (8)	75.2 (8)	56.2 (7)	67.3 (57)
	KI	4.8 (2)	5.1 (8)	5.8 (22)	4.2 (3)	4.6 (8)	6.2 (8)	6.3 (7)	5.7 (57)
	PI	30.1 (2)	28.8 (10)	29.4 (33)	28.5 (2)	29.3 (8)	25.3 (6)	34.0 (7)	31.8 (57)
Mt 3	L	71.6 (2)	72.8 (11)	74.1 (40)	69.6 (4)	72.3 (15)	73.9 (17)	74.2 (13)	77.3 (48)
	KI	7.6 (2)	6.1 (8)	7.4 (24)	5.6 (1)	6.4 (14)	6.0 (15)	7.5 (13)	8.3 (48)
	PI	28.5 (2)	27.1 (10)	27.3 (34)	25.7 (4)	25.5 (14)	24.7 (16)	28.9 (12)	30.3 (48)
Mt 4	L	80.9 (2)	81.8 (8)	82.4 (40)	83.1 (3)	81.6 (14)	80.1 (9)	82.2 (11)	86.4 (55)
	KI	6.3 (1)	7.9 (5)	8.6 (27)	7.2 (3)	6.4 (14)	6.4 (8)	7.9 (11)	7.3 (55)
	PI	24.9 (2)	25.7 (7)	27.7 (40)	27.0 (3)	26.4 (14)	24.3 (7)	30.1 (11)	29.0 (55)

of the postcranial material, because of the incompleteness of most of their elements, and not enough metapodials, the results obtained have a limited value. No substantial differences between the TW material and that from both groups were found in morphology of the postcranial bones. The variability of particular features is so high that it is impossible to establish any characteristics in this matter and should rather be treated as a case of intraspecific variability.

GENERAL REMARKS

All analyses confirmed the assignment of the described material to Ursus deningeri and showed that it resembles that recovered from the other Middle Pleistocene localities dated at MIS 19-13 like Hundsheim, Koněprusy C 178, Kozi Grzbiet, Mosbach 2, and Stránska skálá. However, we found also a set of features, which suggested a higher evolutionary level of these bones and teeth supports a younger age for TW bears, closer to MIS 13-12. Most of these characteristics were found during the study of the teeth, while postcranial bones showed a rather limited biochronological and taxonomical value. Among the most important features, there are the higher proportion of evolutionarily more advanced morphotypes, I3 with a calyx, i1 and i2 with larger and broader crowns and enlarged distoconid, P4 and p4 with morphologically more complicated crowns, M1 with a stronger developed parastyle and lingual cingulum, M2 with a narrower talon, m1 with a longer talonid, m2 with a proportionally narrower and shorter trigonid and a broader and longer talonid, and m3 with a shorter trigonid.

There is also another method to check the taxonomic position of the particular bear palaeopopulation as was shown on the material from the Early Pleistocene Austrian site Deutsch Altenburg (Rabeder et al. 2010). This grouping is based on the functional morphology attempt on two main components. The first is the strong enlargement of the cheek teeth and increased plumpness of the metapodials in spelaeoid bears. The second trend is the remaining of the ancestral cheek teeth and elongation and narrowing of the extremities in arctoid bears (Rabeder et al. 2010). The relation between the dentition and extremities can be shown best by means of the total lengths of the teeth and metapodial bones. In order to include also palaeopopulations with a low number of individuals, like in the case of metapodials from TW, the arithmetic means of all measured lengths of all cheek teeth used in this study (P4/P4, M1/m1, M2/m2 and m3) were correlated to those of the total length of all measurable metapodial bones. For this purpose, all values had to be standardised, and the means of U. s. ingressus from Gamssulzenhöhle served as a such a standard. As expected, the TW bear group is placed together with other deningeroid and spelaeoid bears on a scatter-plot (Fig. 15).

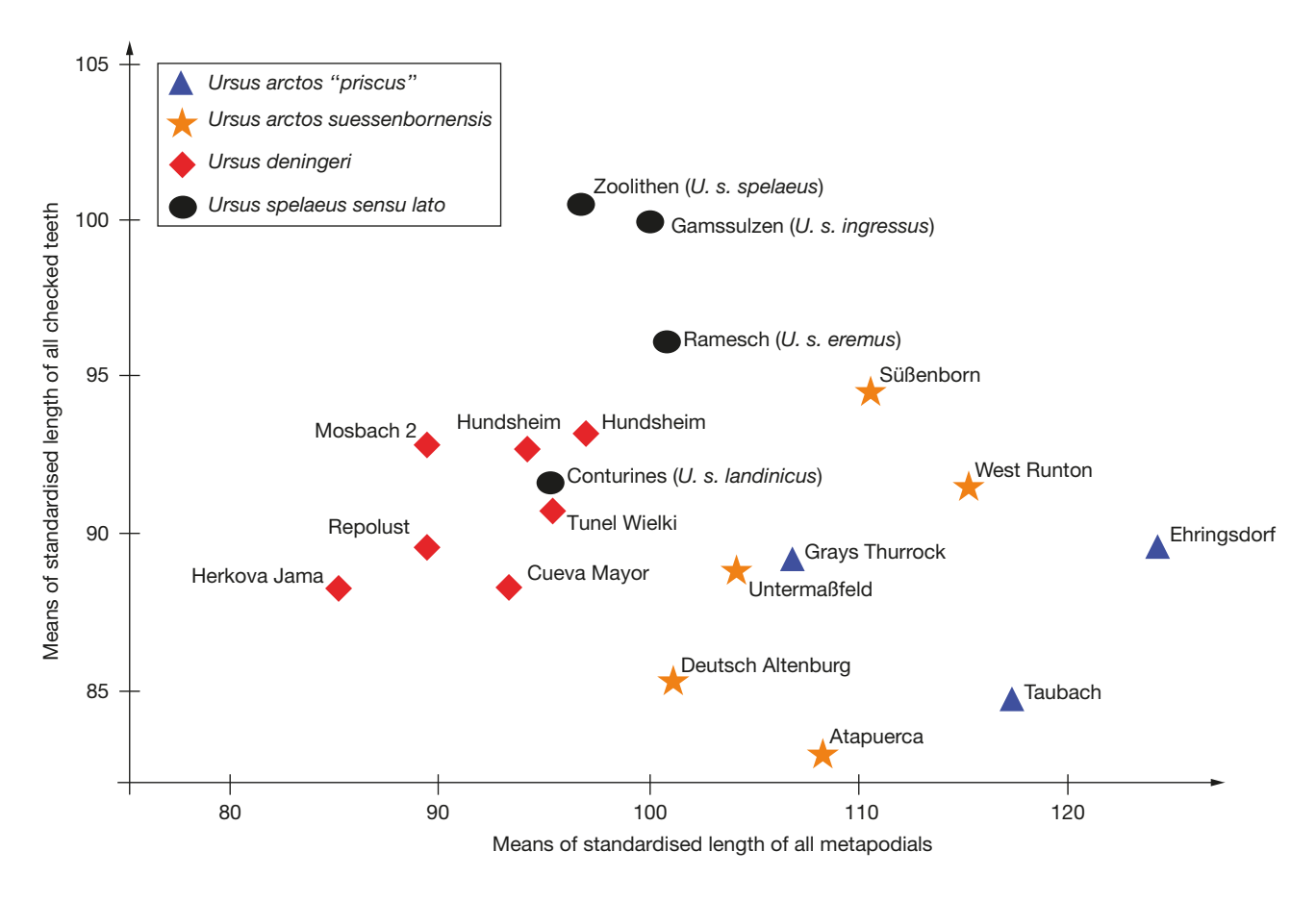


Fig. 15. — Arrangement of different species and supbspecies of the genus Ursus Linnaeus, 1758 populations ordered by tooth and metapodial measurements. The means of standardised lengths of all cheek teeth (P4/p4; M1/m1; M2/m2 and m3) and metapodial bones (mc 1-5; mt 1-5) from populations or from individual skeleton are compared according to the methodology proposed by Rabeder et al. (2010: 109-111; figs 45, 46; table 40).

Ursus sp.

Ursus cf. deningeri

REFERRED MATERIAL. — NISP 308: cranium fr., 2 maxilla fr. (1/1), mandible fr. (2/0), 20 DI/dI, 2 I fr., 139 dC, 50 dC fr., 6 c1 fr., 2 D4, 3 d4, Pm/pm fr., P4 fr., 2 M/m fr., M1 fr., 2 m1 fr., 2 humeri fr. (0/2), 5 radii fr. (4/1), 5 ulnae fr. (4/1), 5 femorae fr. (2/3), 8 tibiae fr. (2/6), fibula fr., 8 pelvis fr. (3/5), calcaneus fr., scapholunar fr., left mc 3, right mc 4, mtpd fr., 7 costae fr., atlas fr., ² cervicale fr., 8 thoracic fr., 2 lumbar fr., 2 vertebra fr., 7 ph 1, 4 ph 2, ph 3 (Appendix 1).

DESCRIPTION

Numerous cranial and postcranial skeletal elements of bears were recovered from TW. Most of them are the remains of neonate or juvenile specimens and milk teeth, but there are also bone fragments belonging to adult individuals. Considering the percentage of the remains of *U. deningeri* and *U. arctos*, the overwhelming number of these bones can be classified as belonging to *U. deningeri*. However, the lack of clear diagnostic features does not allow attributing these remains to *U. deningeri* with confidence. For this reason, we decided to put these remains into the group of *Ursus* cf. deningeri/Ursus sp.

The analysis of the age structure based on the dentition and postcranial skeleton does not quite correspond to expectations from the TW fauna. In addition to the 0-4 month and 12-14 months juveniles died in winter storage, there is a relatively large group of 7-9 month-old bears that apparently died in the den in summer or autumn. The causes of their deaths are unclear. These young bears might have been killed by carnivores and dragged into the den. Biting marks on the bones are rarely observed, so death by a carnivore attack can only be rarely documented (e.g. Marciszak et al. 2024). In such cases, however, biting of the bones does not necessarily have to be visible. Hunting by humans can neither be proven nor disproved. It is also possible that young died very late, e.g. March instead of January. Then they would already go into hibernation at the age of 7-9 months and have not survived the winter due to a lack of sufficient fat reserves (Marciszak et al. 2024). In general, most juvenile bears died in TW were younger than one year. There are significantly fewer finds of 2-3-year-old bears. Compared to the data from the extant *U. arctos*, where it states up to 50% mortality for yearlings (Swenson 2000), the age distribution is relatively normal. In the following two years, the mortality rate is lower and increases again strongly in the case of 3-4-year-old bears that have just became independent. For adult *U. arctos*,

a comparatively low mortality rate of 15% was established (Wittenberg & Wenzelides 2000). This corroborates relatively well with the age data obtained for the TW palaeopopulation. The causes of death in adult animals are very variable. Some of the bears from TW certainly died during the hibernation due to insufficient fat reserves or because of diseases. Some bear individuals may have also fallen as prey to other carnivores. If one assumes that the found age structure really reflects the use of the cave, then the TW seems to have been visited by adult bears, and numerous finds indicate a frequent stay or a higher death rate in the cave. This cave was used by cave bears as a hibernating den.

Ursus arctos taubachensis Rode, 1935 (Fig. 16)

REFERRED MATERIAL. — Among 954 ursid remains from TW, five specimens were determined as belonging to *U. arctos*: a single fragment of the right maxilla with a strongly worn M1 and mesial part of the zygomatic arch (MF/7547, layer K1); one left C1 (MF/7560, layer M2); one crown of the left M2 (TW 825, layer K1); one left, slightly damaged talus (MF/7515, layer O); and one right, slightly damaged talus (MF/7517, layer O).

EMENDED DIAGNOSIS. — About the size of Ursus arctos middendorffi or larger; flat and elongated forehead; large and massive incisors and canines; P1-P3 present; broad and large P4 often with additional cusplets, expanded paracone and enlarged protocone; p1 and p3 usually present; broader and more quadratic in occlusal view M1 with larger paracone and metacone, strong lingual cingulum collared maximally from mesial wall of the protocone to the distal wall of the hypocone and large surface of the inner talon field filed with grooves, lines and additional small cusplets; large and wide M2 with particularly broad and expanded trigon and broad and elongated talon, high and large paracone with strong developed grooves and ridges on their lingual wall, present metastyle and posthypocone, moderately developed distal cingulum, large surface of the inner talon field filed with grooves, lines and additional small cusplets and lingual cingulum reaches maximally after the hypocone; large and robust m1 with blunt mesial margin, double or triple metastylid, double or triple entoconid with their size decreasing significantly mesially, moderately to strong developed enthypoconid; robust m2 with the talonid wider than the trigonid, inner surface of trigonid with moderately to strong developed grooves and ridges, simple metastylid complex, moderately to strong developed enthypoconid; particularly large and broad m3 with mesolophid runs lingually and parallel to the metalophid, single enthypoconid, enthypoconid-hypoconid connection of the centrolophid, entoconid developed in the form of a serie of additional cusps on the lingual edge divided by transverse grooves, inner surface of talonid with moderately to strong developed grooves and ridges; massive metapodials with particularly robust shafts and distal epiphyses (Rode 1935; Baryshnikov 2007).

DESCRIPTION

The complete C1 (MF/7560) metrically (L – 22.74 mm, B – 16.56 mm) falls into the size variability of males and females of *U. deningeri*, therefore it is impossible to recognise the species based on the measurements alone. On average, canines of spelaeoid bears are more robust, and size ranges of bears from arctoid and spelaeoid lineages actually overlap, if we take into consideration *U. a. taubachensis* (Marciszak *et al.*

2019b). In addition, this is regardless of whether we compare not-sexed groups or take into consideration temporarily and sexed populations. Because of the great sexual dimorphism, when comparing different populations from different time periods, the best way is to compare males and females separately. Pleistocene and especially Holocene inidividuals of *U. arctos* are smaller than spelaeoid bears. However, among them there are many large individuals matched or even exceed the size of large individuals of *U. deningeri*. In the case of the canine from TW, it is rather of moderate size, comparable with those in adult males of extant *U. arctos* from Central Europe. The assignation as male canine is confirmed also by a thickened root, the bulging state of which, however, is far away from the massive roots of *U. deningeri*. The tooth is relatively short compared to more elongated and narrower crown in spelaeoid bears; this argument also supports the assignation of the specimen to this species.

The single M2 (TW 825) is a large and broad tooth (1 – 45.56 mm, 2 - 15.74 mm, 3 - 12.79 mm, 4 - 24.56 mm,and 5 - 22.45 mm). Its morphology corresponds well to the size and shape of the M2 of U. a. taubachensis (Fig. 16). An elongated and rectangular M2 has expanded and broad trigon, and elongated and rather wide talon, narrowing gently distally. The rounded and moderately high paracone is placed far from the metacone and separated from it by a shallow and wide valley. Its mesial ridge is in contact with the mesial ridge of the protocone and is characterised by the development of an additional side branch running on the mesio-lingual slope of the parastyle, but not reaching the base of this cusp. In addition, the mesial ridge of the parastyle formed a group of 4-5 cusplets like structures that collared the mesial wall of the trigon (B2). The mesostyle complex is formed by the distal slope of the paracone and the mesial slope of the metacone (B2). The distal arm of the paracone is strongly curved cerntrally, that it lost connection with the mesial arm of the metacone and forms a separate arch. A few pillars, running from the base of the cusp and maximally reaching the half of its height, are situated on the internal wall of the paracone. In the metaloph complex, the metacone and the protocone are not directly connected, a few small cusplets occur between them, and the distally situated hypocone is developed in a double branch (B3). The posteroloph is developed as S-shaped, curved line, formed by a few low and small cusplets running between the metastyle and the hypocone. The entire talon field is covered by numerous small cusplets, which form two regular grooves (B/C). The talon field is collared by a thick wall of the distal cingulum, which forms numerous small cusplets (B). The metastyle and posthypocone are present but weakly developed as small and low cusps. A few pillars reaching the half of the height of the internal wall of the protocone are running from the base of this cusp. The lingual cingulum shows a relatively high evolutionary stage, running through the base of the protocone and terminating between the hypocone and the posthypocone.

Both tali are almost completely preserved, only in the distal-medial part a small piece of the bone is missing, which approximately corresponds to the distal process (Fig. 16).

262

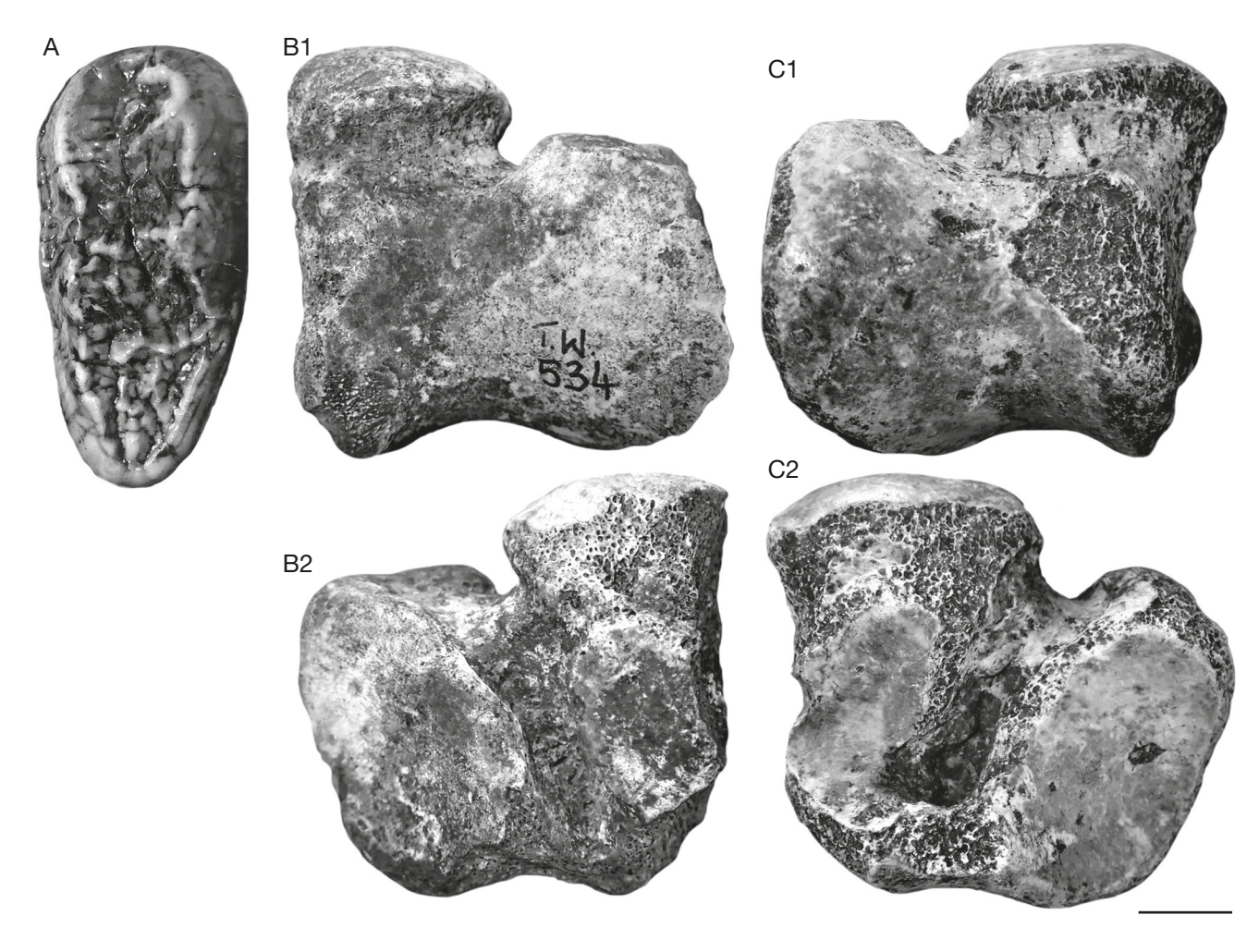


Fig. 16. — Material of Ursus arctos taubachensis Rode, 1935 from Tunel Wielki Cave: A, left M2 (TW 825, occlusal view); B, right talus (MF/7517); C, left talus (MF/7515). Specimens B and C: 1, proximal view; 2, plantar view. Scale bar: 10 mm.

A significant feature distinguishing arctoid and spelaeoid bears is the development of the sulcus tendinis musculi flexoris hallucis longi (Rabeder et al. 2010). In both tali, this measurement cannot be made out quite accurately because of partial damage. In *U. deningeri*, this sulcus is almost twice as wide as in U. a. arctos (Rabeder et al. 2010). In the TW specimens, the sulcus seems to have a similar dimension as in U. a. arctos, but due to the fracture face on the medial edge, this cannot be said with sufficient certainty. The lateral edges of the trochlea run almost parallel, as in *U. a. arctos*. In *U. deningeri*, the medial edge runs sloping from mediodistally to lateral-distally and forms a steep angle with the expansion of the lateral edge (Fig. 16). The inclination of the medial edge of the trochlea is connected to the sprain of the distal epiphysis of the tibia (Mottl 1940; Rabeder et al. 2010). The specimens considered are also smaller than those of *U. deningeri* (MF/7515: 1 – 49.74 mm, 2 – 42.24 mm; MF/7517: 1 - [est. 49.50 mm], 2 - 43.09 mm.

COMPARISON AND REMARKS

The material of *Ursus arctos* from TW is represented only by five specimens, but of great taxonomic value. Among them, the robust M2 is especially noteworthy and documented

the early presence of *U. a. taubachensis* in Europe. The specific cranial and dental characters of many Late Pleistocene brown bears, especially from periglacial areas, cannot be disputed. There is given a good evidence from Central and East Europe to north Siberia (Musil 1964; Ballesio 1983; Baryshnikov & Boeskorov 2005; Marciszak et al. 2019b) that the bears from the Last Glacial were characterised by a unique combination of characters, unknown in extant representatives of this species. The problem is that, with exception of some Eemian sites (e.g. Taubach in Germany, Dziadowa Skała in Poland or Chlupáčova sluj in the Czech Republic), the Late Pleistocene record of brown bears is rather fragmentary not allowing characterising sufficiently the population variability. We therefore decided to leave open the question of the taxonomic status of Late Pleistocene bears, and used informal taxa for describing the morphological characters of the specimens studied. We use the term *U. a. taubachensis* for a large form corresponding to the traditional concept of 'U. a. priscus' (leaving aside the fact that these phenotypic characteristics do not fit the holotype of *U. a. priscus* itself). *Ursus arctos arctos* is restricted to the European Late Pleistocene brown bears, identical to the recent, nominotypical subspecies *U. a. arctos*.

DISCUSSION

The results obtained for bear palaeopopulation from TW are corroborated with general evolutionary trends documented within the MIS 19-9 time interval and are the important source of knowledge about these changes within the Central Europe (Wiszniowska 1989; Wagner 2004, 2005b, 2010, 2014). Most of the features show low or insignificant time-dependent differences and trends or they were effectively diluted by a considerable variability. This is well documented in the P4 and p4 analysis, where the higher amount of more advanced morphotypes was found in comparison with the group 1 (MIS 19-13). However, no substantial differences in indices (e.g. B/L) have been found. Naturally, the absence of distinguishing metric characters and values does not mean that there is no morphological differentiation but it suggests that those hypothetical morphological changes and trends do not reach a high enough level to exceed the interpopulation and intraspecific metric differences (Wagner 2014).

Comparison of the mean values of the TW metrical and morphological features with respect to both biostratigraphic group 1 (MIS 19-13) and group 2 (MIS 11-9) recognised the differences between them. It is also documented the intermediate position of the TW palaeopopulation, closer to the group 1 (MIS 19-13) with many deningeroid characteristics, but already with some advanced (i.e., spelaeoid) features. The most notable evolutionary trends to be found included, among others, an advanced molarisation correlated with an increase in broadening of the cheek teeth (Rabeder 1983, 1989; Wiszniowska 1989; Wagner 2004, 2005b, 2010, 2014). It is well documented in the higher proportion of evolutionary more advanced morphotypes in all teeth and more complicated occlusal surface of P4, M1, M2/p4, m1, m2, m3. Incisors tend to have larger and broader crowns and stronger developed additional structures on the crowns, like a calyx on I3 or distoconid on i1-i2.

The M1 has a stronger developed parastyle and the lingual cingulum, and the paracone is higher than the metacone. The tendency to increase the paracone height in relation to the metacone is known (Rabeder 1983, 1989; Wiszniowska 1989; Wagner 2004, 2005b, 2010, 2014). This tooth is traditionally used for distinguishing U. deningeri, U. spelaeus and *U. arctos*. The spelaeoid (typical for *Ursus* gr. *spelaeus*) features are the increasing in size and percentage of the teeth with the paracone higher and longer than the metacone and the mesial lobe broader than the distal one (Rode 1931, 1935; Kurtén 1959; Rabeder 1983, 1989; Wiszniowska 1989; Wagner 2004, 2005b, 2010, 2014). Among the specimens from Mosbach 2 (MIS 15-13), the paracone higher than the metacone was found in 41% teeth, in Za Hájovnou Cave it varies between 70 and 80%, and it equals 72% in TW. A tendency for the talonid to lengthening was found, but it does not increase in a linear pattern, since L ta/L tr in Kozi Grzbiet is 102.8, in TW is 105.1, in Hundsheim is 106.9, and is 109.1 in Za Hájovnou Cave. Simultaneously it is 107.9 in Mosbach 2 and 106.2 in the layers 19a-d in Biśnik Cave (Table 5). A trend towards increasing the width was also found, although the differences found are quite minor, but the trend is noticeable (Table 5).

In the evolution of the M2, the most noticeable trend is the increase in size of the tooth and the widening of its crown. It can be easily traced from Kozi Grzbiet (L M2 – 39.7 mm) and Stránska skálá (40.8 mm) (MIS 19-17), through TW (41.6 mm, MIS 13-12), Za Hájovnou Cave (42.3 mm, MIS 11) up to layers 19a-d in Biśnik Cave (42.9 mm, MIS 9-8) (Table 6). The increase broadening of the M2 crown is primarily related to the enlargement of the trigon, which is well documented by two indices. A significant increase in the paracone length in relation to the metacone length was found. In the L me/L pa ratio, the M2 from TW (58.3) is placed within the group 2 (MIS 11-9) and away from the group 1 (MIS 19-13). The second index (B ta/B tr), showing the broadening of the trigon, is even stronger marked, with a constant increasing tendency (Table 6). In respect to the B ta/B tr index, the TW population shows intermediate values between the groups dated on MIS 19-13 and MIS 11-8 (Table 6).

Concerning the maximal length of the m1, no substantial clinal changes has been found between the groups. The L m1 from the group 2 (MIS 11-9) is slightly higher than that of the gropu 1 (MIS 19-13) and TW. A tendency to widening the talonid was noted for the m1 (Rabeder 1983, 1989; Wiszniowska 1989; Wagner 2004, 2005b, 2010, 2014), but our analysis only weakly supported that (Table 7). Contrary, a clear tendency to the increase in the talonid length was found, where B ta/B tr index increasing from Kozi Grzbiet (59.4) or Stránska skálá (61.7) through Mosbach 2 (61.7), Hundsheim (62.5) up to Za Hájovnou Cave (65.1) and layers 19a-d in Biśnik Cave (69.7). In the value of this ratio (64.6), the TW population is closer to within the group 2 (MIS 11-9) than the group 1 (MIS 19-13) (Table 7). The significance of the height and length of both entoconids or their complexes respectively is questionable. There was noted a trend for an increase in spelaeoid characters manifesting itself in the increase in size of the entoconid 2 relative to the entoconid 1 (Rabeder 1983, 1989; Wiszniowska 1989; Wagner 2004, 2005b, 2010, 2014). In the material younger than 0.6 mya, there are no specimens without the entoconid 2 (Wagner 2014). In the TW population, the m1 have sometimes double (n = 7), the most often triple (n = 19), and even quadruple (A4, n = 4) entoconid. This documented the age younger than 0.6 mya, and relatively high evolutionary level indicate age closer to the group 2 (MIS 11-9) than the group 1 (MIS 19-13).

The average values do not show apparent tendency towards an increase of the maximal size, where the oldest sample from Kozi Grzbiet (L 29.3 mm) is among the largest, while the m2 from younger Mosbach 2 (L 26.9 mm) and especially Za Hájovnou Cave (L 27.8 mm) are among the smallest ones (Table 8). The TW palaeopopulation is also among small-sized m2s (L 27.6 mm). There was found a general tendency to lengthening and broadening of the m2 talonid (Table 8). In both indices, L ta/L tr and B ta/B tr, the TW population grouped with the group 2 (MIS 11-9) than the group 1 (MIS 19-13). The values obtained for both

264

ratios are almost the same as those for Za Hájovnou Cave (MIS 11), and differ from those dated on MIS 19-13. The higher values of this index of the group 2 (MIS 11-9) ursids probably reflect a more open crown compared to the group 1 (MIS 19-13) (Wagner 2014). The occlusal surface of the m2 from TW is also more complicated, which is especially well documented in the stage of developing the metalophid and mesolophid complexes. A tendency to broadening and lengthening the talonid has also been documented from other European sites (Rabeder 1983, 1989; Wiszniowska 1989; Wagner 2004, 2005b, 2010, 2014).

Contrary to other cheek teeth, the m3s do not show such well-expressed, progressive features when compared the specimens from TW with those from older populations. Linear dimensions of the m3 from TW are among the smallest, and identical to those from Mosbach 2 (L 23.9 mm) (Table 9). There is no apparent tendency towards an increase in the average values of the maximal size or width from the group 1 (MIS 19-13) to the group 2 (MIS 11-9). In the L ta/L tr ratio, the TW palaeopopulation is grouped with the group 2 (MIS 11-9) and away from the group 1 (MIS 19-13). In addition, the occlusal surface of the m3 shows to be more complicated than that of populations from the group 1 (MIS 19-13) (Table 9).

In order for the examined dentognathic material to be useful in such analyses, the study of the postcranial material was also performed. It must meet several specific criteria: 1) they must be found in numbers that allow for statistically reliable results; 2) in the case of the postcranial skeleton, these should not be elements that are too heavily covered with a muscular layer, which can significantly affect their massiveness and the occurrence of deformations; and 3) their morphology should be characterised by the presence of easy-to-define and measurable features. Long bones are an example for this type of remains, but usually a relatively small number of complete specimens limits their usefulness. In turn, vertebrae and ribs, occuring in large numbers, are usually omitted due to their morphology, which makes it difficult to select points that are easy to identify and measure. In addition, they are most often incomplete to some extent, which hinders the possibility of using them as a material for analyses. The biggest problem with the eight wrist bones (scaphoid, semilunar, triquetral, pisiform, trapezium, capitate, hamate) and seven foot bones (talus, calcaneus, cuboid, three cuneiforms, and navicular) is their highly diverse morphology, which complicates the definition of easily recognisable and measurable points. Paradoxically, these bones, due to their massive structure, are usually preserved in a complete state. At the same time, their number at a given site is usually subject to large fluctuations, and their diverse morphology does not facilitate the analysis. The phalanges, which are among the most numerous and best-preserved elements of the postcranial skeleton and which are also characterised by a fairly uniform structure, seem to be ideal bones for such type of analysis. However, morphological changes observed on them practically do not correlate with evolutionary changes over time. In addition, the extremely high percentage of undergrown individuals

among the palaeopopulations from Sudeten caves significantly complicates or even prevents such analyses. Despite the existence of these facts, an attempt was made to examine their usefulness in these analyses.

In the metric analyses of the evolution of cave bears, three values based on metacarpals and metatarsals are the most important. Those are the total length of the bone and two coefficients, namely the width of the shaft to the total length (PI index) and the width of the distal epiphysis to the total length (KI index). Despite the relatively large number of analysed European sites yielding the *U. deningeri* remains, it was only in the case of the material from Einhornhöhle, Hundsheim, Urdhöhle, and, to a lesser extent, Za Hájovnou Cave and Biśnik Cave (layers 19ad), that it was possible to analyse these parameters for all complete metacarpals and metatarsals. Since all metapodials except for mt 5, are represented in the TW material, it was possible measurements to be made.

However, with the exception of mc 5 and mt 1, where five specimens were measured, the number of all the remaining specimens is only two. Although even single specimens from a given site show a certain trend, especially if individual bones show a similar set of features compared to other populations, they absolutely do not reflect the full variability. Frequency plays a role in the analyses of metapodials, and with such a relatively low sample sizes, it is quite easy to overinterpret or overemphasise individuals with dimensions significantly below or above the average, which automatically translates into a decrease or increase in the average values. In the case of these analyses of *U. deningeri*, where the ranges of variability largely overlap and the basic value used in them is the average, this is extremely important. For this reason, in the analyses below, concerning individual bones, only the palaeopopulations from Einhornhöhle, Hundsheim, Urdhöhle, Za Hájovnou Cave and Biśnik Cave (lavers 19ad-19) can be treated as those whose values and coefficients obtained on their basis provide a picture of the full population variability. In the case of the *U. deningeri* material from TW, similarly to the teeth from this site, they were also subjected to analysis. However, their low sample size and the related interpretational limitations were noted. In most values, metapodials from TW stay closer to the group 2 (MIS 11-9) than to the group 1 (MIS 19-13). Similar results for *U. deningeri* were obtained by Schütt (1968), Feustel et al. (1971), Musil (2005), and Athen (2007). Even despite the comparison, especially of the postcranial material, was based on a limited number of localities and specimens, some of the results appear to be of interest and may be generally valid for *U. deningeri*:

1) The teeth and metapodials are most suitable for morphodynamic analyses. The most valuable are the premolars (P4/p4) and molars (M1/m1, M2/m2 and m3) followed by the incisors (i1, I2/i2 and I3/i3) with the I1 thread. The remaining teeth, i.e. the canines (C1/c1) and additional premolars (P1/p1, P2/p2 and P3/p3) are not useful in morphodynamic analyses. Some usefulness, but limited due to, among other elements, their relatively rare occurrence, is also demonstrated by skulls. The remaining skeletal elements are useless in such analysis.

- 2) In the evolution on the incisors, an increase in size, broadening the crown and complexity of the morphology of the mesial and chewing surfaces, consisting in the production of additional cusplets and structures is observed.
- 3) In the evolution of the P4/p4, there is observed a significant increase in the broadening of the crown and the degree of complexity of the crown surface through the development of additional cusplets and structures.
- 4) In the evolution of the M1, an increase in dimensions, development and gradual strengthening of grooves and edges on the inner walls of the main cusps (paracone, metacone, protocone, mesocone, and hypocone), an increase in the size of the parastyle, which became more strongly separated from the rest of the crown, an increase in the length of the lingual cingulum and an increase in the degree of complexity of the occlusal surface of the talon through the development of numerous grooves, small cusplets and additional edges.
- 5) Due to the active role played in grinding food, the M2 morphology underwent the most significant changes among the upper dentition. There was an increase in the dimensions and mass of the M2, the development and gradual strengthening of grooves and edges on the inner walls of the main cusps (paracone, metacone, protocone and hypocone), an increase in the size of the parastyle, which became more strongly separated from the rest of the crown, an increase in the length of the lingual cingulum and an increase in the degree of complexity of the talon occlusal surface through the development of numerous grooves, small cusplets and additional edges. Additional structures (e.g. metastyle, metaloph, and posteroloph) are also developed and gradually strengthened.
- 6) In the evolution of the m1, the development of a metastyle located mesially to the metaconid, a doubling number of entoconids, the development of an enthypoconid and their gradual differentiation into 2-3 cusps, the development and gradual strengthening of edges on the inner wall of the entoconid, development of a mesoconid on the distal edge of the protoconid and the medial edge and strengthening the distal edge were noted.
- 7) In the evolution of the m2, an increase in the broadening the crown, development and gradual strengthening of structures (edges, grooves) on the surface of the hemitrigonid and talonid, development and multiplication of the metalophid, metastylid, mesolophid, entoconid, enthypoconid and hypoconid were noted.
- 8) Of all molars, m3 shows the greatest variation in the outline of the crown in the occlusal view. In the evolution of the m3, an increase in the dimensions and broadening, changes in the shape of the crown, development and gradual strengthening of the edges of the protoconid, structures on the metaconid, hypoconid, centrolophid, entoconid and talonid field were noted, along with an increase in its complexity.
- 9) Analysis of the metacarpals and metatarsals showed an increase in their size and mass, especially in the shaft and distal epiphysis.
- 10) Cave bear remains are difficult to interpret. Despite the abundance of often well-preserved material, the features differentiating them are poorly expressed. Many of them are

characterised by a strong anatomical conservatism and their separation based on these features in a binary approach is very difficult or even impossible. These features are very rarely developed in the absence or presence of some structure or its characteristic shape, which would allow for unambiguous distinction of particular chronosubspecies. However, they usually develop gradually, and the degree of their variability is expressed rather in changes in proportions or shape. The interpretation of these changes is often ambiguous based on subjective view and/or comparative sample. Even with extremes, e.g. minimum and maximum development of a given feature when comparing two individuals from a given population. This is well illustrated by the example of the analysis of changes in skull morphology.

Ursus deningeri was an animal characterised by a long growth period, up to 6-7 years for 99 and even 13-14 years for $\partial \partial$, comparable to extant large subspecies of brown or polar bears. The degree of development of a given diagnostic feature depends on the individual's age and is additionally subject to convergence. The degree of verticalisation and development of the frontal part, which increases with age and is much more strongly expressed in $\partial \partial$ than in QQ. This feature changes not only during ontogenetic but also phylogenetic development. It is one of the bases on which many authors distinguish or divide cave bear material in a given profile or site. In such a system, the frequency of a given feature may be rather an expression of intraspecific variability and the basis for designating chronosubspecies in the fossil material than separate species, which was often postulated by earlier authors. In the case of *U. deningeri* studies, metric indices should be calculated based on a representative and sufficiently large sample, for which there is certainty that they come from a given chronosubspecies. It is more difficult to determine whether they come from a given sex. While in the case of the skull, mandible, long bones or some tarsal bones, such as the calcaneus, it is possible to determine the sex of the individual with a high degree of probability, in the case of the metacarpal or metatarsal bones it is a difficult task. It is known that extreme adult individuals most likely represent different sexes, minimum \mathcal{P} and maximum \mathcal{P} . However, in this work, the range of variability that would allow for distinguishing two sexes was not captured, and the division of metacarpals or metatarsals into sexes is omitted. This process still requires correlating the dimensions of the fossil material with large subspecies of the modern brown bear and comparing them with series with a determined sex. This will allow us extrapolating the results and attempt to distribute these bones in a given population. Considering all the data presented above, the remains of deningeroid ursids from TW were classified as Ursus deningeri hercynicus Rode, 1935 sensu Baryshnikov (2007). The detailed analysis of the palaeopopulation shows their intermediate morphodynamic position between the group 1 (MIS 19-13) like Kozi Grzbiet, Stránská Skála, Koněprusy C 718 Cave, Hundsheim, Mauer, Mosbach 2, Urdhöhle and the group 2 (MIS 11-9) populations like those from Einhornhöhle, Vértesszőlős 2, Za Hájovnou Cave, Draby, and layers 19ad-19 of the Biśnik

Cave. This chronosubspecies was described as medium-sized, with common P3 and triple entoconid on m1, the occurrence of which covered a timespan between MIS 12 and 7 (Baryshnikov 2007). In the overhelming number of features, the TW material represents a higher evolutionary level than the nominotypical chronosubspecies *Ursus deningeri deningeri* (von Reichenau, 1904), known from the group 1 (MIS 19-13). It was determined as a large form, with often reduced P1-P3/ p1-p3, broad P4 and the double entoconid on m1, which occurs in MIS 17-12 (Baryshnikov 2007). The morphodynamic analysis performed also corroborates this statement.

Ursus deningeri was a permanent member of the Middle Pleistocene palaeoguilds and ancestor to spelaeoid ursids, the most common large carnivore between MIS 7-2 (Baryshnikov 2007; Wagner 2010). Its extrtaordinary geographical range was spatially restricted to Eurasia (England to China) and temporarly between 1.1 and 0.3 mya (von Reichenau 1904, 1906; Zapfe 1948; Heller 1975; Prat & Thibault 1976; Kurtén & Poulianos 1977, 1981; Azzaroli et al. 1986; Tsoukala 1991; Argant & Argant 2002; Baryshnikov 2007; Wagner & Sabol 2007; Argant 2009; Ghezzo et al. 2014; Madurell-Malapeira et al. 2009; Wagner 2010; Jiangzuo et al. 2018; Stefaniak et al. 2022). The evolution of deningeroid = > spelaeoid lineage was characterised by the increase of body size and cheek-teeth complexity (Wagner 2010, 2014; Marciszak & Lipecki 2020). The evolution of spelaeoid bears from deningeroid forerunner is differently dated from European sites, with the possible earliest appearance of *U. spelaeus s.l.* noted from the English site Swanscombe already during MIS 11 (Kurtén 1959; McFarlane et al. 2011). This British records is, however, highly uncertain, since the sample is too small to allow a clear distinguishing between *U. spelaeus* and derived *U. deningeri*. These differences should be based on population characteristics, not on one or a few individuals. The more appearance of this species from the most territory of Europe took place later, and generally it is acceptable that U. spelaeus s. l. appeared during MIS 7 (Rabeder 1999; Argant & Argant 2002; Hilpert 2006; Baryshnikov 2007; Argant 2009; Marciszak et al. 2023).

The occurrence of Ursus arctos taubachensis in TW is also notable. Firstly, the Middle Pleistocene records of this species in Europe are scarce and their evolutionary history remains poorly known. From 0.9-0.8 mya, there are also known some arctoid ursids (Soergel 1926; Jánossy 1963; Ambros et al. 2005; Baryshnikov 2007; Wagner & Sabol 2007; Rabeder et al. 2010; Wagner 2010). The species became more common and widespread in Eurasia since MIS 15 (Moigne et al. 2006; Jiangzuo et al. 2018; Marciszak et al. 2019b; Conti et al. 2021; Villalba de Alvarado et al. 2022). The oldest Polish record of *U. arctos* comes from Kozi Grzbiet and Południowa Cave (0.8-0.7 mya) (Marciszak & Lipecki 2020). Early and mid-Middle Pleistocene specimens were described as small or at least medium-sized individuals, comparable metrically to the extant *U. a. arctos* (Wagner 2010; Rabeder et al. 2010; Marciszak & Lipecki 2020). However, since MIS 12, the long period of cold and continental climatic conditions between 480 and 430 kyr, drastically changed the Palaearctic faunal pattern (Kahlke et al. 2011; Kahlke 2014). It covered the main part of the Central European territory. Species of the Central Asian steppe origin spread into northern and western Palaearctic regions. This was a part of a longer period lasted between 0.8 and 0.4 mya, and characterised by climate changes, particularly the increasing severity and duration of cold stages, had a profound effect on biota and physical landscape, especially in the Northern Hemisphere (Maslin & Ridgwell 2005; Kahlke et al. 2011; Kahlke 2014). One of the very first faunal assemblages termed the Mammoth Fauna, associated with steppe-tundra conditions, was the fauna of Bad Frankenhausen (c. 460 kya) (Kahlke 2014). Elements of steppe and tundra origin co-occurred, and the structure of the Mammoth Fauna appeared for the first time. Similarly dated (MIS 13-12) is the fauna from Tunel Wielki Cave (Berto et al. 2021; Kot et al. 2022). Ursus arctos taubachensis also appeared in Europe roughly at the same time (Rode 1931, 1935; Musil 1964; Baryshnikov 2007; Rabeder et al. 2010; Marciszak et al. 2019b). The presence of this subspecies is regularly noted until MIS 1 (Kurtén 1956, 1959, 1968; Thenius 1956; Musil 1964; Ballesio 1983; Sabol 2001a, b; Baryshnikov & Boeskorov 2004; Pacher 2007; Rabeder & Frischauf 2016; Marciszak et al. 2016, 2019a, b, 2020).

CONCLUSIONS

The analysis of the ursid material from the Tunel Wielki Cave showed the presence of two species, Ursus deningeri hercynicus and Ursus arctos taubachensis. Abundant and well-preserved material of *Ursus deningeri hercynicus* allows to do a detailed morphometrical analysis, which can be potentially useful in the biochronological context. This material is represented by almost all skeletal elements, with the predominance of isolated teeth, metapodials and phalanges. Analysis showed that the remains of *Ursus deningeri hercynicus* from TW have had intermediate features and values between the early and mid-Middle Pleistocene (MIS 19-13) sites Hundsheim, Koněprusy C 178, Kozi Grzbiet, Mosbach 2, and Stránska skálá and those from the late Middle Pleistocene (MIS 11-9) like Einhornhöhle, Vértesszőlős 2, Za Hájovnou Cave, Draby and layers 19ad-19 of the Biśnik Cave.

A set of features suggests a higher evolutionary level and connected with a supposed slightly younger age, closer to MIS 13-12. Most of these characters were found in the dental material while postcranial bones have a rather limited biochronological and taxonomic value. The most important features are a higher proportion of more evolutionarily advanced morphotypes, I3 with a calyx, i1 and i2 with larger and broader crowns and enlarged distoconid, P4 and p4 with more complicated crowns, M1 with a stronger developed parastyle and the lingual cingulum, M2 with a broader trigon, m1 with a slightly longer talonid, m2 with a broader and longer talonid, m3 with a shorter trigonid as well as more massive metapodials.

The presence of *Ursus arctos* in TW is also noteworthy, since the early and mid-Middle Pleistocene history of this species is poorly known in Europe. The TW material is represented by five bones revealing the presence of two brown bear forms. A presence of the form morphologically indistinguishable from the Holocene and extant Central European *Ursus arctos arctos* was documented based on five bones recovered from the Middle Pleistocene horizon. A single M2 confirms the occurrence of *Ursus arctos taubachensis*, a member of the Mammoth Fauna, the first arrival of which to Europe is dated at MIS 12. Together with the German site Bad Frankenhausen, Tunel Wielki Cave probably documents the first appearance of the species related to the Mammoth Fauna of Asian origin in Europe.

Acknowledgements

The research was financed by subsidies for the activities of the University of Wrocław, no. 2020 (501). It was also supported by an internal grant from the Faculty of Biological Sciences, University of Wrocław entitled "The Middle Pleistocene Revolution - How the Modern Theriofauna of Eurasia was developed", as part of the programme "Inicjatywa Doskonałości - Uczelnia Badawcza (IDUB)", grant no. BPIDUB.4610.6.2021.KP.A. New fieldworks in Tunel Wielki Cave and analyses of newly discovered collections were financed by the National Science Centre, Poland, grant: 2016/22/E/HS3/00486.

Author contributions

Investigation, writing, methodology, writing - review and editing, supervision, project administration, funding acquisition, investigation, A.M.; funding acquisition, project administration, data collection, writing - review and editing, M.K.; investigation, methodology, visualization, writing, K.Z.-S.; G.L.: investigation, methodology, visualization, writing.

Data availability statement

All the information containing the research data required to reproduce the work, e.g. status of the material, its location, collection numbers etc., is presented in the main text and in both appendices. All the material, if currently present, is available to study in particular museums and private collections.

REFERENCES

- Ambros D., Hilpert B. & Kaulich B. 2005. Das Windloch bei Sackdilling (Fränkische Alb, Süddeutschland). Lage Forschungsgeschichte, Geologie, Paläontologie und Archäologie. *Abhandlungen der Naturhistorischen Gesellschaft Nürnberg* 45: 365-382.
- ARGANT A. 2009. Biochronologie et grands mammifères au pleistocène moyen et supérieur en Europe Occidentale: l'apport des canidés, des ursidés et des carnivores en général. *Quaternaire* 20 (4): 467-480. https://doi.org/10.4000/quaternaire.5334
- Argant A. 2010. Carnivores (Canidae, Felidae et Ursidae) of Romain-la-Roche (Doubs, France). *Revue de Paleobiologie* 29 (2): 495-601. https://shs.hal.science/halshs-00586673v1

- ARGANT A. & ARGANT J. 2002. Die Bären von Château (Burgund, Frankreich). *Abhandlungen zur Karst- und Höhlenkunde* 34: 57-63.
- ATHEN K. 2007. Biometrische Untersuchungen des Stylopodiums, Zygopodiums und Metapodiums pleistozäner Ursiden im Hinblick auf die Evolution des Höhlenbären und die Klassifizierung des Fundmaterials Einhornhöhle/Harz. PhD thesis, Universität Tübingen, 358 p.
- AZZAROLI A., GIULI C. DE, FICCARELLI G. & TORRE D. 1986. Mammal succession of the Plio-Pleistocene of Italy. *Memorie della Societa Geologica Italiana* 31: 213-218.
- Ballesio R. 1983. Le gisement Pléistocène supérieur de la grotte de Jaurens á Nespouls, Corrèze, France : les Carnivores (Mammalia, Carnivora). III. Ursidae *Ursus arctos* Linnaeus. *Nouvelles Archives du Musée d'Histoire Naturelle Lyon* 21: 9-43. https://doi.org/10.15298/rusjtheriol.03.2.04
- BARTOLOMEI G., CHALINE J., FEJFAR O., JÁNOSSY D., JEANNET M., VON KOENIGSWALD W. & KOWALSKI K. 1975. *Pliomys lenki* (Heller, 1930) (Rodentia, Mammalia) en Europe. *Acta Zoologica Cracoviensia* 20 (10): 393-467.
- BARYSHNIKOV G. F. 2007. Semejstvo medvezhi (Carnivora, Ursidae). Nauka, Sankt-Peterburg, 541 p.
- BARYSHNIKOV G. F. & BOESKOROV G. G. 2004. Skull of the Pleistocene brown bear (*Ursus arctos*) from Yakutia, Russia. *Russian Journal of Theriology* 3 (2): 71-75.
- Berto C., Nadachowski A., Pereswiet-Soltan A., Lemanik A. & Kot M. 2021. The Middle Pleistocene small mammals from the lower layers of Tunel Wielki Cave (Kraków-Częstochowa Upland): An Early Toringian assemblage in Poland. *Quaternary International* 577: 52-70. https://doi.org/10.1016/j.quaint.2020.10.023
- BOĆHEŃSKI Z. 1974. *Ptaki młodszego czwartorzędu Polski*. Państwowe Wydawnictwo Naukowe, Warszaw, 212 p.
- BOCHEŃSKI Z. 1988. Kopalne ptaki z jaskiń i schronisk Doliny Sąspowskiej, in CHMIELEWSKI W. (ed.), Jaskinie Doliny Sąspowskiej. Tło przyrodnicze osadnictwa pradziejowego. Prace Instytutu Archeologii Uniwersytetu Warszawskiego, Warszawa: 47-77.
- CONTI J., BELLUCCI L., IURINO D. A., STRANI F. & SARDELLA R. 2021. Review of *Ursus* material from Fontana Ranuccio (Middle Pleistocene, Central Italy): new insights on the first occurrence of the brown bear in Italy. *Alpine and Mediterranean Quaternary* 34 (1): 55-68. https://doi.org/10.26382/AMQ.2021.14.
- Chmielewski W., Nadachowski A., Stworzewicz E., Bocheński Z. & Madeyska T. 1988. *Jaskinie Doliny Sąspowskiej. Tło przyrodnicze osadnictwa pradziejowego*. Wydawnictwo Uniwersytetu Warszawskiego, Warszawa, 69 p.
- Erbaeva M. A., Montuire S. & Chaline J. 2001. New ochotonids (Lagomorpha) from the Pleistocene of France. *Geodiversitas* 23 (3): 395-409.
- FEUSTEL R., KERKMANN K., SCHMID E., MUSIL R., MANIA D., VON KNORRE D. & JAKOB H. 1971. Die Urdhöhle bei Döbritz. *Alt-Thüringen* 11: 131-226.
- GARCÍA N. & ARSUAGA J. L. 2001. *Ursus dolinensis*: a new species of Early Pleistocene ursid from Trinchera Dolina, Atapuerca (Spain). *Comptes Rendus de l'Académie des Sciences. Série II, Sciences de la Terre et des Planètes* 332 (11): 717-725. https://doi.org/10.1016/S1251-8050(01)01588-9
- GHEZZO E., BERTÉ D. F. & SALA B. 2014. The revaluation of Galerian Canidae, Felidae and Mustelidae of the Cerè Cave (Verona, north-eastern Italy). *Quaternary International* 339-340: 76-89. https://doi.org/10.1016/j.quaint.2012.12.031
- GIBBARD P. 2015. The Quaternary System/Period and its major subdivisions. *Russian Geology and Geophysics* 56 (4): 686-688. https://doi.org/10.1016/j.rgg.2015.03.015
- GIBBARD P. & COHEN K. M. 2019. Global chronostratigraphical correlation table for the last 2.7 million years, version 2019 QI-500. Quaternary International 500: 20-31. https://doi.org/10.1016/j.quaint.2019.03.009

268

- GIMRANOV D., LAVROV A., PRAT-VERICAT M., MADURELL-MALAPEIRA J. & LOPATIN A. V. 2023. — *Ursus etruscus* from the late Early Pleistocene of the Taurida Cave (Crimean Peninsula). Historical Biology 35 (6): 843-856. https://doi.org/10.10 80/08912963.2022.2067993.
- Głazek J., Lindner L. & Wysoczański-Minkowicz T. 1976a. Interglacial Mindel I/Mindel II in fossil-bearing karst at Kozi Grzbiet in the Holy Cross Mts. Acta Geologica Polonica 26 (3): 377-393.
- Głazek J., Sulimski A., Szynkiewicz A. & Wysoczański-MINKOWICZ T. 1976b. — Middle Pleistocene karst deposits with Ursus spelaeus at Draby near Działoszyn, Central Poland. Acta Geologica Polonica 26 (3): 451-466.
- GŁAZEK J., KOWALSKI K., LINDNER L., MŁYNARSKI M., STWOrzewicz E. & Wysoczański-Minkowicz T. 1977a. — Kozi Grzbiet - podział stratygraficzny starszej części zlodowacenia krakowskiego (Mindel) w oparciu o badania stanowiska fauny interglacjalnej typu kromerskiego, in LINDNER L. & MICHALSKA Z. (eds), "Czwartorzęd zachodniej części regionu świętokrzyskiego", Bocheniec-Kielce, 6-10.06.1977r. Wydawnictwo Geologiczne, Warszawa: 15-24.
- GŁAZEK J., LINDNER L., KOWALSKI K., MŁYNARSKI M., STWORZEwicz E., Tuchołka P. & Wysoczański-Minkowicz T. 1977b. -Cave deposits at Kozi Grzbiet (Holy Cross Mts., Central Poland) with vertebrate and snail faunas of the Mindelian I/Mindelian II interglacial and their stratigraphic correlations, in Proceedings of the 7th International Speleological Congress, Sheffield: 211-214.
- Głazek J., Lindner L. & Wysoczański-Minkowicz T. 1977c. Geologiczna interpretacja stanowiska fauny staroplejstoceńskiej Kozi Grzbiet w Górach Świętokrzyskich. Kras i Speleologia 1 (5):13-28.
- GŁAZEK J., SULIMSKI A., SZYNKIEWICZ A. & WYSOCZAŃSKI-MINKOWICZ T. 1977d. — Kopalny kras ze środkowoplejstoceńskimi szczątkami kręgowców w Drabach koło Działoszyna. Kras i Speleologia 185: 42-58.
- HELLER F. 1975. Ein neuer Vertreter des *Ursus deningeri*-Formkreises aus der altquartären Wirbeltierfauna von Erpfingen (Schwäbische Alb). Mitteilungen aus dem Geologisch-Paläontologischen Institut der Universität Hamburg 44: 111-122.
- HILPERT B. 2006. Die Ürsiden aus Hunas Revision und Neubearbeitung der Bärenfunde aus der Steinberg-Höhlenruine bei Hunas (Gde. Pommelsbrunn, Mittelfranken, Bayern). PhD dissertation, University of Erlangen-Nürnberg, 91 p.
- JÁNOSSY D. 1963. Die altpleistozäne Wirbeltierfauna von Kövesvárad bei Répáshuta (Bükk-Gebirge). Annales Historico-Naturales Musei Nationalis Hungarici, Pars Mineralogica et Palaeontologica 55: 109-141.
- JÁNOSSY D. 1990. Vertebrate fauna of site II, in KRETZOI M. & Dobosi V. T. (eds), Vértesszőlős. Site, man and culture. Akademiai Kiado, Budapest: 187-219
- Jiangzuo Q., Wagner J., Chen J., Dong C., Wei J., Ning J. &LIU J. 2018. — Presence of the Middle Pleistocene cave bears in China confirmed - evidence from Zhoukoudian area. Quaternary Science Review 199: 1-17. https://doi.org/10.1016/j. quascirev.2018.09.012
- KAHLKE R.-D. 2014. The origin of Eurasian mammoth faunas (Mammuthus-Coelodonta Faunal Complex). Quaternary Science Reviews 96: 32-49. https://doi.org/10.1016/j.quascirev.2013.01.012
- KAHLKE R.-D., GARCIA N., KOSTOPOULOS D. S., LACOMBAT F., LISTER A. M., MAZZA P. P. A., SPASSOV N. & TITOV V. V. 2011. — Western Palaearctic palaeoenvironment conditions during communities, and implications for hominin dispersal in Europe. Quaternary Science Review 30 (11-12): 1368-1395. https://doi.org/10.1016/j.quascirev.2010.07.020
- KOT M., BERTO C., KRAJCARZ M. T., MOSKAL-DEL HOYO M., Gryczewska N., Szymanek M., Marciszak A., Stefaniak K., ZARZECKA-SZUBIŃSKA K., LIPECKI G., WERTZ K. & MADEYSKA T.

- 2022. Frontiers of the Lower Palaeolithic expansion in Europe: Tunel Wielki Cave (Poland). Scientific Reports 12: 16355. https:// doi.org/10.1038/s41598-022-20582-0
- Koufos G. D., Konidaris G. E. & Harvati K. 2018. Revisiting Ursus etruscus (Carnivora, Mammalia) from the Early Pleistocene of Greece with description of new material. Quaternary International 497: 222-239. https://doi.org/10.1016/j.quaint.2017.09.043
- KOWALSKI K. 1951. Jaskinie Polski cz. 1. Państwowe Muzeum Archeologiczne, Warszawa, 466 pp.
- Krajcarz M. T., Cyrek K., Krajcarz M., Mroczek P., Sudoł M., SZYMANEK M., TOMEK T. & MADEYSKA T. 2016. — Loess in a cave: lithostratigraphic and correlative value of loess and loess-like layers in caves from the Kraków-Częstochowa Upland (Poland). Quaternary International 399: 13-30. https://doi.org/10.1016/j. quaint.2015.08.069
- Kurtén B. 1956. - The bears and hyenas of the interglacials. Quaternaria 4:1-13.
- KURTÉN B. 1959. On the bears of the Holsteinian Interglacial. Stockholm Contributions in Geology 2: 73-102.
- Kurtén B. 1968. *Pleistocene mammals of Europe*. Weidenfeld and Nicolson, London: 317 p.
- Kurtén B. & Poulianos A. N. 1977. New stratigraphic and faunal material from Petralona Cave with special reference to the Carnivora. Anthropos 4: 47-130.
- KURTÉN B. & POULIANOS A. N. 1981. Fossil Carnivora of Petralona Cave: status of 1980. Anthropos 8: 9-56.
- MADEYSKA T. 1988. Osady jaskiń i schronisk Doliny Sąspowskiej, in CHMIELEWSKI W. (ed.), Jaskinie Doliny Sąspowskiej. Tło przyrodnicze osadnictwa pradziejowego. Prace Instytutu Archeologii Uniwersytetu Warszawskiego, Warszawa: 77-173.
- Madurell-Malapeira J., Alba D. M. & Moyà-Solà S. 2009. Carnivora from the late Early Pleistocene of Cal Guardiola (Terrassa, Vallès-Penedès Basin, Catalonia, Spain). Journal of Paleontology 83 (6): 969-974. https://doi.org/10.1666/09-054.1
- MARCISZAK A. & LIPECKI G. 2020a. Fossil bear material from the oldest deposits in the Jasna Strzegowska cave (Silesia, southern Poland). Geological Quarterly 64 (4): 861-875. https://doi. org/10.7306/gq.1556
- MARCISZAK A. & LIPECKI G. 2020b. The history of bears (Ursidae, Carnivora, Mammalia) from Silesia (southern Poland) and the neighbouring areas. Geological Quarterly 64 (4): 876-897. https://doi.org/10.7306/gq.1565
- MARCISZAK A. & LIPECKI G. 2022. Panthera gombaszoegensis (Kretzoi, 1938) from Poland in the scope of the species evolution. Quaternary International 633: 36-51. https://doi.org/10.1016/j. quaint.2021.07.002
- Marciszak A., Socha P., Nadachowski A. & Stefaniak K. 2011. — Carnivores from Biśnik Cave. Quaternaire, Hors-serie 4: 101-106.
- MARCISZAK A., STEFANIAK K. & GORNIG W. 2016. Fossil theriofauna from the Sudety Mts (SW Poland). The state of research. Cranium 33 (1): 31-41.
- Marciszak A., Schouwenburg C., Gornig W., Lipecki G. & MACKIEWICZ P. 2019a. — Morphometric comparison of Panthera spelaea (Goldfuss, 1810) from Poland with the lion remains from Eurasia over the last 700 ka. Quaternary Science Reviews 223: 105950. https://doi.org/10.1016/j.quascirev.2019.105950
- Marciszak A., Schouwenburg C., Lipecki G., Talamo S., SHPANSKY A., MALIKOV D. & GORNIG W. 2019b. — Steppe brown bear Ursus arctos "priscus" from the Late Pleistocene of Europe. Quaternary International 534: 158-170. https://doi. org/10.1016/j.quaint.2019.02.042
- Marciszak A., Sobczyk A., Kasprzak M., Gornig W., Rata-JCZAK U., WIŚNIEWSKI A. & STEFANIAK K. 2020. — Taphonomic and paleoecological aspects of large mammals from Sudety Mts (Silesia, SW Poland), with particular interest to the carnivores. Quaternary International 546: 42-63. https://doi.org/10.1016/j. quaint.2019.11.009

- MARCISZAK A., LIPECKI G., PAWŁOWSKA K., JAKUBOWSKI G., RATAJCZAK-SKRZATEK U., ZARZECKA-SZUBIŃSKA K., NADACHOWSKI A. 2021. The Pleistocene lion *Panthera spelaea* (Goldfuss, 1810) from Poland a review. *Quaternary International* 605-606: 213-240. https://doi.org/10.1016/j.quaint.2020.12.018
- MARCISZAK A., GORNIG W. & SZYNKIEWICZ A. 2023. Carnivores from Draby 3 (central Poland): The latest record of *Lycaon lyca-onoides* (Kretzoi, 1938) and the final accord in the long history of ancient faunas. *Quaternary International* 674-675: 62-86. https://doi.org/10.1016/j.quaint.2023.03.012
- MARCISZAK A., MACKIEWICZ P., BORÓWKA R. K., CAPALBO C., CHIBOWSKI P., GĄSIOROWSKI M., HERCMAN H., CEDRO B., KROPCZYK A., GORNIG W., MOSKA P., NOWAKOWSKI D., RATAJCZAK-SKRZATEK U., SOBCZYK A., SYKUT M. T., ZARZECKA-SZUBIŃSKA K., KOVALCHUK O., BARKASZI Z., STEFANIAK K. & MAZZA P. P. A. 2024. Fate and preservation of the Late Pleistocene cave bears from Niedźwiedzia Cave in Poland, through taphonomy, pathology, and geochemistry. *Scientific Reports* 14: 9775. https://doi.org/10.1038/s41598-024-60222-3
- MASLIN M. A. & RIDGWELL A. J. 2005. Mid-Pleistocene revolution and the 'eccentricity myth, in HEAD M. J. & GIBBARD P. L. (eds), Middle Pleistocene transitions: the land ocean evidence. Early Special Publication of the Geological Society of London 247 (1): 19-34. https://doi.org/10.1144/GSL.SP.2005.247.01.02
- MCFARLANE D. A., SABOL M. & LUNDBERG J. 2011. A unique population of cave bears (Carnivora: Ursidae) from the Middle Pleistocene of Kents Cavern, England, based on dental morphometrics. *Historical Biology* 23 (2-3): 131-137. https://doi.org/10.1080/08912963.2010.483730
- MOIGNE A.-M., PALOMBO M. R., BELDA V., HERIECH-BRIKI D., KACIMI S., LACOMBAT F., LUMLEY A.-M. D., MOUTOUSSAMY J., RIVALS F., QUILÈS J. & TESTU A. 2006. Les faunes de grands mammifères de la Caune de l'Arago (Tautavel) dans le cadre biochronologique des faunes du Pléistocène moyen italien. *L'Anthropologie* 110 (5): 788-831. https://doi.org/10.1016/j.anthro.2006.10.011
- MOTTL M. 1940. Die Fauna der Mussolinihohle. *Geologica Hungarica* 14: 1-352.
- MOTTL M. 1964. Bärenphylogenese in Südost-Österreich. Mitteilungen des Museums für Bergbau, Geologie und Technik am Landesmuseum Joanneum Graz 26: 1-56
- MOULLÉ P.-E. 1992. Les grands mammifères du Pleistocène inferieur de la grotte du Vallonnet (Roquebrune-Cap-Martin, Alpes-Maritimes). Étude paléontologique des Carnivores, Equidé, Suidé et Bovidés. PhD Thesis, Muséum national d'Histoire naturelle à l'Institut de Paléontologie Humaine, Paris: 1-302.
- MUSIL R. 1964. Die Braunbären aus dem Ende des lezten Glazials. Časopis Moravského musea, Vědy přirodní 49: 83-102.
- MUSIL Ř. 1972. Die Bären der Stránská skála. *Anthropos* 20: 107-112.
- MUSIL R. 2001. Die Ursiden-Reste aus dem Unterpleistozän von Untermassfeld. *Monographien des Römisch-Germanischen Zentralsmuseums* 40 (2): 633-658.
- MUSIL R. 2005. Metapodia a prstní články medvědů z jeskyně "Za Hájovnou", Javoříčský kras. *Přírodovědné studie Muzea Prostějovska* 8: 143-151.
- NADACHOWSKI A. 1982. Late Quaternary rodents of Poland with special reference to morphotype dentition analysis of voles. Państwowe Wydawnictwo Naukowe, Warszawa-Kraków, 108 p.
- NADACHOWSKI A. 1988. Fauna kopalna płazów, gadów i ssaków w osadach jaskiń i schronisk Doliny Sąspowskiej, *in* CHMIELEWSKI W. (ed.), *Jaskinie Doliny Sąspowskiej. Tło przyrodnicze osadnictwa pradziejowego*. Prace Instytutu Archeologii Uniwersytetu Warszawskiego, Warszawa: 9-39.
- NADACHOWSKI A. 1989. Review of fossil Rodentia from Poland. Senckenbergiana Biologica 70 (4-6): 229-250.
- NADACHOWSKI A. 1990. Lower Pleistocene rodents of Poland: faunal succession and biostratigraphy. *Quartärpaläontologie* 8: 215-223. https://doi.org/10.1515/9783112760833-017

- OLIVE F. 2006. Évolution des grands Carnivores au Plio Pléistocène en Afrique et en Europe occidentale. *L'Anthropologie* 110 (5): 850-869. https://doi.org/10.1016/j.anthro.2006.10.005
- PACHER M. 2007. The type specimen of *Ursus priscus* Goldfuss, 1810 and the uncertain status of Late Pleistocene brown bears. *Neues Jahrbuch für Geologie und Paläontologie Abhandlungen* 245 (3): 331-339. https://doi.org/10.1127/0077-7749/2007/0245-0331
- Prat F. & Thibault C. 1976. Le Gisement de Nauterie à la Romieu (Gers). Fouilles de 1967 a 1973. Nauterie I. Muséum national d'Histoire naturelle, Paris, 82 p. (Mémoires du Muséum national d'Histoire naturelle, Sér. C Sciences de la Terre (1950-1992); 35).
- RABEDER G. 1983. Neues von Höhlenbären: Zur Morphogenetik der Backenzähne. *Die Höhle* 34 (2): 67-85.
- RABEDER G. 1989. Modus und Geschwindigkeit der Hohlenbaren-Evolution. Schriften des Vereins zur Verbreitung naturwissenschaftlicher Kenntnisse Wien 127-128: 105-126.
- RABEDER G. 1992. Das Evolutionsniveau des Nixloch bei Losenstein-Ternberg (O.Ö.). Mitteilungen der Kommission für Quartärforschung der Österreichischen Akademie der Wissenschaften 8: 133-141.
- RABEDER G. 1995a. Die Gamssulzenhöhle im Toten Gebirge. Mitteilungen der Kommission für Quartärforschung der Österreichischen Akademie der Wissenschaften 9: 1-133.
- RABEDER G. 1995b. Evolutionsniveau und Chronologie der Höhlenbären aus der Gamssulzen-Höhle im Toten Gebirge (Oberösterreich). Mitteilungen der Kommission für Quartärforschung der Österreichischen Akademie der Wissenschaften 9: 69-81.
- RABEDER G. 1999. Die Evolution des Höhlenbärengebisses. *Mitteilungen der Kommission für Quartärforschung der Österreichischen Akademie der Wissenschaften* 11: 1-102.
- RABEDER G. & FRISCHAUF C. 2016. Fossile Bären in Höhlen, in SPÖTL C., PLAN L. & CHRISTIAN E. (eds), Höhlen und Karst in Österreich. *Denisia* 37: 183-198.
- RABEDER G., HOFREITER M., NAGEL D. & WITHALM G. 2004. New taxa of Alpine cave bears (Ursidae, Carnivora). *Cahiers Scientific, Horse série* 2: 49-67.
- RABEDER G., PACHER M. & WITHALM G. 2010. Early Pleistocene bear remains from Deutsch-Altenburg (Lower Austria). *Mitteilungen der Kommission für Quartärforschung der Österreichischen Akademie der Wissenschaften* 17: 1-135.
- RODE K. 1931. Über die Bären von Taubach und Ehringsdorf. Paläontologische Zeitschrift 13: 61-72.
- RODE K. 1935. Untersuchungen uber das Gebiss der Bären. Monographien zur Geologie und Paläontologie 2 (7): 1-162.
- RUSTIONI M. & MAZZA P. 1993. The genus *Ursus* in Eurasia: dispersal events and stratigraphical significance. *Rivista Italiana di Paleontologia e Stratigrafia* 98 (4): 487-494.
- SABOL M. 2001a. Fossil and subfossil findings of brown bears from selected localities in Slovakia. *Slovak Geological Magazine* 7: 3-17.
- SABOL M. 2001b. Fossil brown bears of Slovakia. *Cadernos Laboratorium Xeolóxico de Laxe* 26: 311-316.
- Schütt G. 1968. Die cromzeitlichen Bären aus der Einhornhöhle bei Scharzfeld. *Mitteilungen aus dem Geologischen Institut der Technischen Hochschule Hannover* 7: 1-121.
- SOERGEL W. 1926. Der Bär von Süßenborn. Ein Beitrag zur näheren Kenntnis der diluvialen Bären. *Neues Jahrbuch für Mineralogie, Geologie und Paläontologie B* 54: 115-156.
- STEFANIAK K., KOVALCHUK O., MARCISZAK A., STEPANCHUK V., REKOVETS L., VAN DER MADE J., YANENKO V., TSVELYKH A., RATAJCZAK-SKRZATEK U., KOTOWSKI A., GORNIG W. & BARKASZI Z. 2022. Middle Pleistocene faunal and palaeoenvironmental changes in the south of Eastern Europe: a case study of the Medzhybizh 1 locality (MIS 11, Ukraine). *Quaternary International* 633: 103-117. https://doi.org/10.1016/j.quaint.2021.07.013
- SWENSON J. 2000. Der Braunbär (*Ursus arctos*) in Eurasien, *in* GANSLOSSER U. (ed.), *Die Bären*. Filander Verlag, Fürth: 89-108.

- THENIUS E. 1956. Zur Kenntnis der fossilen Braunbären (Ursidae, Mammalia). Sitzungsberichte der Österreichische Akademie der Wissenschaften. Mathematisch Naturwissenschaftliche Klasse, Abteilung 1: Biologie, Mineralogie, Erdkunde und Verwandte Wissenschaften 165: 153-172.
- TORRES PÉREZ-HIDALGO T. J. DE 1992. The European descendants of *Ursus etruscus* C. Cuvier (Mammalia, Carnivora, Ursidae). Boletin Geológico y Minero 103 (4): 632-642.
- TSOUKALA E. 1991. Contribution to the study of the Pleistocene fauna of large mammals (Carnivora, Perissodactyla, Artiodactyla) from Petralona Cave (Chalkidiki, N. Greece). Preliminary report. Comptes Rendus de l'Académie des Sciences. Série II, Mecanique, Physique, Chimie, Sciences de la Terre, Sciences de l'University 312 (2): 331-336.
- VILLALBA DE ALVARADO M., COLLADO GIRALDO H., ARSUAGA J. L., Bello Rodrigo J. R., van Heteren A. H. & Gómez-OLIVENCIA A. 2022. — Looking for the earliest evidence of Ursus arctos Linnaeus, 1758 in the Iberian Peninsula: the Middle Pleistocene site of Postes cave. Boreas 51 (1): 159-184. https:// doi.org/10.1111/bor.12537
- VON REICHENAU W. 1904. Über eine neue fossile Bären-Art *Ursus* deningeri aus den fluviatilen Sanden von Mosbach. Jahrbücher des Nassauischen Vereins für Naturkunde 57: 1-11.
- VON REICHENAU W. 1906. Beiträge zur näheren Kenntnis der Carnivoren aus den Sanden von Mauer und Mosbach. Abhandlunge der Grossherzoglich Hessischen Geologischen Landesanstalt zu Darmstadt 4: 189-313.
- WAGNER J. 2004. A taxonomic revision of bears from selected Biharian localities of the Czech Republic. A preliminary report: I. C 718, Chlum I, Chlum IV. Cahiers Scientifiques, Hors-Série 2: 139-144.
- WAGNER J. 2005a. Morfometrická charakteristika dentálního materiálu medvědů z jeskyně "Za Hájovnou", Javoříčský kras. Přírodovědné studie Muzea Prostějovska 8: 109-142.
- WAGNER J. 2005b. A taxonomic revision of bears from selected Biharian localities of the Czech Republic. A preliminary report. II. Koněprusy caves - an old collection. Bulletin de la Société d'Histoire Naturelle de Toulouse et de Midi-Pyrenees 141 (1): 51-54.

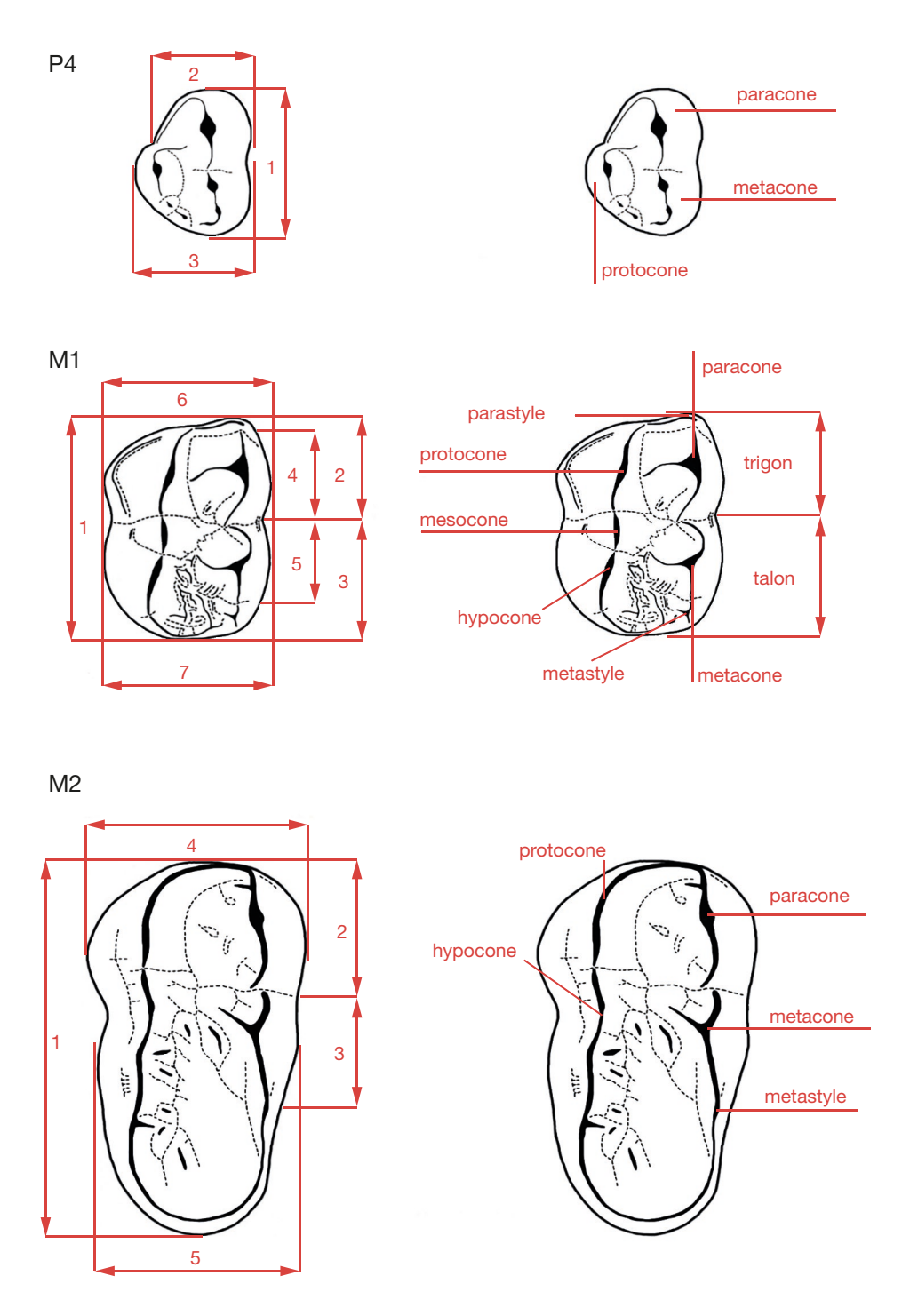
- WAGNER J. 2006. A list of craniodental material of Pliocene ursids (genus Ursus) in the collection of Naturhistorisches Museum Basel. Scientific Annals, School of Geology Aristotle University of Thessaloniki 98: 127-139.
- WAGNER J. 2010. Pliocene to early Middle Pleistocene ursine bears in Europe: a taxonomic overview. Journal of the National Museum of Prague, Natural History Series 179 (20): 197-215.
- WAGNER J. 2014. Metric characteristics of ursid cheek teeth from Za Hájovnou Cave (Javoříčko Karst, the Czech Republic) and its taxonomical implication. Acta Musei Nationalis Pragae, Series *B - Historia Naturalis* 70 (1-2): 71-90. https://doi.org/10.14446/ AMNP.2014.71
- Wagner J. & Čermák S. 2012. Revision of the early Middle Pleistocene bears (Ursidae, Mammalia) of Central Europe, with special respect to possible co-occurrence of spelaeoid and arctoid lineages. Bulletin of Geosciences 87 (3): 461-496.
- WAGNER J. & SABOL M. 2007. Remarks on Biharian bears (Ursidae: Ursus) from the territory of Slovakia. Scripta Facultatis Scientiarum Naturalium Universitatis Masarykianae Brunensis 35: 159-164.
- WITTENBERG V. & WENZELIDES L. 2000. Die Braunbären Nordamerikas, in GANSLOSSER U. (ed.), Die Bären. Filander Verlag, Fürth: 109-146.
- WISZNIOWSKA T. 1989. Middle Pleistocene Carnivora (Mammalia) from Kozi Grzbiet in the Świętokrzyskie Mts, Poland. Acta Zoologica Cracoviensia 32 (14): 589-630.
- WITHALM G. 2001. Die Evolution der Metapodien in der Höhlenbären-Gruppe (Ursidae, Mammalia). Beiträge zur Paläontologie 26: 169-249.
- Wojenka M., Krajcarz M. T., Szczepanek A. & Wilczyński J. 2017. — Sprawozdanie z badań wykopaliskowych przeprowadzonych w Jaskini Tunel Wielki w Wąwozie Koziarnia w 2016 roku. Prądnik: Prace i Materiały Muzeum im. Prof. Władysława Szafera 27: 147-168.
- Woroncowa-Marcinowska K., Pawłowska K., Żarski M. & URBAN J. 2017. — Zespoły plejstoceńskiej fauny (zbiory Muzeum Geologicznego PIG-PIB) w ujęciu stratygraficznym, geologicznym i tafonomicznym. Przegląd Geologiczny 65 (1): 53-62.
- ZAPFE H. 1948. Die altplistozänen Bären von Hundsheim in Niederösterreich. Jahrbuch der Geologischen Bundesanstalt 91: 95-164.

Submitted on 13 September 2024; accepted on 16 January 2025; published on 21 May 2025.

APPENDICES

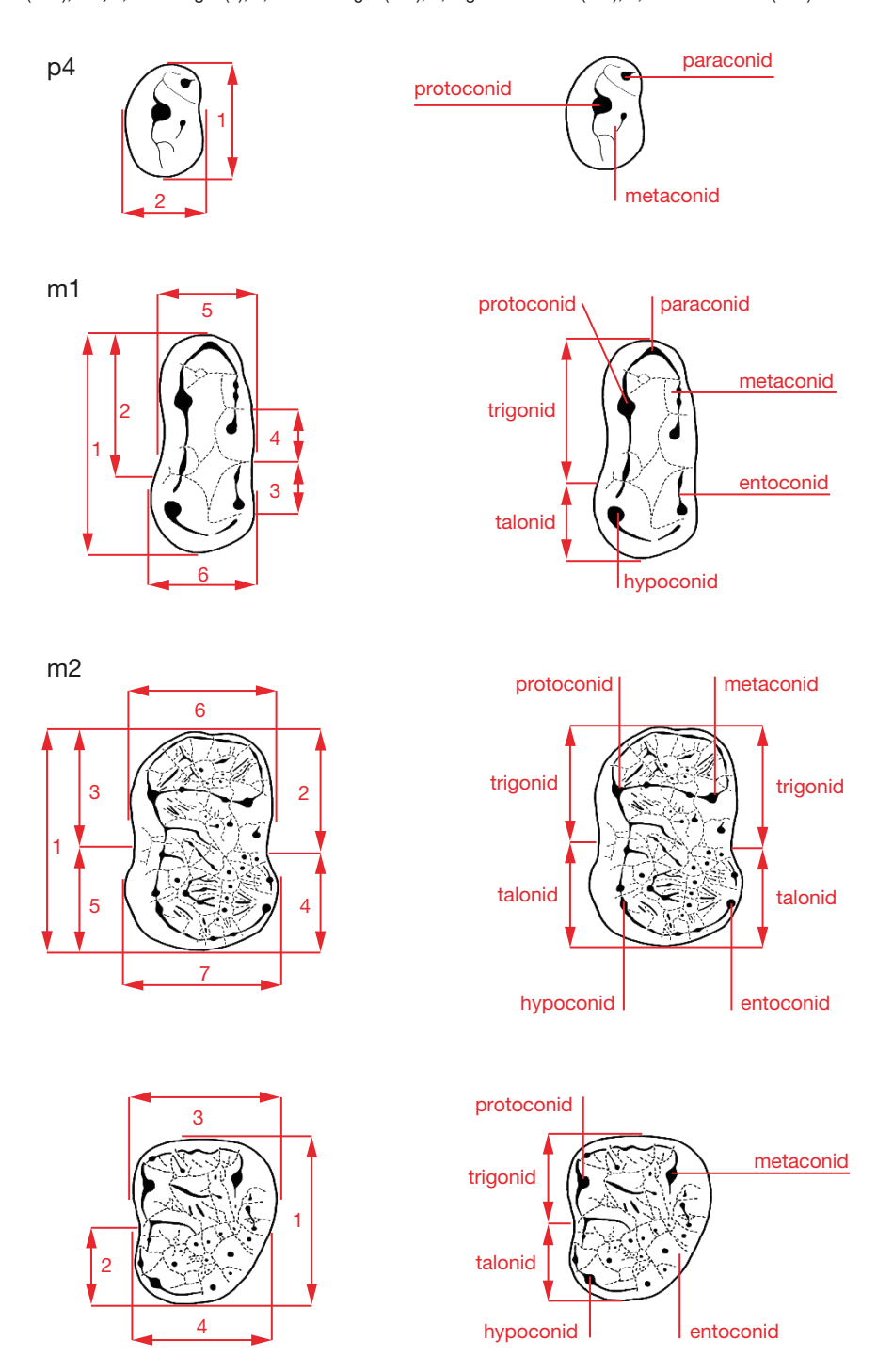
APPENDIX 1. — Catalogue, measurements and detail morphodynamic analysis of the ursid material from Tunel Wielki Cave. Available at: https://doi.org/10.5852/cr-palevol2025v24a14_s1

APPENDIX 2. — Scheme of measurements and cusps terminology of the ursid upper cheek tête: P4, 1, total length (L); 2, trigon breadth (B tr); 3, talon breadth (B ta); M1, 1, total length (L); 2, trigon length (L tr); 3, talon length (L ta); 4, paracone length (L pa); 5, metacone length (L me); 6, trigon breadth (B tr); 7, talon breadth (B ta); M2, 1, total length (L); 2, paracone length (L pa); 3, metacone length (L me); 4, trigon breadth (B tr); 5, talon breadth (B ta).

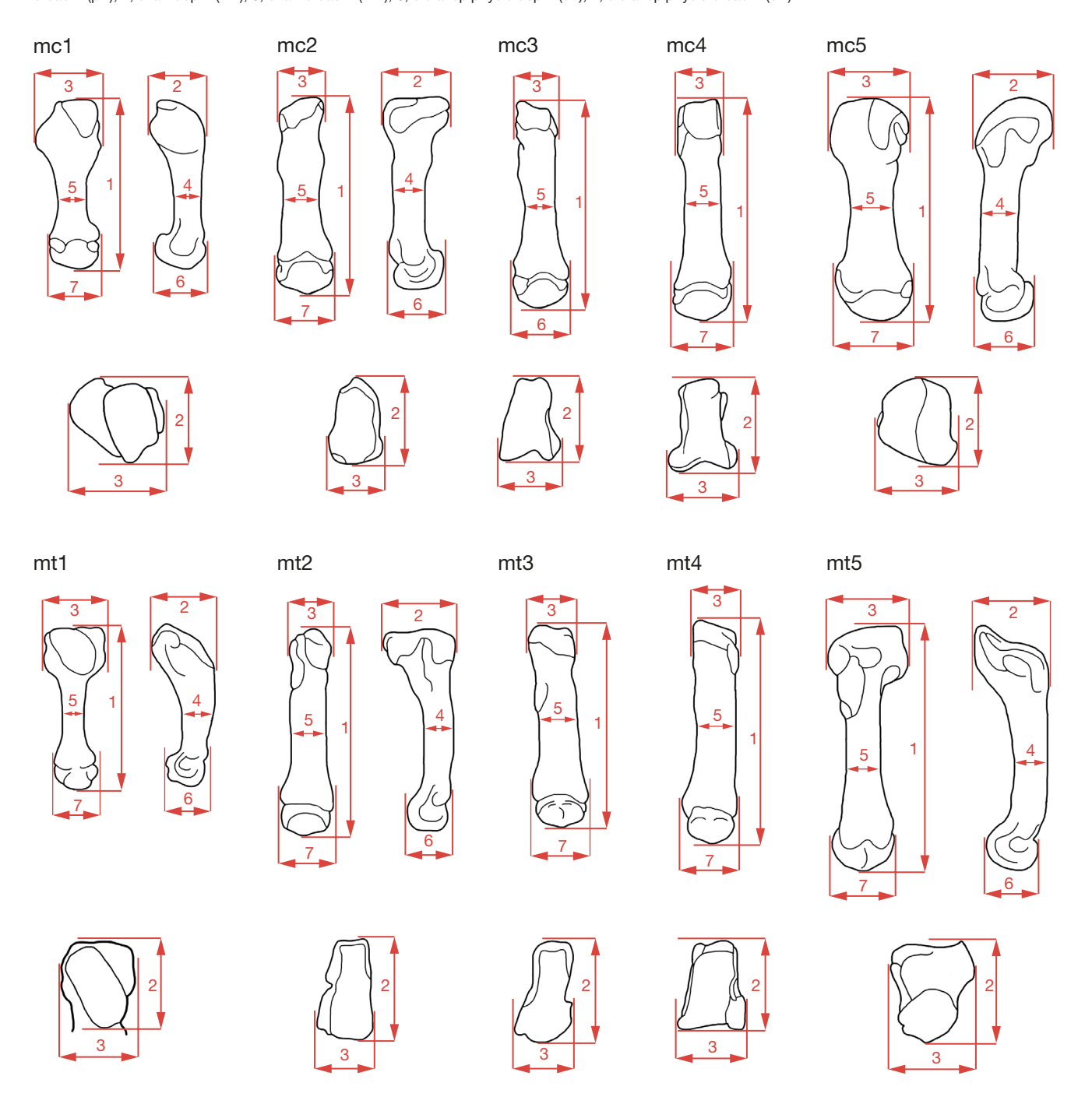


272

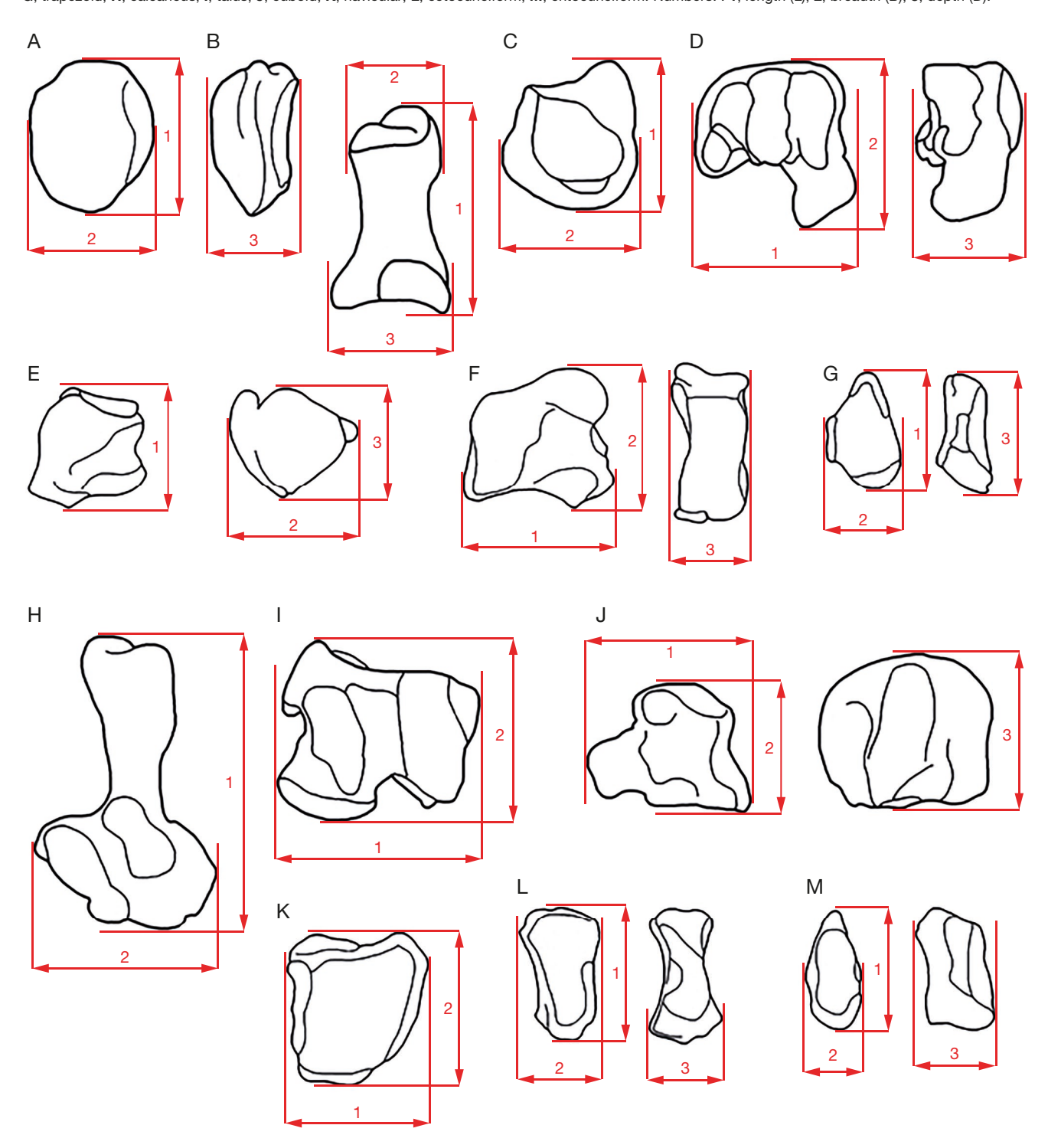
APPENDIX 3. — Scheme of measurements and cusps terminology of the ursid lower cheek teeth: p4, 1, total length (L); 2, total breadth (B); m1, 1, total length (L); 2, trigonid length (L tr); 3, length of distal entoconid (L e1); 4, length of mesial entoconid (L e2); 5, trigonid breadth (B tr); 6, talonid breadth (B ta); m2, 1, total length (L); 2, trigonid lingual length (L tr 1); 3, trigonid buccal length (L tr 2); 4, talonid lingual length (L ta 1); 5, talonid buccal length (L ta 2); 6, trigonid breadth (B tr); 7, talonid breadth (B ta); m3, 1, total length (L); 2, talonid length (L la); 3, trigonid breadth (B tr); 4, talonid breadth (B ta).



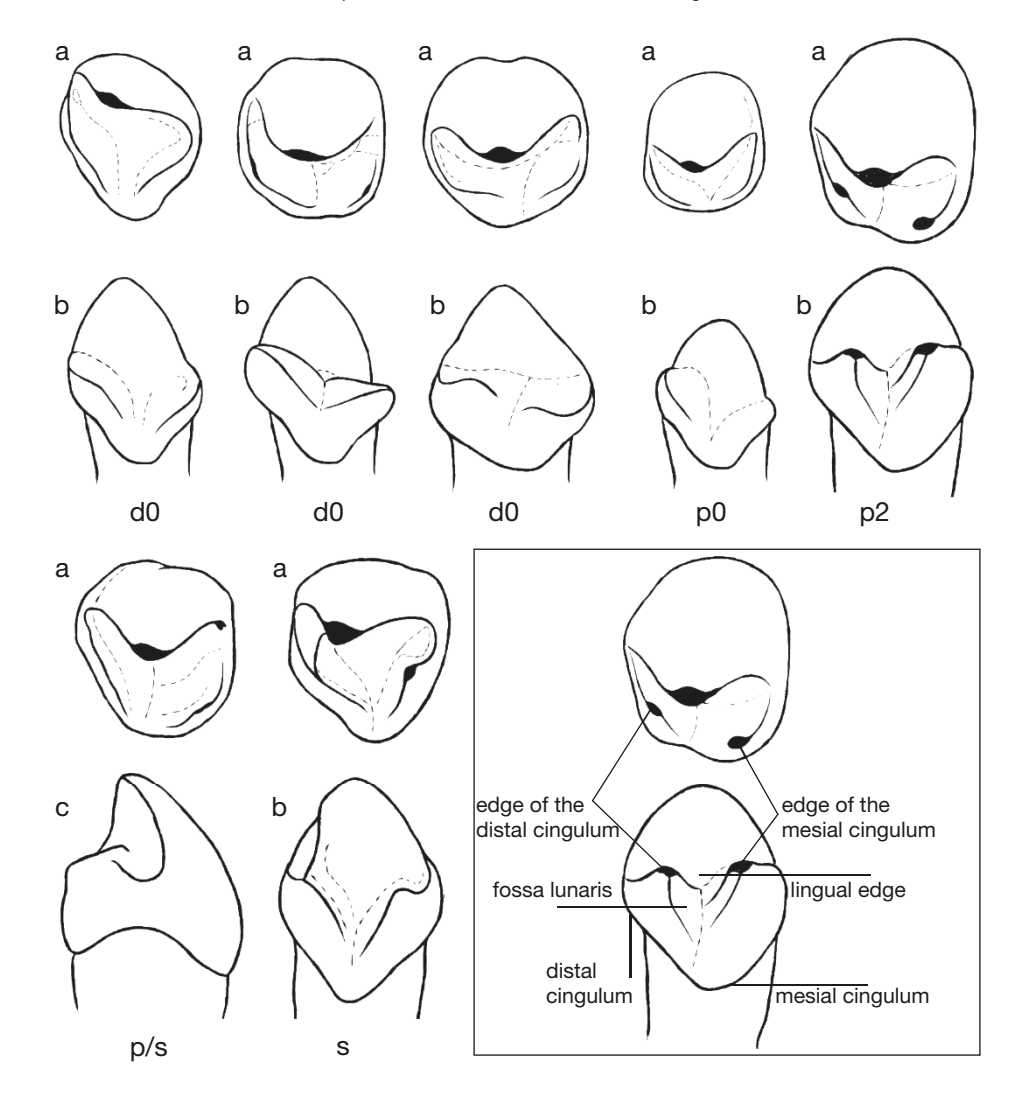
 $\label{eq:Appendix 4.} Appendix 4. - Scheme of measurements of ursid metacarpals and metatarsals: \textbf{1}, total length (L); \textbf{2}, proximal epiphysis depth (pL); \textbf{3}, proximal epiphysis breadth (pB); \textbf{4}, shaft depth (mL); \textbf{5}, shaft breadth (mB); \textbf{6}, distal epiphysis depth (dL); \textbf{7}, distal epiphysis breadth (dB).$



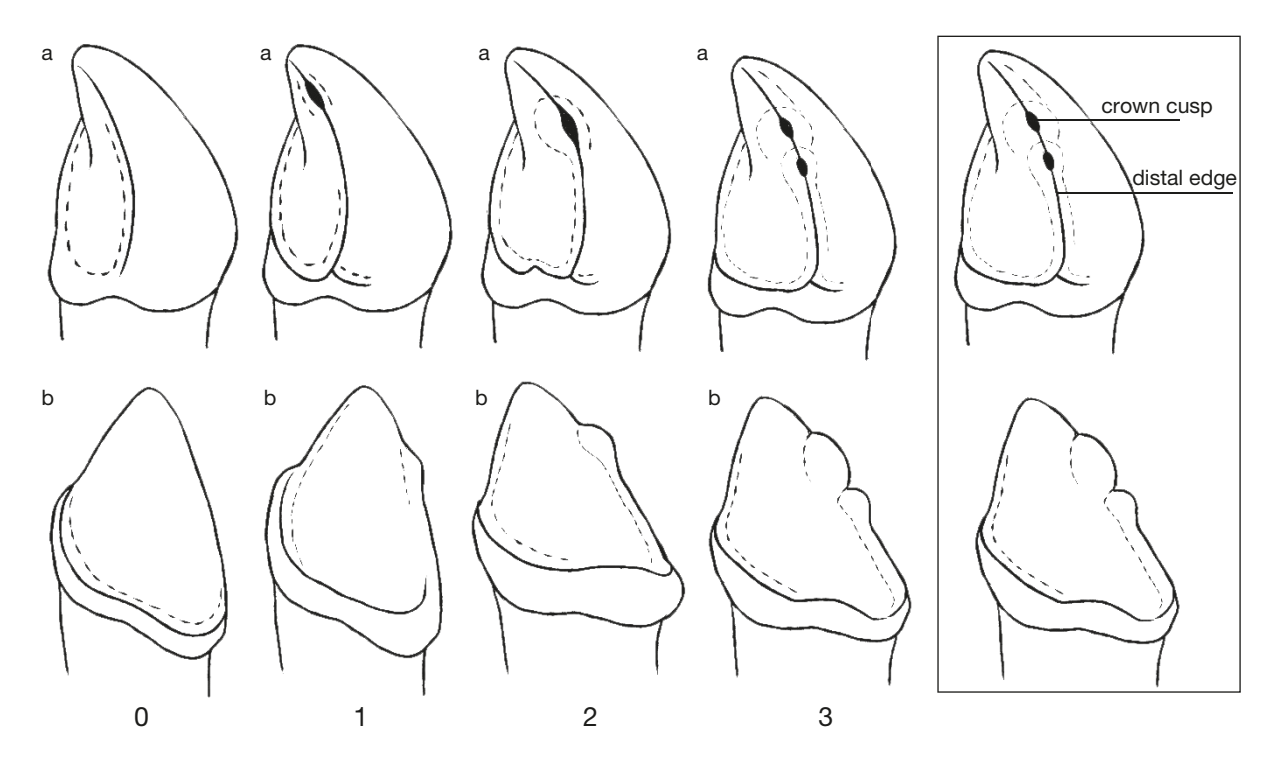
 $A \texttt{PPENDIX} \ 5. \ - \ S \texttt{cheme} \ of \ measurements \ of \ ursid \ carpals \ and \ tarsals: \ \textbf{A}, \ patella; \ \textbf{B}, \ pisiform; \ \textbf{C}, \ triquetrum; \ \textbf{D}, \ scapholunatum; \ \textbf{E}, \ hamatum; \ \textbf{F}, \ capitatum; \ \textbf{G}, \ trapezoid; \ \textbf{H}, \ calcaneus; \ \textbf{I}, \ talus; \ \textbf{J}, \ cuboid; \ \textbf{K}, \ navicular; \ \textbf{L}, \ ectocuneiform; \ \textbf{M}, \ entocuneiform. \ Numbers: : 1, \ length \ (L); \ \textbf{2}, \ breadth \ (B); \ \textbf{3}, \ depth \ (D).$



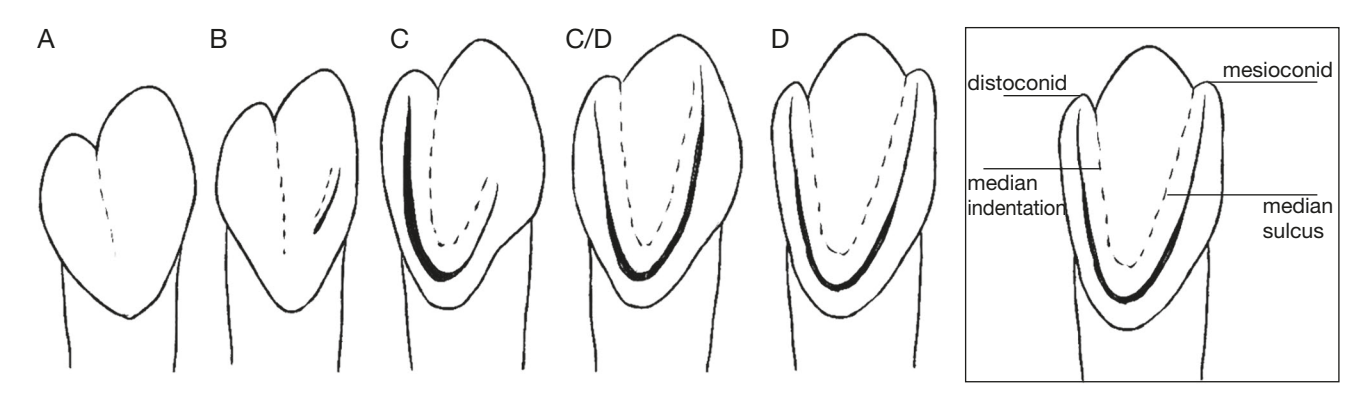
APPENDIX 6. — First and second upper incisor (I1-I2). Description. A large series of I1 and I2 allows to distinguish the differences between them, with I1 being smaller, with a simpler and more compact crown, and straighter root. The I1 crown of TW bears is simply build, relatively short mesio-distally and moderately expanded bucco-lingually. The crown is asymmetrical, and its main axis runs diagonally from the upwards and lingual sides to the downwards and buccal ones. The crown apex is oriented mesio-buccally, and forms an asymmetrical triangle. The mesial and distal edges are of similar size or distal one is larger. The mesial valley between them is U- or V-shaped, shallow, and both edges are connected to each other. Morphotypes of the I2: d, small size; narrow and simple structured crown, poorly distinguished crown apex; the division of the cingulum into two parts is weakly marked by a narrow and poorly developed notch; p, the mesial and distal sections of the cingulum are divided by a wide, V-shaped valley; the edges of the cingulum reach the base of the lingual side; fossa lunaris is not developed; s, large, wide, bilaterally developed crown; cingulum well developed and distinctly separated, with a strongly developed lingual edge and fossa lunaris; wide and flattened shaft of the distal cingulum is covered with thickenings and small tubercles, the number of which is variable. Based on Rabeder (1999: 76, fig. 46, modified). The numbers indicate the number of cusplets on the crown: a, occlusal view; b, lingual view; c, mesial view.



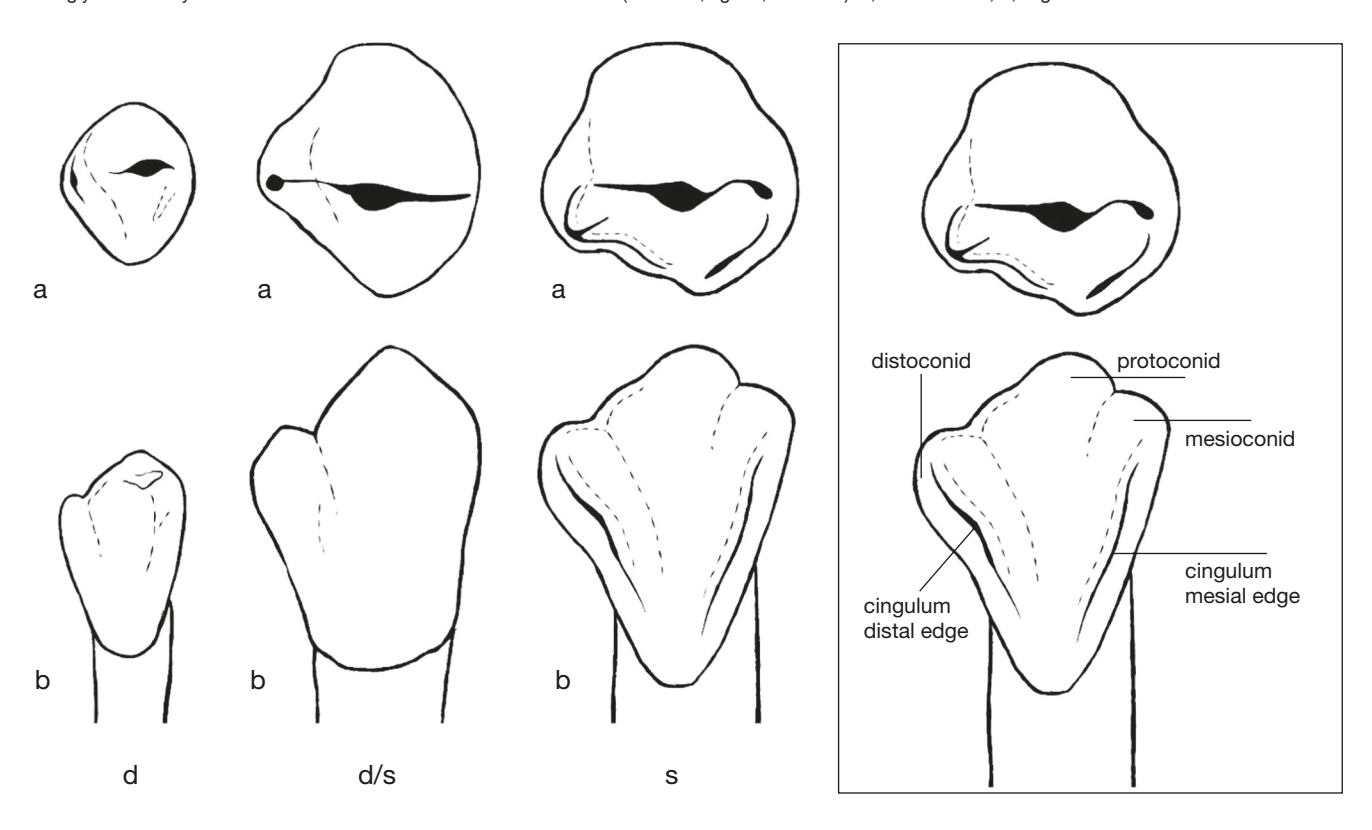
APPENDIX 7. — Third upper incisor (I3), Description, Large, caniniform I3 has the crown located at an angle of 400 to the root axis (Fig. 2, Table S6). The crown itself appears in the medio-lingual direction of the point. In terms of its cross-section, the point mediates between the chisel-shaped main point, and the crown is compressed longitudinally. The medial and distal ridges appear less sharply in its apex area than those in spelaeoid bears. The distal edge gradually lifts up against the lingual crown surface. A little below the apex, the medial edge divides downwards into two divergent parts, which enclose a gusset-like depression. The medial and distal edge bends at the base lingually and merges into a cingulum that hems inside of the entire tooth. The I3 from TW has a developed lingual edge and fossa lunaris that occurs as a clearly visible pit on the mesial side of the tooth. The cingulum is very weak and sometimes even absent as well. In all 13 from TW, the mesial and distal edges delimit a somewhat recessed field with the lingual cingulum. In the hollow, small often develop on the medial base of the main cusp and occasionally on its distal base. The medial swelling always rises at the point where the lingual part of the edge joins the cingulum. It tends to be less sharply opposed to this than to the dropping of the main point stacked side stools on the distal base. The upper one is separated from the descending edge by a notch; the lower one seems to represent an elevation of the cingulum. This stool-like elevation of the cingulum apparently has a local bulge in the base of the crown, while the other cusp is otherwise below the distal edge tends to reach the deepest one. The I3 morphotypes: A1, present two main crown edges, slender and elongated crown, without additional structures; A2, more complex morphology, an angle formed by the proximal and lingual edge with the fossa lunaris appears; A3, fossa lunaris strongly developed; a small cusp is located on the lingual side in the contact zone between the anterior gyrus of the crown and the lingual edge; A4, fossa lunaris strongly developed; a lingual cusplet located between the anterior gyrus of the crown and its lingual edge; B1, strongly developed fossa lunaris; two additional lingual cusplets present in the contact zone between the lingual gyrus and the lingual crest; B2, strongly developed fossa lunaris; three strongly developed and easily defined lingual cusplets present at the base of the lingual crest. Based on Rabeder (1999: 72, fig. 42, modified): a, occlusal side; b, lingual side; c, mesial side.



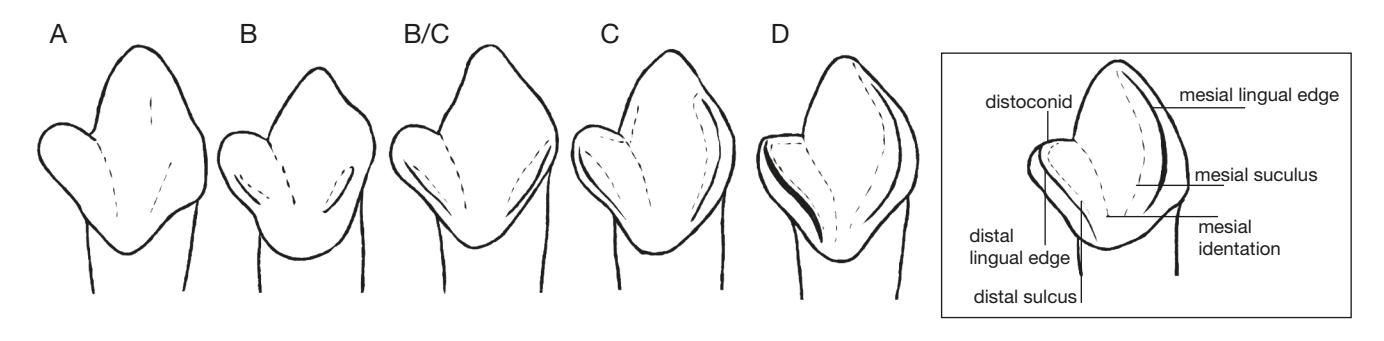
APPENDIX 8. — First lower incisor (i1). Description. Small and thin i1 is simply build, one-rooted tooth, with a narrow crown consisting of two cusps. The crown is straight, with an apex oriented almost vertically, and c. 2/3 of the crown is developed from the main cusp, the protoconid that is located on the median side. Closely associated with the protoconid is the laterally positioned distoconid, which is also lower; there is no sign of mesioconid. Simply build crown has only one lingual groove that is deep, thin, and running from the saddle between the protoconid and distoconid into the median part of the base. The i1 morphotypes: A, small size; simple structured of a strongly verticalised crown, and slender structure. The distoconid is separated by a narrow and shallow medial sulcus, reaching halfway up the crown. It divides the lingual wall of the crown into a wider mesial and narrower distal part; B, slightly wider crown; the medial sulcus reaches the base of the crown; mesial sulcus relatively short, deep and well defined; C, relatively short mesial sulcus, often comes into contact with the medial sulcus, creating a single, thickened sulcus; Through this development, a connection with the cingulum is also created and longitudinally running edges are formed; C/D, mesial sulcus reaches the crown apex; mesioconid is not developed; D, mesial sulcus reaches the apexes of both cusps, creating an additional, small indentation; present a small mesioconid. Based on Rabeder (1999: 79,fig. 49, modified). The diagram shows the left i1 from the distal side.



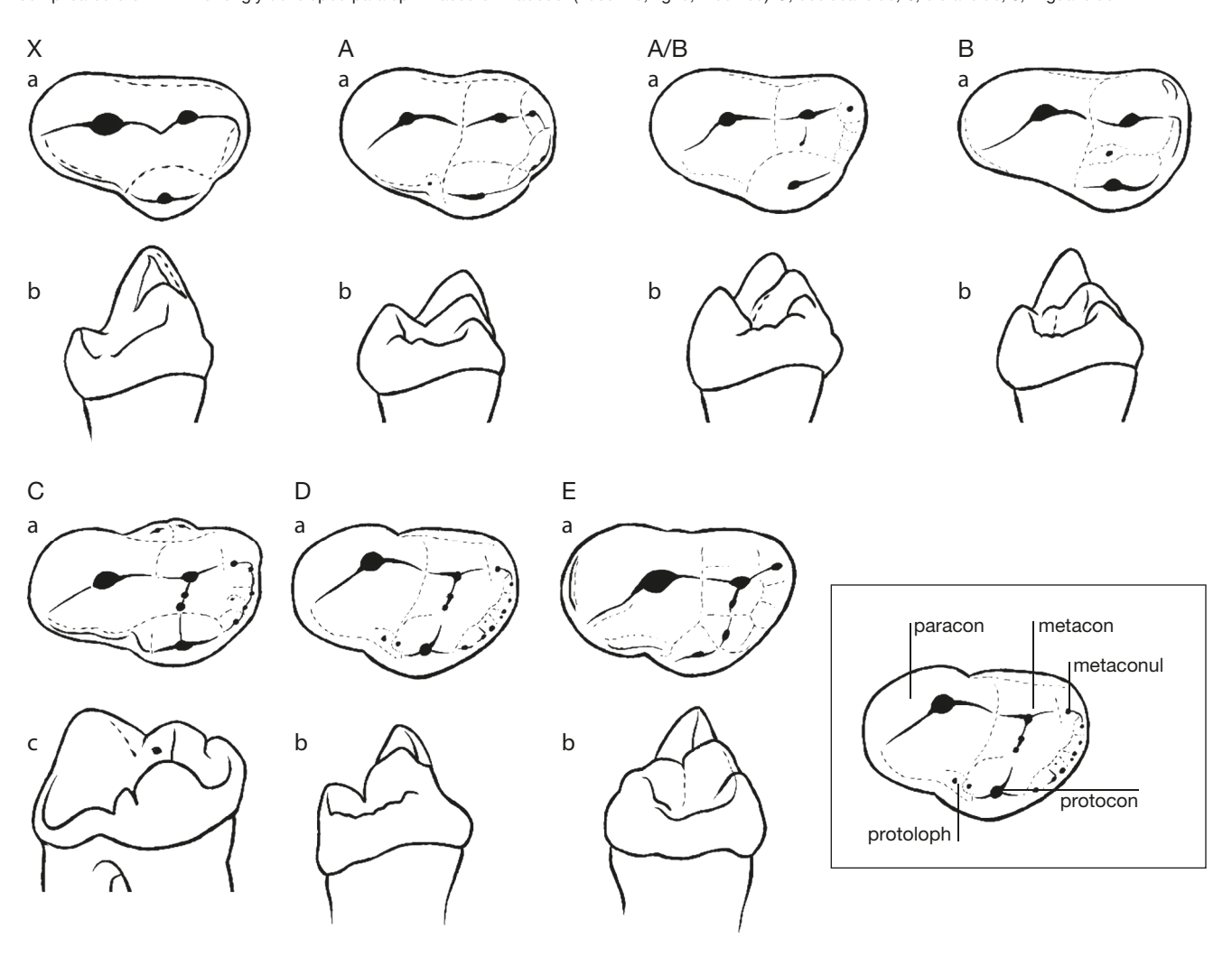
APPENDIX 9. — Second lower incisor (i2). Description. Larger, but morphologically similar i2 has one long root with the tip oriented laterally The relatively large crown is divided into two (in most specimens) or three (in a few teeth) parts, and its apex is oriented vertically and slightly distally, being oval-shaped in occlusal view. About 70% of the crown surface is represented by the main cusp, the protoconid, which is developed as a flat and elongated cusp. Closely associated with the protoconid is laterally oriented distoconid, which is poorly developed and gently separated from the main cusp by a thin and shallow groove. The i2 morphotypes: d, without mesioconid; distoconid strongly associated with the protoconid, the apex of which is more vertically aligned; d/s has, without or weak development mesioconid; the apex of the distoconid is more horizontally oriented in the buccal directed; s, strong mesioconid; the apex of the distoconid is strongly horizontally oriented in the buccal directed. Based on Rabeder (1999: 77, fig. 47, modified): a, occlusal side; b, lingual side.



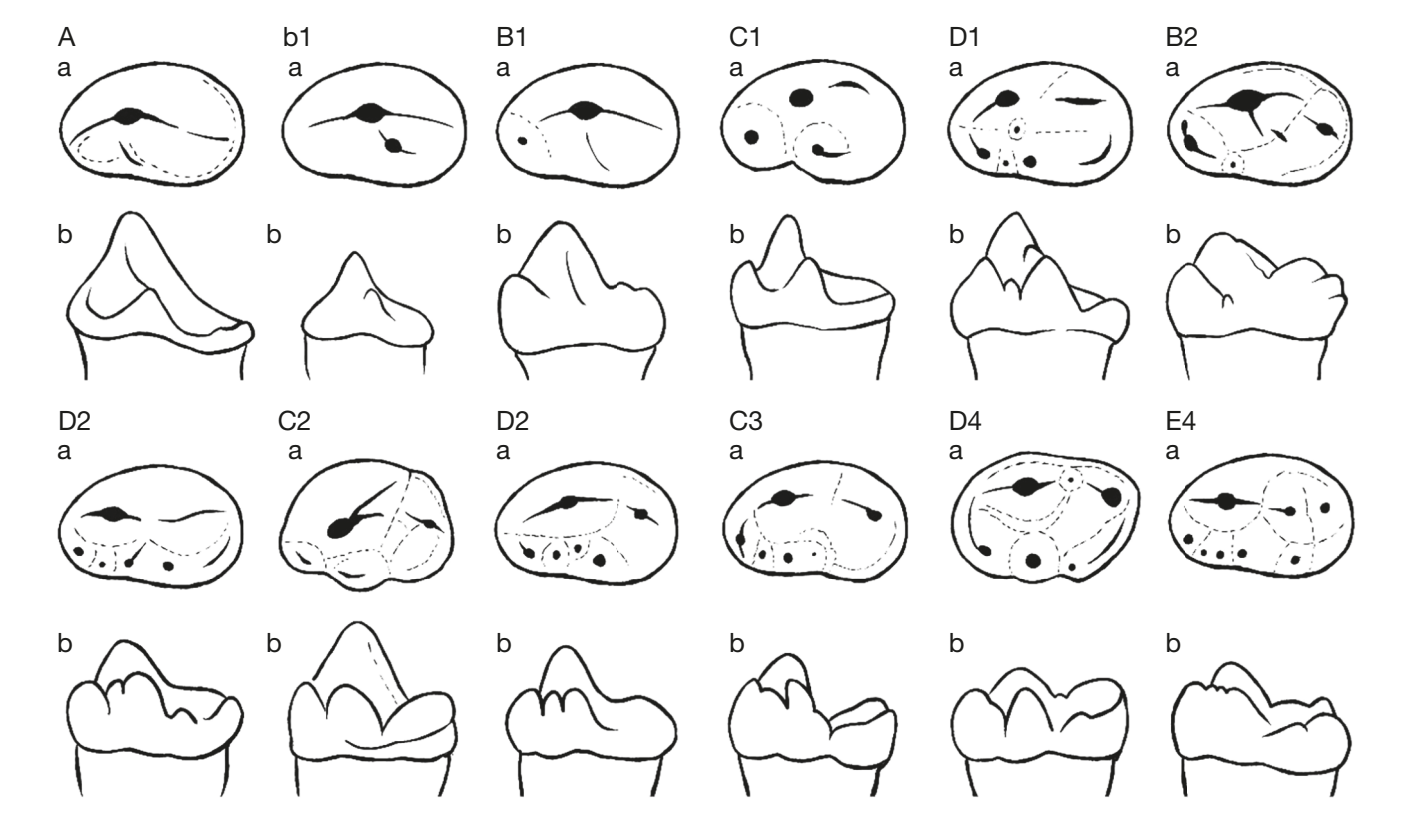
APPENDIX 10. — Third lower incisor (i3). Description. Among incisors, i3 shows the greater morphological variability. The i3 is a tooth with particularly elongated, massive root, which apex is oriented buccally and is oval in cross-section. The crown is rounded to oval in occlusal view, asymmetrical in mesio-distal side, and enlarged distally. The main cusp, the protoconid, occupies c. 65 % of the crown surface. It vertical apex is massive and rather blunt. The distoconid is well developed and clearly distinct from the protoconid, oriented buccally and separated by a thin and shallow notch running almost up to the crown base. The distal surface of the crown is almost completely smooth. A weakly developed groove is located on the disto-lingual surface of the crown. This ridge (sulcus medialis) is even better developed in the morphotype B/C, where it reaches the middle point of the crown. The i3 morphotypes: A, proportionally the smallest (in relation to the size of the protoconid) distoconid; weakly developed medial notch and medial sulcus; B, moderately developed distoconid, moderately deep medial notch and a slightly deepened medial sulcus reaching a maximum of 1/3 of the crown height; B/C, medial sulcus reaching half the crown height; C, clearly distinguished and buccally directed distoconid; strongly developed lingual edge; deep medial sulcus reaching the crown apex; D, largest distoconid; strongly developed lingual edge; deep medial sulcus reaching the crown apex. Based on Rabeder (1999: 72, fig. 42, modified). The diagram shows the left i3 from the distal side.



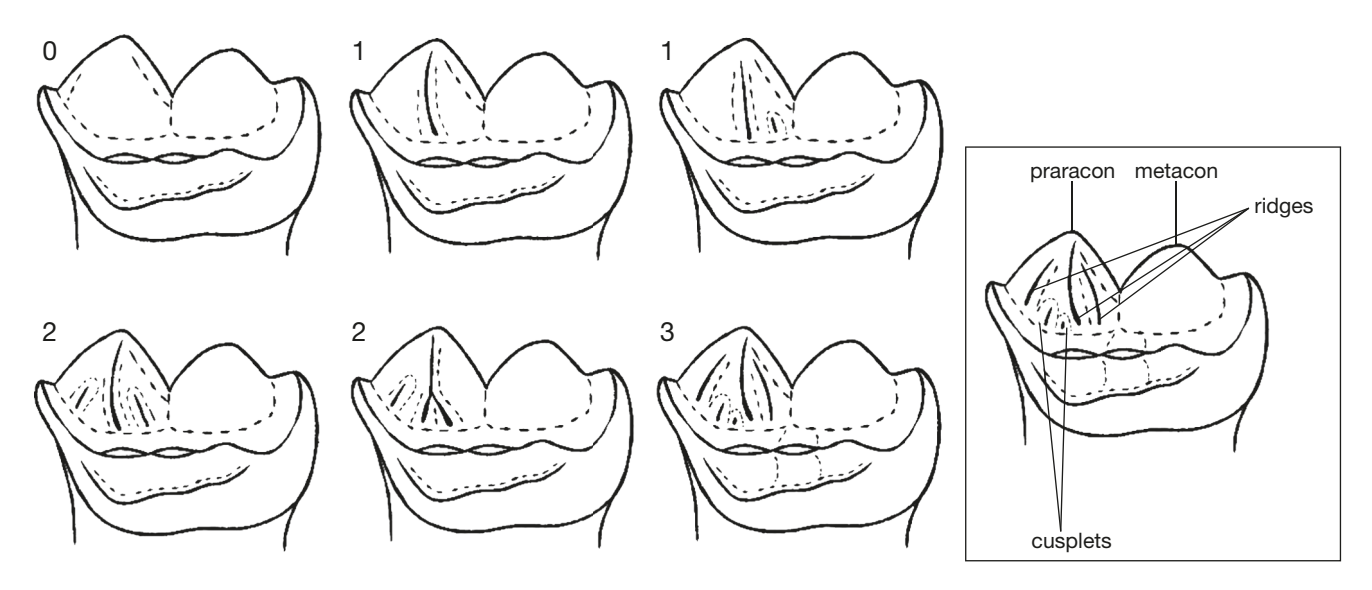
APPENDIX 11. — Fourt upper premolar (P4). Description. Triangular tooth, with the buccal margin of the tooth is concave in the median part, and the size of the convexity varies considerably, from the gently to the very deep one. The lingual, mesial and distal margins are blunt or rounded. Paracone is large, round and quite low. The metacone is almost equal in size to the paracone, but lower, and more oval, the valley between them is strongly pronounced. An elongated, oval and low protocone is well developed, and sharply delineated from the remaining part of the crown. Its mesial margin forms a wide, open angle with the distal margin of the paracone. Cingulum is weakly developed, but stronger (forms a small crest) in disto-buccal part of the crown. The P4 morphotypes: A, triangular crown with a simple morphology, without additional cusps such as protoloph and metaconule; A/B, lower crown; a small, additional cusplet present between the protocone and the metacone; enlarged metacone; enlargement protocone shifting more mesially; **B**, low crown; enlarged and massive paracone; enlargement protocone shifting considerably mesially; distinct metacone; **C**, a small cusplet located on the mesio-lingual side of the protocone; metaloph not present or weakly developed; distal edge of the high and rounded protocone has a several small cusplets and cingulum thickenings; D, strong cusplet on the distal edge of the metacone, metacone, metacone, metacone and protocone connected into one continuous edge; on the lingual wall of the metacone, next to the strongly developed metaconule, is present located small cusplet; enlarged and more medially shifted protocone has a main axis running almost parallel to the axes of the paracone and metacone; E, all distal cusps (protocone, metacone, metaconule and cusplet on the protocone) are connected by a strongly developed metaloph; F, the most complicated crown with strongly developed paraloph. Based on Rabeder (1983: 78, fig. 6, modified): **a**, occlusal side; **b**, distal side; **c**, lingual side.



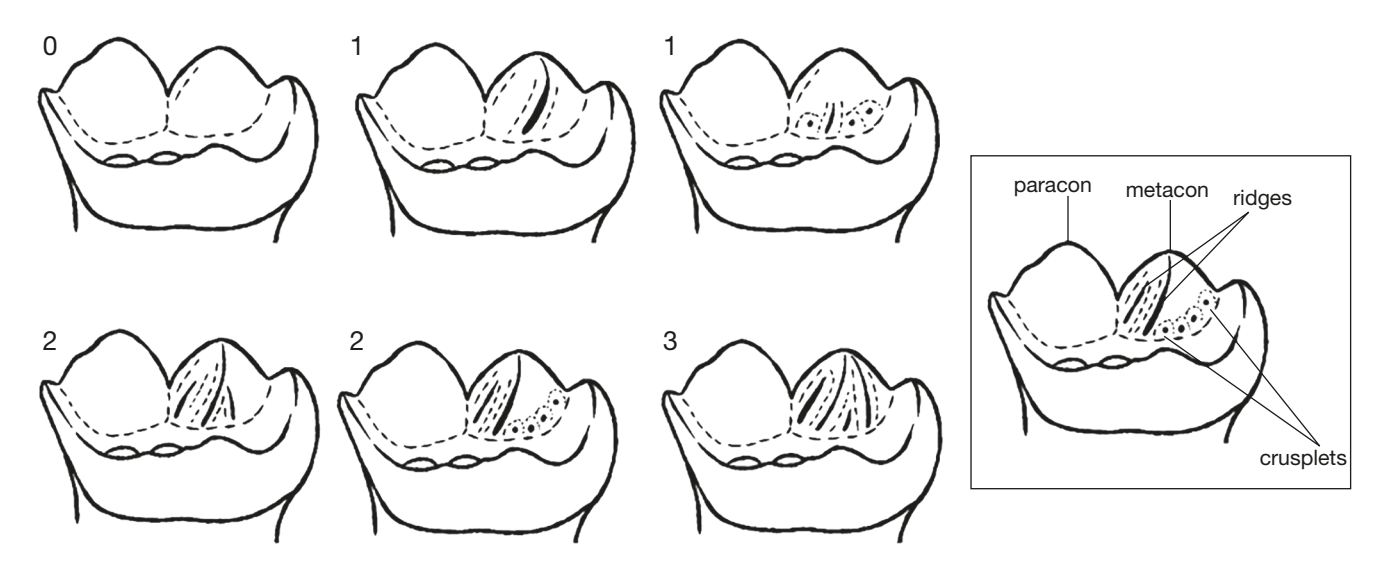
APPENDIX 12. — Fourth lower premolar (p4). The p4 morphotypes: **A**, simply structured crown, lack of additional cusplets; high and strongly developed protoconid; **b1**, without metaconid, paraconid and parallel distal crests or they are present (rather rare) in s weak forms; **B1**, oval or ovoid shaped with regular outline crown; behind the vertical and moderately high protoconid is located weak metaconid; mesio-lingually from the protoconid is located conical and prominent paraconid; talonid with the median edge; **B2**, prominent paraconid; low and elongated hypoconid shifted disto-lingually; strong distal cingulum without additional structures on its surface; **C1**, strongly developed metaconid and paraconid; **C2**, strongly developed hypoconid and metaconid; **C3**, irregular and robust crown; strongly developed hypoconid and metaconid; low and rounded entoconid, located in the middle part on the lingual side; small, additional cusplets located between paraconid or before metaconid; **D**, two cusplets located buccally to the metaconid; weakly developed metalophid; **D1**, between the metaconid paraconid present 1-2 cusplets of variable size; **D2**, small and rounded hypoconid located in the distal part of the crown; **D3**, small entoconid located on the disto-lingual part of the crown; **E**, metaconid is connected to a row of tubercles within the metalophid with a main crest leading from the protoconid to the hypoconid; between the distal part of the metaconid and the hypoconid there is a second, transverse hypolophid crest; **E2**, without entoconid; **E3**, entoconid present; **E4**, numerous cusplets of variable size on the trigonid; 3 talonid main cusps (entoconid). Based on Rabeder (1983: 74, fig. 3, modified): **a**, occlusal side; **b**, lingual side.



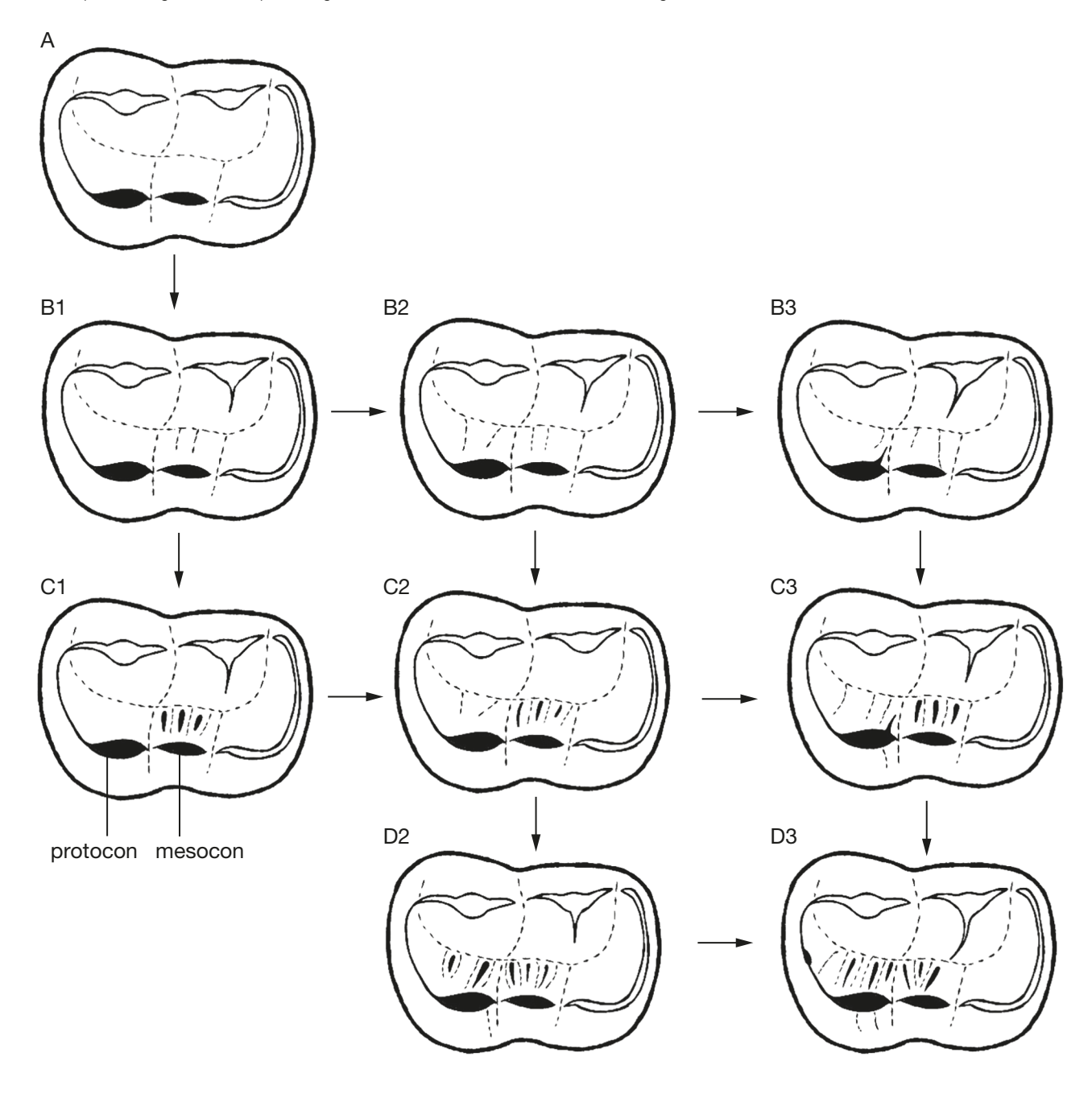
APPENDIX 13. — First upper molar (M1). Description. Square-shaped M1 is symmetrical in occlusal view, with a talon that is slightly longer and broader than the trigon The mesial margin of the tooth is blunt to rounded, with moderately expanded parastyle, while the distal margin is rounded. The buccal side is mostly straight; it is moderately concave only on the transition between the trigon and talon. The lingual margin of the trigon is straight, while the lingual margin of the talon is expanded and rounded; a gentle, median concavity occurs between them. The low and triangular parastyle is variably developed, from small to moderately large one. In most M1, it is small to moderately large, separated from the paracone and associated with the mesial cingulum. Its interior crest ends without forming a cusp, however a small cuspid occurs in six specimens. The paracone and metacone are rounded, high and almost equal in size, the valley that separates them is deep. They are well separated from the buccal cingulum. Morphotypes of the lingual (inner) wall of the M1 paracone: 0, smooth, devoid of any structures; 0.5, at the base of the wall very delicate and barely visible, grooves and lines are marked; 1, strongly developed and outlined single edge running from the base of the wall to the top of the paracone; 1.5, a single ridge is accompanied by a second, smaller, 1/3-length groove, which also starts at the base of the wall; 2, strongly developed and thick edge, running from the base of the wall to its top, along with two accompanying edges, reaching approximately half the height of the wall; 3, one large edge and several longer and shorter thickened accompanying lines. Based on Rabeder (1999: 45, fig. 25, modified). The diagram shows the lingual side of the left M1.



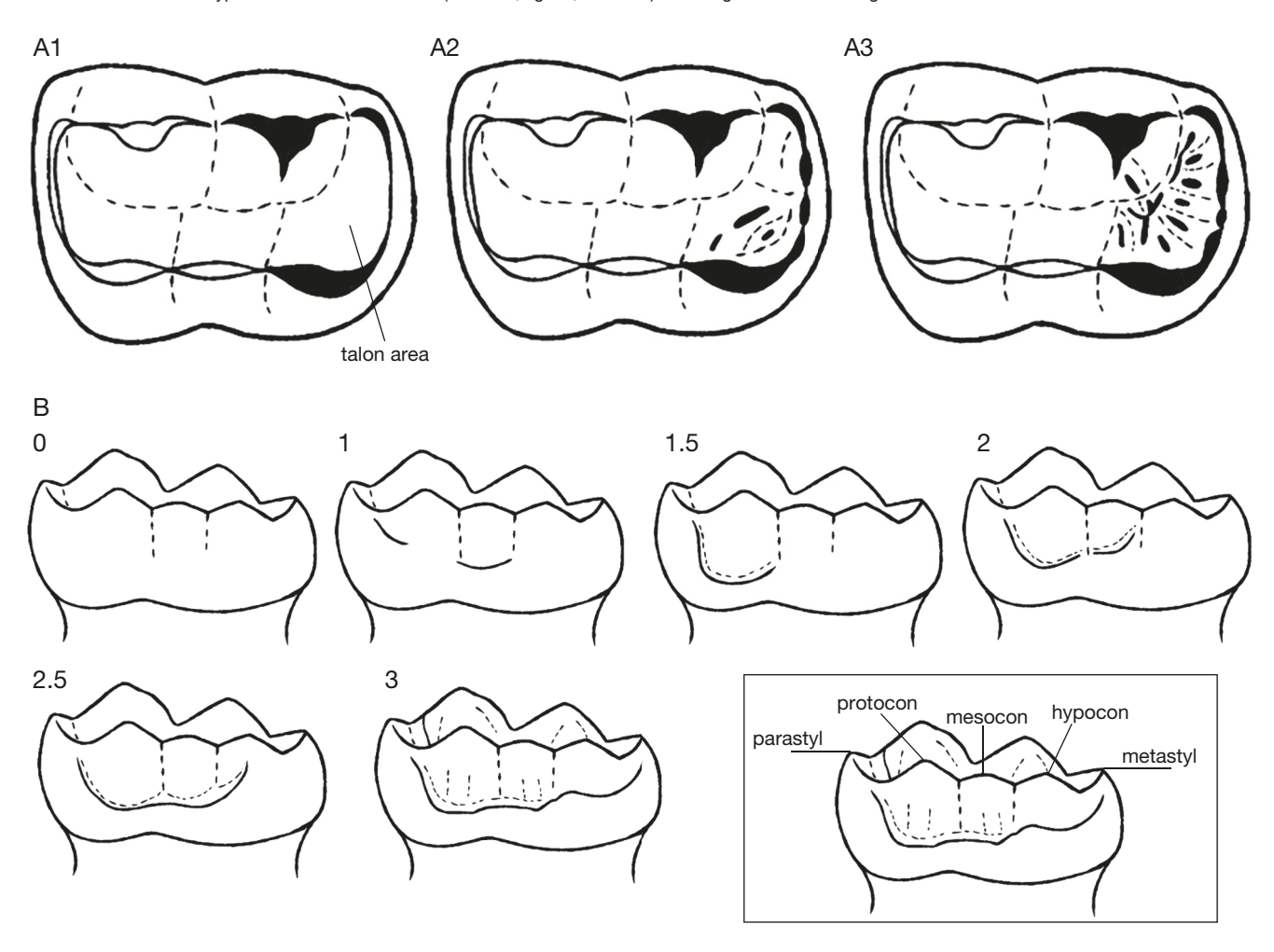
APPENDIX 14. — Morphotypes of the lingual (inner) wall of the M1 metacone: 0, completely smooth inner wall; 0.5, main edge ending halfway (0.5) or of the height of the inner wall of the metacone; 1, single, strongly developed edge, running from the base of the wall to the top of the metacone; 1.25/1.5/1.75, main edge is accompanied by 1-2 grooves, additional structures and tubercles, which concentrated mainly at the base of the wall; 2, strongly developed main ridge, running in the form of a thick strip from the top of the crown in the mesio-medial direction, we also deal with 1-2 accompanying ridges and a series of 4-6 additional, small cusplets. They form a series running from the base of the wall at its junction with the main ridge to the distal edge of the metacone; 2.5, stronger development of structures accompanying the main edge than in the morphotype 2, of which 2-3 additional ones reach 3/4 of the height of the wall. Based on Rabeder (1999: 46, fig. 26, modified). The diagram shows the lingual side of the left M1.



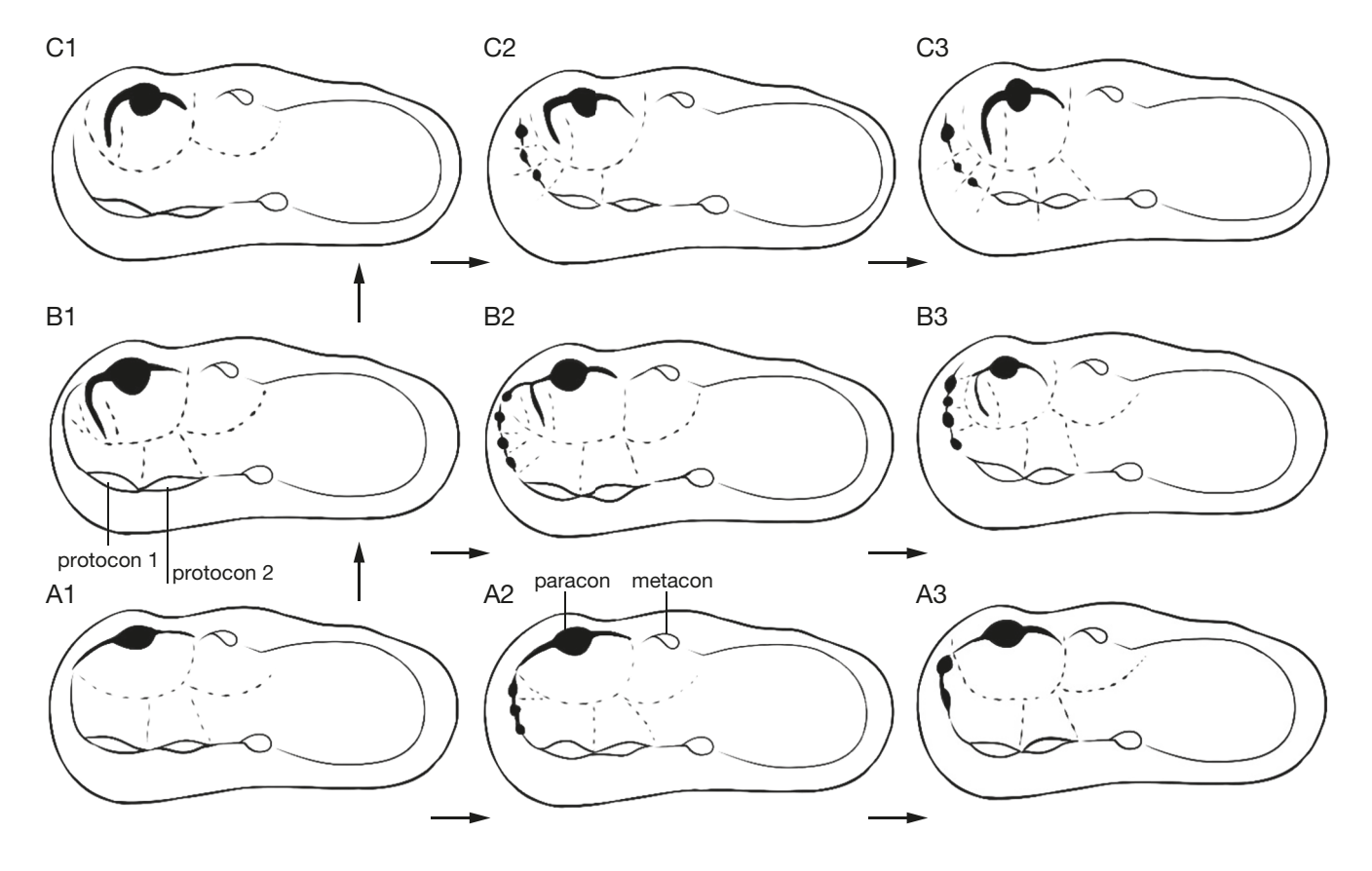
APPENDIX 15. — Morphotypes of the buccal (inner) wall of the M1 protocone and mesocone: **A**, simple structure and inner walls devoid of any grooves, edges and structures. They are also absent from the wide and deep transverse groove separating them; **B1**, first, still thin and narrow grooves and lines are delicately marked at the base of the inner wall of the protocone; **B2**, moderately developed lines and structures are also present on the mesocone; **B3**, strongly developed grooves and lines; low and transverse cusplet is present on the transverse groove separating the walls of the protocone and mesocone; **C1/C2/C3**, presence of thickened and strongly developed grooves, lines and edges at the base of the inner wall of the mesocone; **D2**, thick and strongly developed, numerous grooves and edges present on the inner walls of the protocone and mesocone, the length of which reaches 2/3 of the height of these walls; **D3**, numerous, exceptionally strongly developed grooves and edges ending slightly below the apexes of both cusps and with one continuous edge running parallel to both cusps. Based on Rabeder (1999: 47, fig. 28, modified). The diagram shows a view from the occlusal side of the right M1.



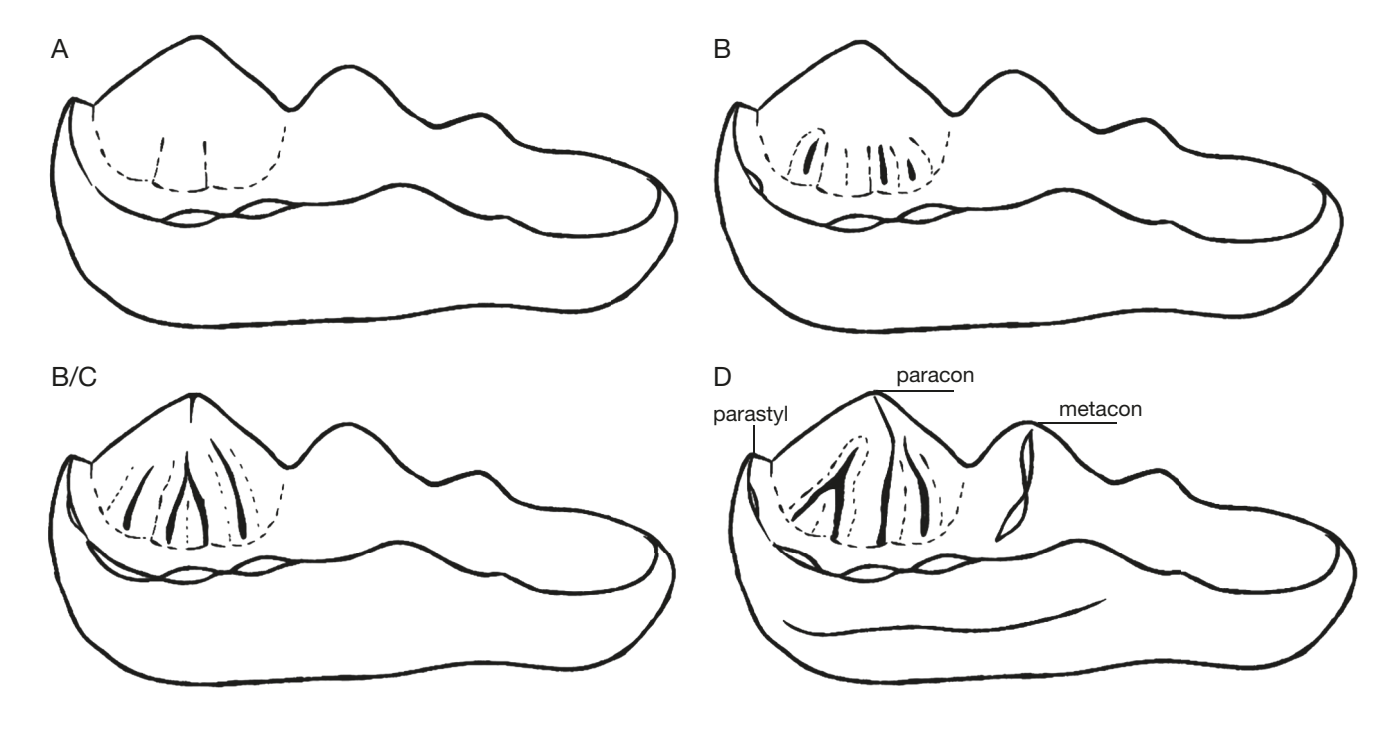
APPENDIX 16. — A, Morphotypes of the inner talon field M1: A1, smooth or almost smooth surface; A2, several longitudinal grooves, lines and additional small cusplets; A3, several longitudinal grooves, lines and additional small cusplets filed the area; B, morphotypes of the M1 lingual cingulum: 0, without a lingual cingulum; 1, poorly developed lingual cingulum, present in the mesocone; 1.5/1.75, lingual cingulum occurs at the base of the protocone and the mesial wall of the mesocone (1.5), reaching 2/3 of its height (1.75); 2, well-developed lingual cingulum reaches from the mesial wall of the protocone, along its base, to the notch between the mesocone and the hypocone; 2.5, well-developed lingual cingulum reaches half the length and height of the hypocone; 2.75, the lingual cingulum reaches up to 3/4 of the length and height of the hypocone; 3, the lingual cingulum runs along the entire length of the crown, from the mesial wall of the protocone to the distal wall of the hypocone. Based on Rabeder (1999: 46, fig. 27, modified). The diagram shows the lingual view of the left M1.



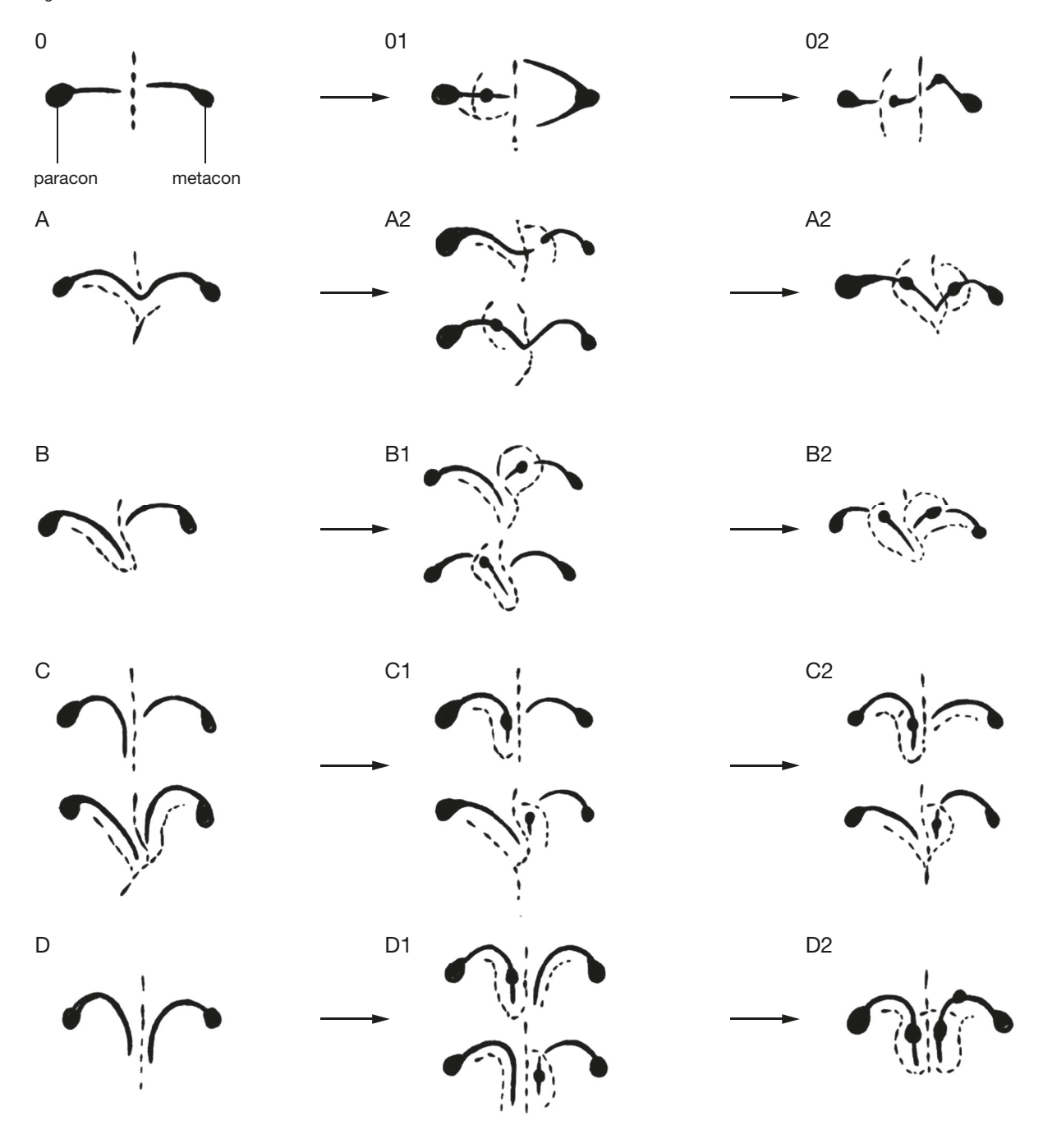
APPENDIX 17. — Second upper molar (M2). Description. An elongated and rectangular M2 has all main cusps connected by a crest running by almost entire crown length and following the tooth outline. The trigon in most specimens is quite expanded and broad, while the talon is elongated and narrowing distally. The rounded, high paracone is located far from the metacone and separated from it by a shallow but distinctive valley. Morphotypes of the M2 parastyle complex: A1, single parastyle edge connected to the protocone edge, without any cusplets in the mesial part; A2, A3, similarly as in A1 developed connection between the parastyle and metastyle edges, distinguished by having 1-4 small cusplets in the mesial part of the protocone edge (A2) or 1-2 larger ones, one of which can already be defined as a parastyle on the mesial side of the protocone edge (A3); B1/B2, an additional, lateral edge that runs through the transverse groove. The degree of development of the cusps is identical to that of the adequate ones in morphotypes A1-A3; C1/C2/C3, broken connection between the edges of the parastyle and protocon. Based on Rabeder (1999: 61, fig. 31, modified). The diagram shows the occlusal side view of the left M2.



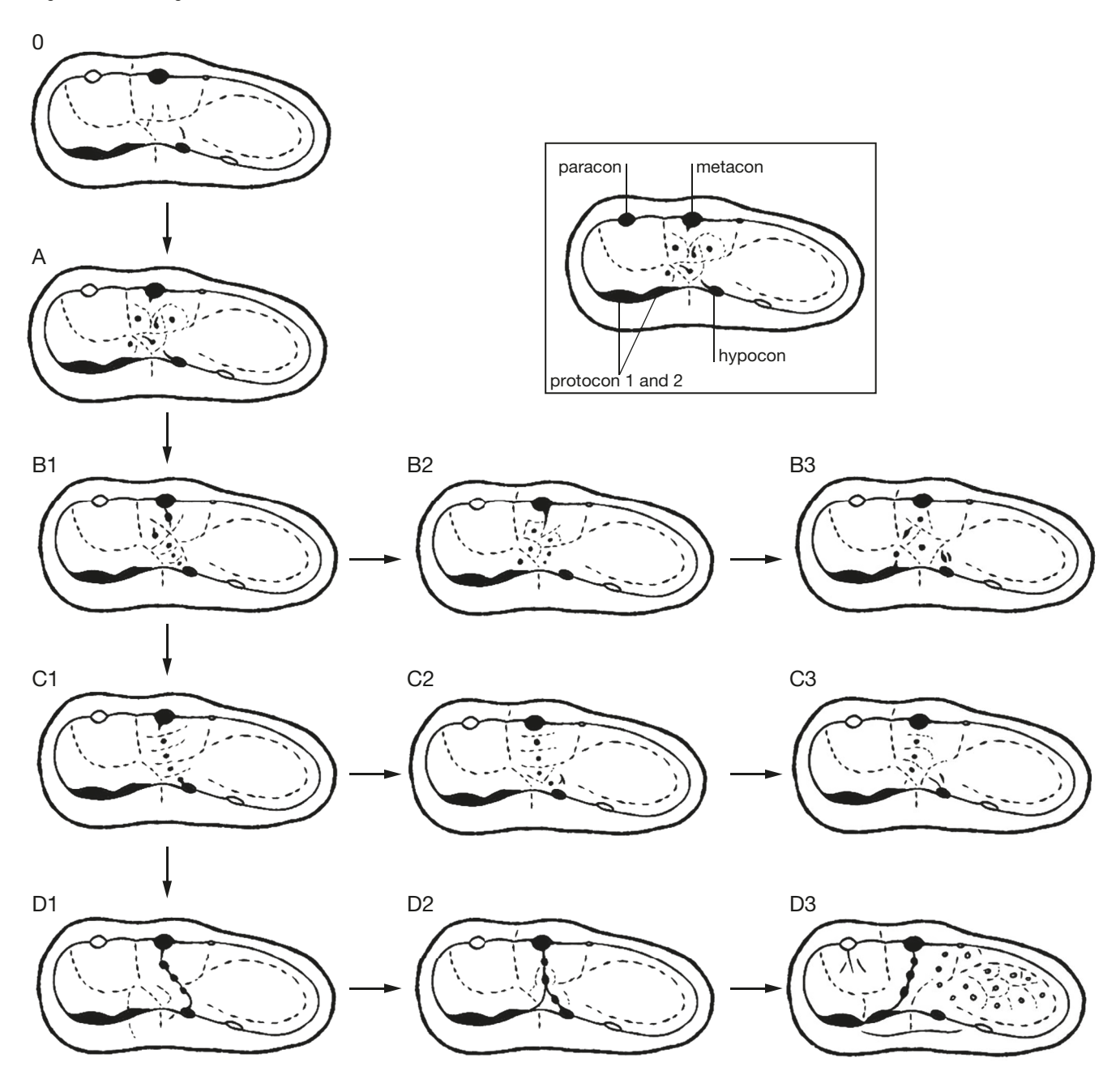
APPENDIX 18. — Morphotypes of the M2 groove and ridge formation on the lingual (inner) wall of the paracone: **A**, completely smooth, inner wall; **A/B**, **B**, present short and weakly developed lines and ridges, reaching a maximum of 1/2 the height of the inner wall of the paracone; B/C, present strongly developed and marked lines and edges, which reach up to 3/4 of the wall height; **C**, present one, dominant edge, which runs along the entire height of the inner paracone wall from the base to its apex. Based on Rabeder (1999: 65, fig. 36, modified). The diagram shows a view from the lingual side of the left M2.



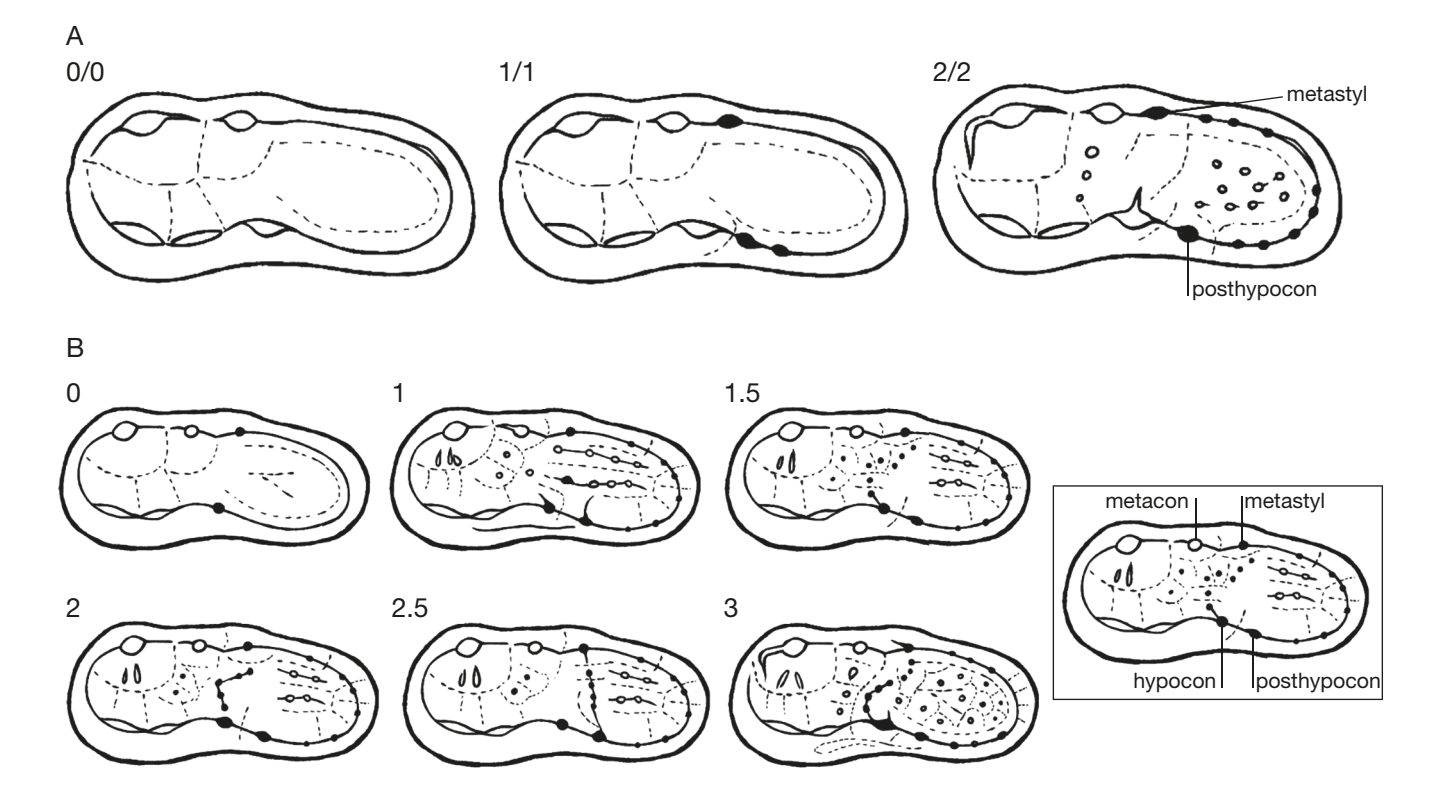
APPENDIX 19. — Morphotypes of the M2 mesostyl complex: **0**, one straight line, the rear edge of the paracone and the front edge of the metacone, without any additional structures; **A**, the rear edge of the paracone and the front edge of the metacone form a characteristic M-shaped complex with rounded edges; **A1**, one small cusplet on one of the edges; **A2**, on both edges several small and well recognised cusplets; **B**, without additional cusplets and structures, distal edge of the paracone is so strongly bent that the connection with the front edge of the metacone was lost. The transverse furrow is arched as a result; **C**, morphotype was found, characterized by a strongly curved of one of the edges and without additional structures; **D/D1**, strongly curved both edges; **D** without additional structures; **D1**, with a large cusplet on the front edge of the metacone. Based on Rabeder (1999: 62, fig. 32, changed). The diagram shows the view from the lingual side of the left M2.



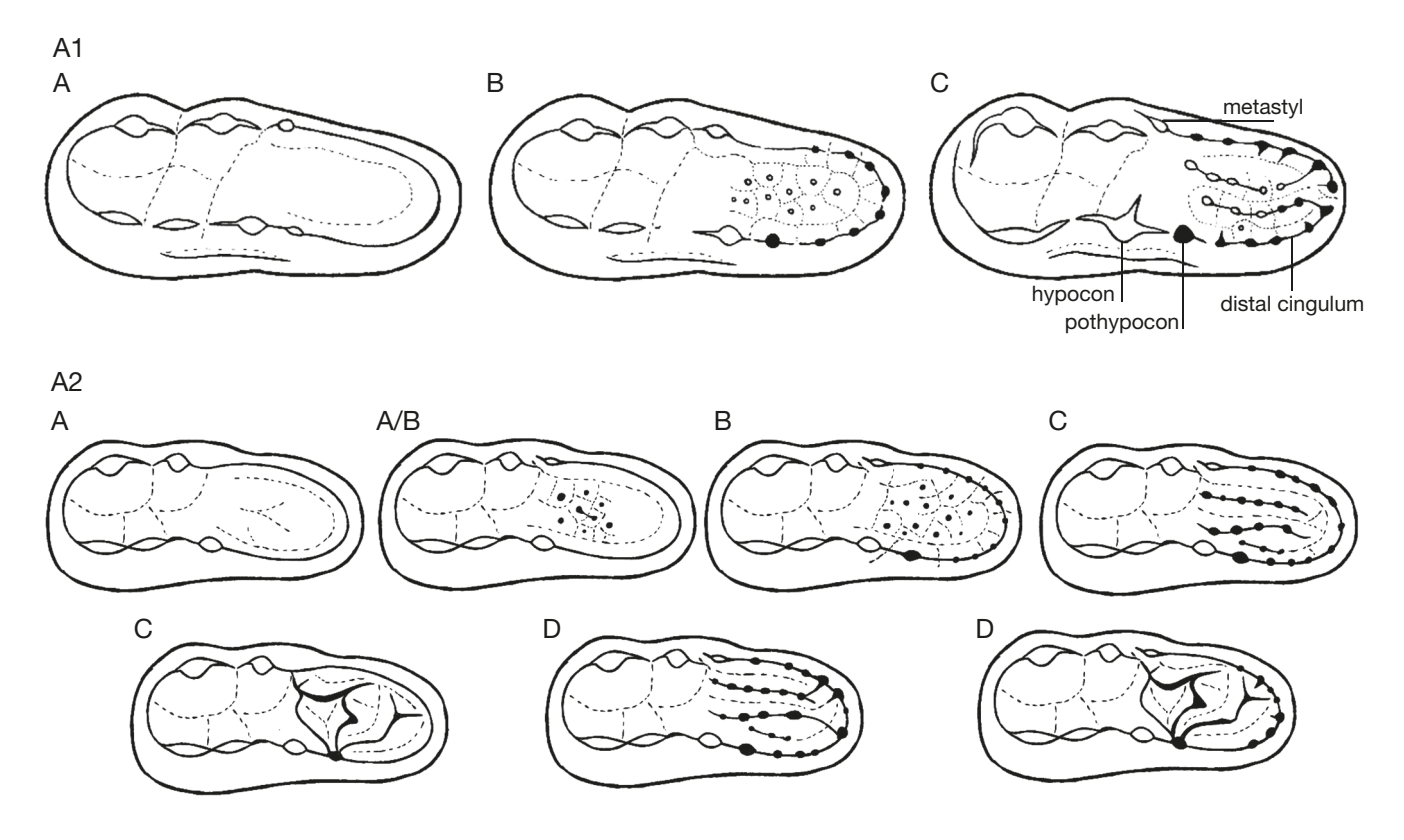
APPENDIX 20. — Morphotypes of the M2 metalophe: A, between the metacone and the edge of the protocone there is an enlarged one cusp, but the entire structure is completely disorganised; **B1**, between the metacone and the hypocone there is a poorly developed and organized row of small cusplets, in some interrupted, while in a few there are only 2-3 enlarged cusplets; **B2**, weakly developed and organised series of cusplets, running between the second protocone and the hypocone, in some they are connected; B3, moderately developed series of cusplets, running between the metacone and the second protocone; C1, well-developed, more regular-shaped row of cusplets runs between the hypocone and the metacone; C2, well-developed, regularly-shaped row of cusplets runs from the metacone between the second protocone and the hypocone or bifurcates between them; C3, strong developed and regular row of cusplets runs between the metacone and the second protocone; **D1**, strongly developed row of cusplets in the form of a relatively high edge and with a regular shape runs between the metacone and the inner wall of the protocone; **D2**, thick and high edge, formed by a row of cusplets, runs from the base of the metacone and runs, bifurcating, towards the hypocone and protocone or between these two tubercles, heading towards the inner surface; Based on Rabeder (1999: 63, fig. 33, modified). The diagram shows the lingual view of the left M2.



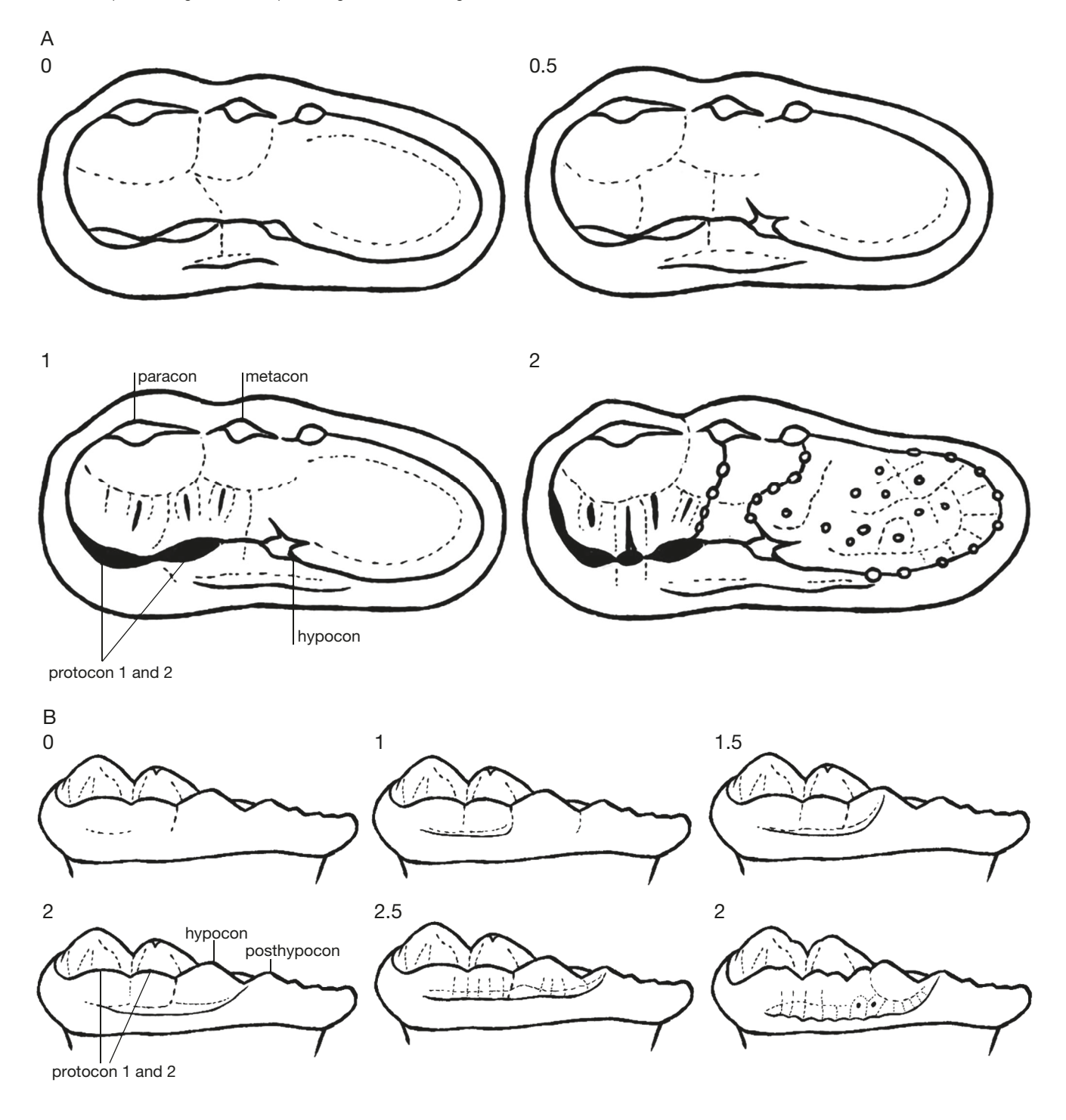
APPENDIX 21. — **A**, Morphotypes of the M2 metastyle and posthypocon: **0**, lack of metastyle; **1**, small metastyle, developed in the form of a low and rounded cusp; **2**, strongly developed and large metastyle. Based on Rabeder (1999: 65, fig. 38, modified). The diagram shows the lingual view of the left M2; **B**, morphotypes of the M2 posteroloph: **0**, there are no cusplets between the metastyle and the hypocone; **1**, small, weakly developed cusplets located between the metastyle and the hypocone do not form a transverse, regular row; **1.5**, half of cusplets between the metastyle and the hypocone formed in a fairly regular row; **2**, well developed teeth row located between the metastyle and the hypocone, still has 20-30% of its surface developed in a poorly organised or incompletely developed form. Sometimes an additional, less marked tooth row appears, located behind the posteroloph line; **3**, well-developed and fully formed tooth row in a regular. Based on Rabeder (1999: 64, fig. 34, modified). The diagram shows the lingual view of the left M2.



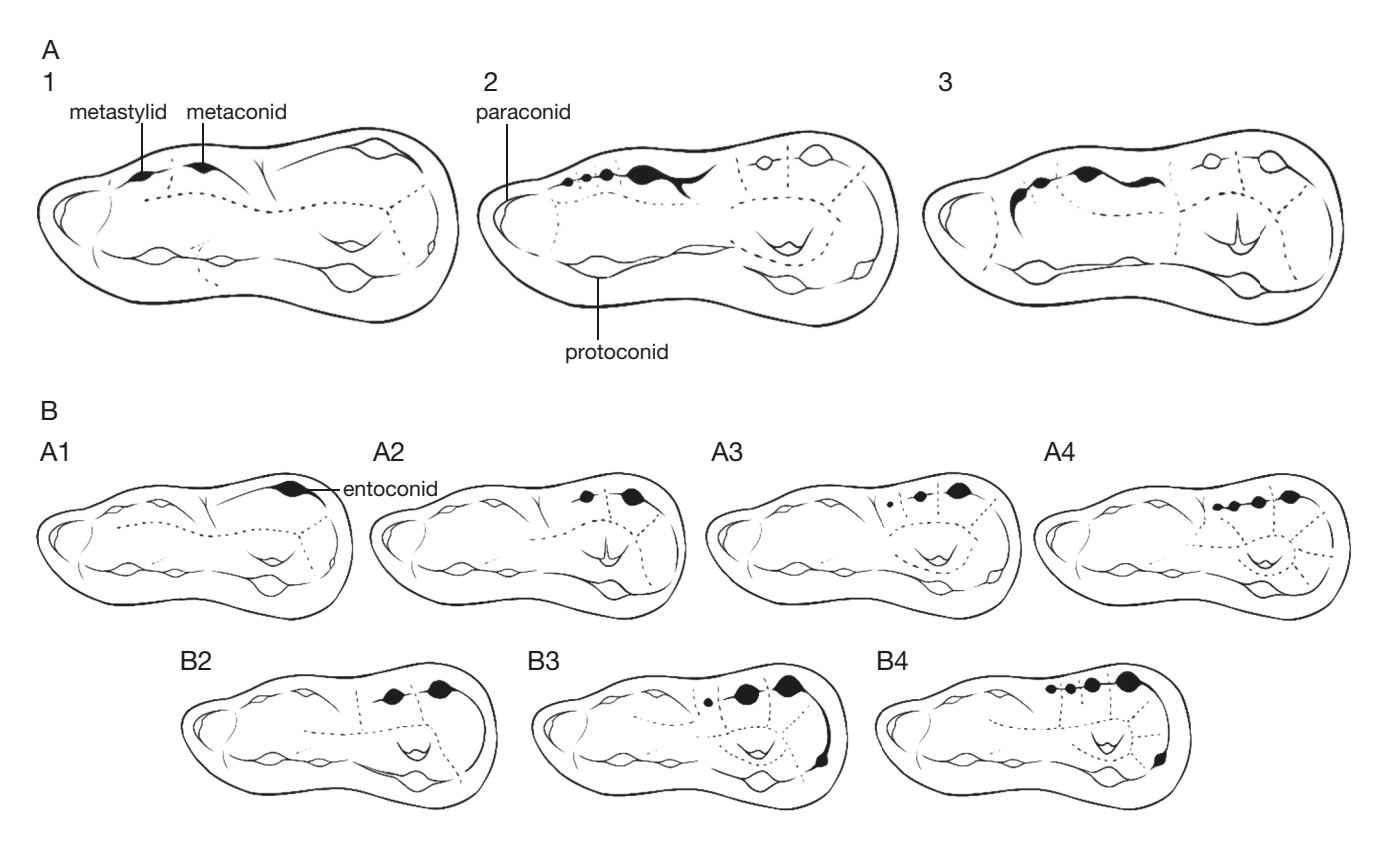
APPENDIX 22. - A1, Morphotypes of the M2 distal cingulum: A, smooth distal cingulum; absence of cusplets between the metastyle and the posthypocone; A/B, stronger development of the distal cingulum, with stronger grooves and small and weakly developed cusplets; B, distal cingulum with weakly to moderately developed cusplets and moderately developed additional structures between the metacone and the hypocone; cusplets developed in regular series; grooves and lines strongly marked; C, strongly developed and complicated distal cingulum, with a series of cusplets, grooves, lines and other structures, that often come into contact with the elements of the occlusal surface of the talon. Based on Rabeder (1999: 65, fig. 37, modified). The diagram shows the occlusal view of the left M2; A2, morphotypes of the M2 talon structures: A, smooth surface without any structures; A/B, weakly developed cusplets, grooves and other structures cover approximately half of the talon surface; B, the talon surface is completely covered with moderately strong developed structures, which occur in an irregular form; B/C, strongly developed structures begin to take on, at least in part, already regulated forms of elongated, longitudinal lines; at the same time, a large part of this area still has a strongly irregular character; C, strong structures are developed as elongated, thick and longitudinal lines cover completely talon surface; these thick grooves, lines or rows of cusplets still do not connect with the distal cingulum; D, strongly developed cusplets, grooves and other structures create thick, longitudinal edges, coming into contact with the distal cingulum and co-creating cusplets. Based on Rabeder (1999: 64, fig. 35, modified). The diagram shows the occlusal view of the left M2.



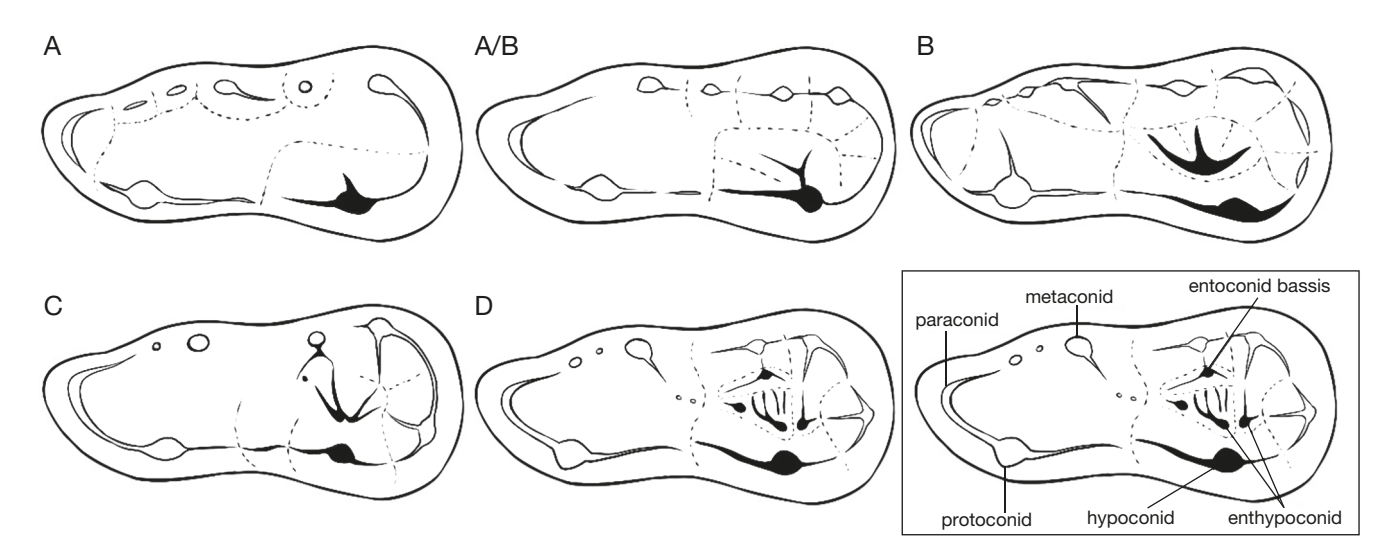
APPENDIX 23. — **A**, Morphotypes of the M2 lingual (inner) wall structures of the protocone: **0/0.5**, smooth inner wall; **1**, few weakly developed grooves and lines that run lingually but reach a maximum of half the protocone height of the tubercle wall; **1.5**, many of these structures are more strongly developed and transformed into thin but clearly marked edges reaching the first protocone; **2**, numerous, strongly developed and thick grooves, lines and edges. Based on Rabeder (1999: 66, fig. 39, modified). The diagram shows the occlusal view of the left M2; **B**, morphotypes of the M2 lingual cingulum: **A**, lack of lingual cingulum development or its presence only in the form of a short and thin groove; **0.5**, cingulum extends from the base of protocone 1 to the indentation between protocone 2 and hypocone; **1.5**, cingulum runs from the base of the protocone 1 and reaches behind the hypocone; present 1-2 small cusplets; **2**, strong cingulum reaches the border of the hypocone and posthypocone; **2.5/3/3.5**, strong lingual cingulum in the form of a wide and flattened edge extends to the base of the posthypocone; on its surface present large 1 (3) or 2 (3.5) cusplets. Based on Rabeder (1999: 66, fig. 40, modified). The diagram shows the lingual view of the left M2.



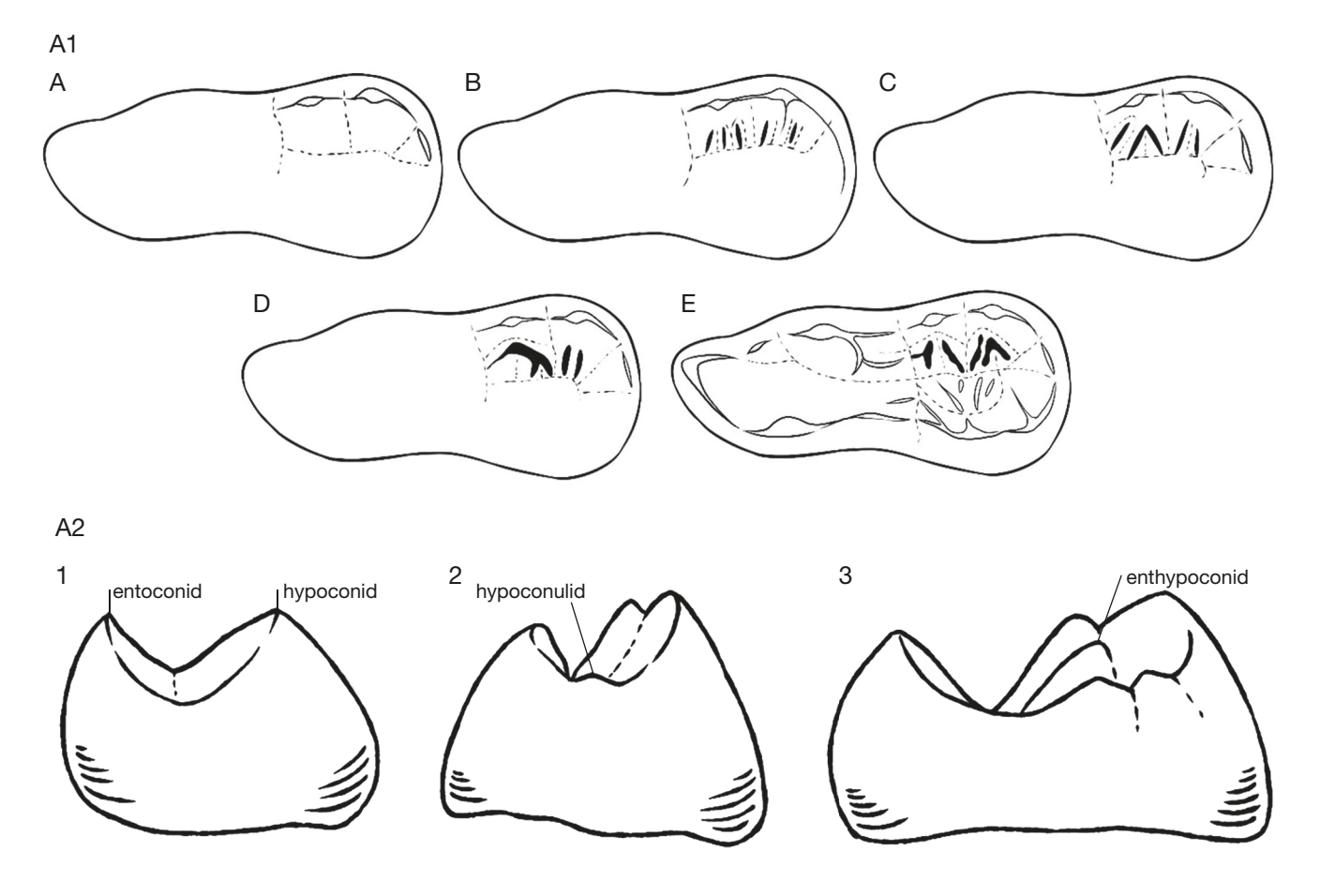
APPENDIX 24. — First lower molar (m1): A, Morphotypes of the m1 metastylid: 1, single metastylid; 1.5/2.5, metastylids most often occur in the form of a short row of teeth, located one behind the other, usually slightly smaller and more closely positioned in relation to the full morphotypes. This row of teeth connects with the lingual arm of the paraconid; 2, double metastylid; 3, triple metastylid, developed on one edge, running from the metaconid to the protoconid. Based on Rabeder (1999: 21, fig. 3, modified). The diagram shows the occlusal side view of the left m1; B, Morphotypes of the m1 entoconid number: A1, simple structured single entoconid, lack of any additional structures; A2, double entoconid; mesial entoconid 2 smaller; A3, triple entoconid, forming an arched row, with their size decreasing mesially; A4, quadruple entoconid, with their size decreasing significantly mesially; B2, double entoconid, both cusps of similar size; B3, triple entoconid has two distal cusps of similar dimensions, the most mesially located constitutes about 1/3 of their size; B4, quadruple entoconid forms weak curve and runs almost parallel to the edge of the m1 talonid; the most distally located cusp is the largest, while the 3 others constitute 40-50% of its size. Based on Rabeder (1999: 21, fig. 4, modified). The diagram shows the occlusal side view of the left m1.



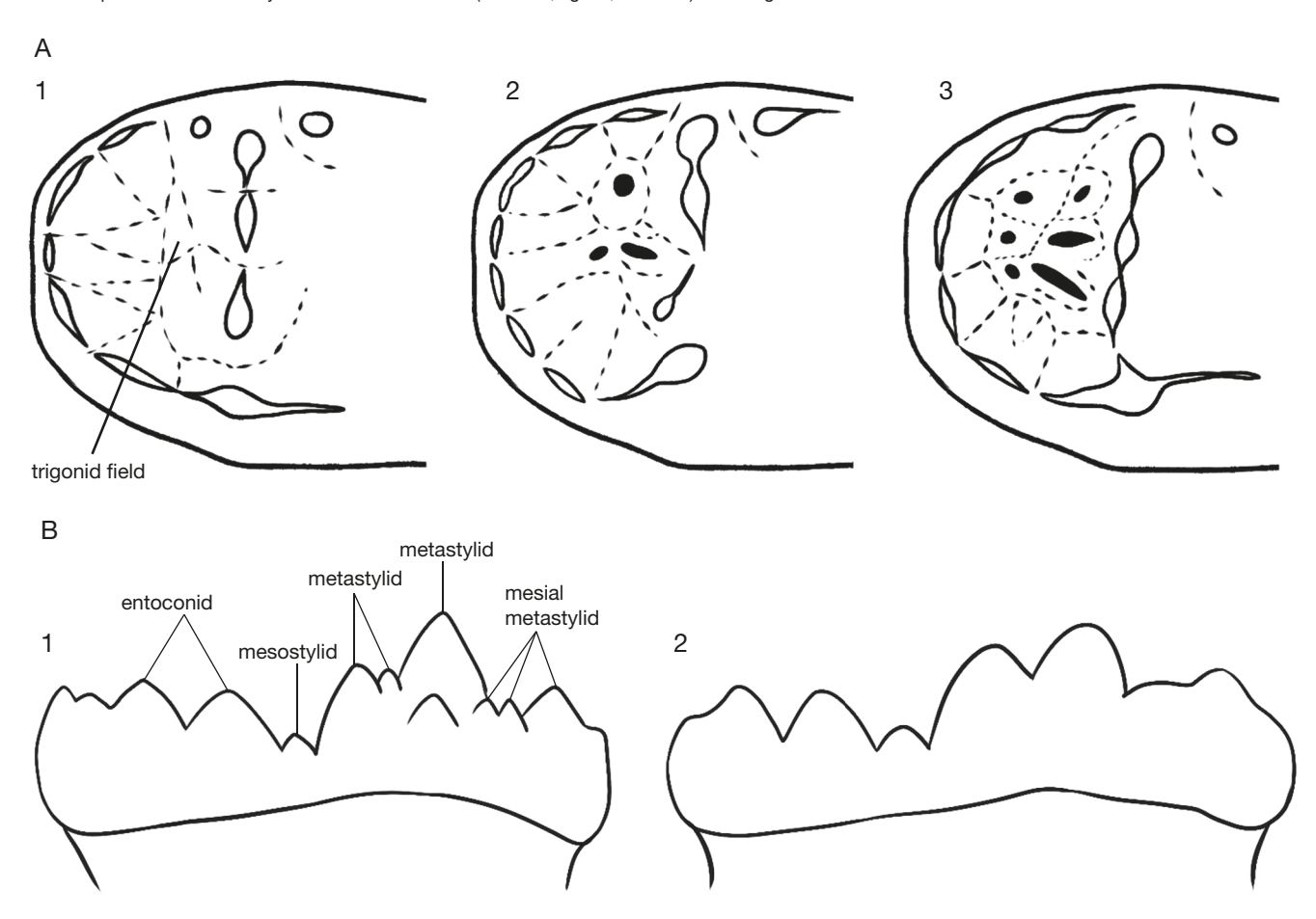
APPENDIX 25. — Morphotypes of the m1 enthypoconid; A, without additional structures; A/B, weakly developed enthypoconid, which is not separated from the hypoconid by a longitudinal groove; most often Y-shaped branched structure; B, well-developed enthypoconid separated from the hypoconid by a groove; C, strong enthypoconid with thin grooves and lines on its lingual wall, which often connect with similar structures on the longitudinal groove, separating it from the hypoconid; D, bipartite or tripartite enthypoconid and the above-mentioned structures are considerably strongly developed. Based on Rabeder (1999: 22, fig. 5, modified). The diagram shows the view from the occlusal side of the left m1.



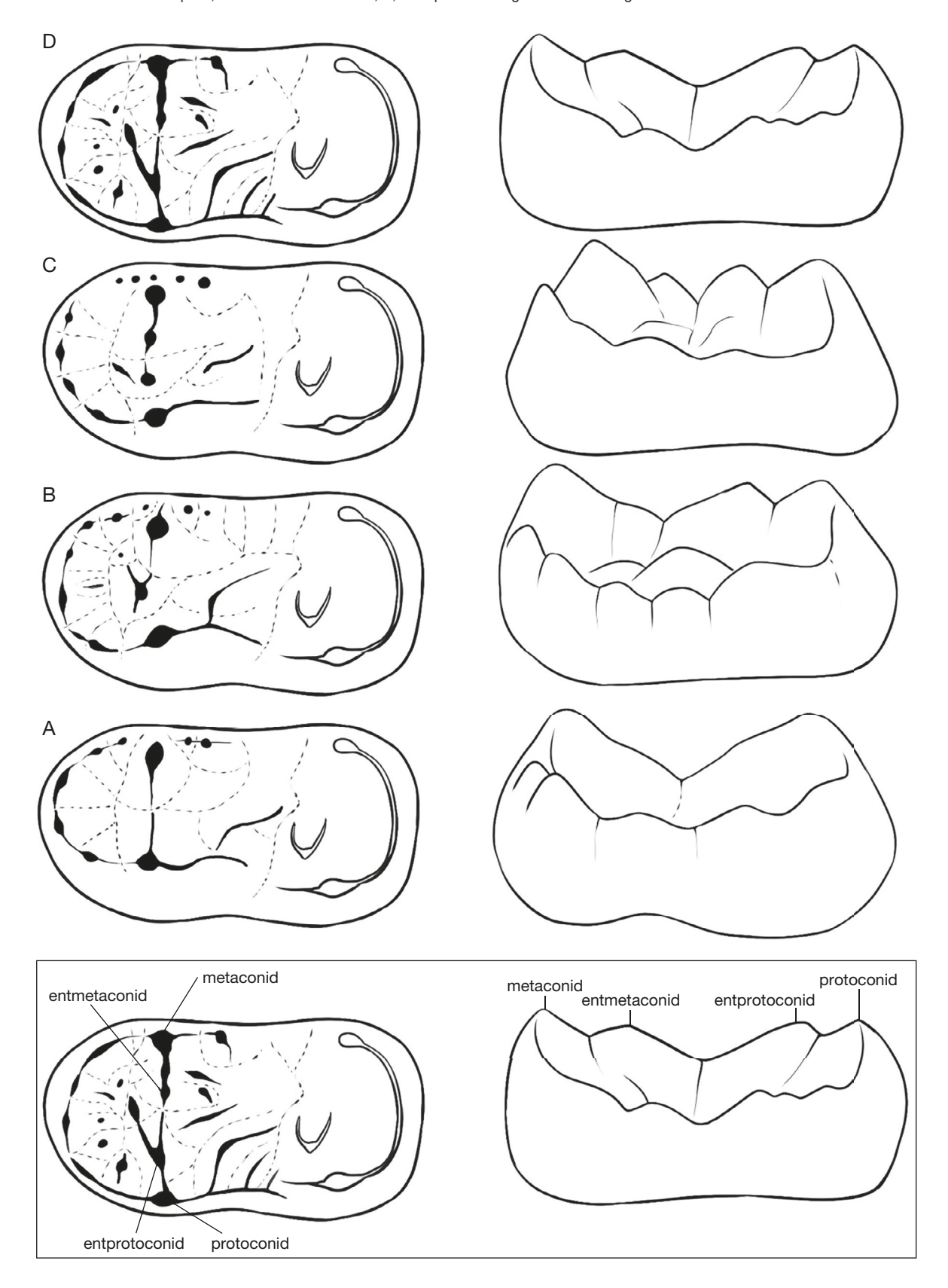
APPENDIX 26. — A1, Morphotypes of structures on the inner wall of m1 entoconid: presentation of the evolution of the development of from the most primitive (A) to the most advanced (C) and the terminology of the basic tubercles and structures based on which they were designated: A, absence of any structures; A/B, several thin and weakly developed lines are delicately outlined on the basis; B, moderately developed grooves and lines reach up to half the height of the lingual wall of the entoconid; B/C, strong structures; present a longitudinal groove separating entoconid 1 and 2, separation is not fully developed and occupies 1/2 of the length encompassing the lingual wall of the entoconid; C, strong structures and a longitudinal groove separating entoconid 1 and 2, which covers approximately 2/3 of the length; D, strong grooves and lines and the longitudinal groove separates it along its entire length entoconid 1 and 2; E, considerably strong structures in the form of thick edges; present second longitudinal groove on the inner wall of entoconid 1, which partially or completely separates it from the other entoconids. Based on Rabeder (1999: 22, fig. 6, modified). The diagram shows a view from the occlusal side of the left m1; A2, morphotypes of the m1 talonid distal edge: 1, deeply indented and narrow; 2, decidedly widened, with 1-2 cusplets; 3, considerably wide, with 2 cusplets, and the hypoconulid which developed an edge that, running in the lingual-mesial direction, comes into contact with the enthypoconid and with its edges creates a strongly developed, relatively thin but high, zigzag-curved edge. Based on Rabeder (1999: 23, fig. 7, modified). The diagram shows a distal view of the left m1.



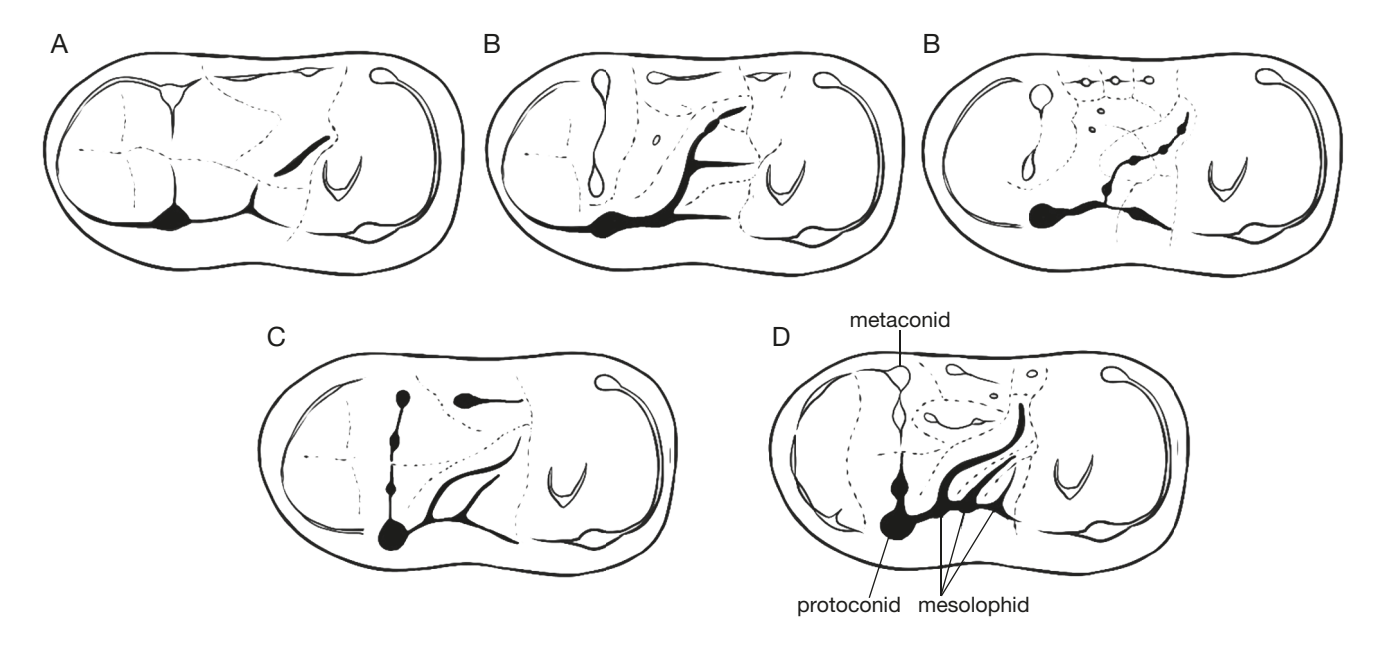
APPENDIX 27. — Second lower molar (m2): **A**, morphotypes of the structures on the inner surface of the m2 trigonid: **1**, without any structures or with very weakly developed; **2**, moderately developed 2-3 cusplets; **3**, strong 5-8 cusplets and lines. Based on Rabeder (1999: 29, fig. 10, modified). The diagram shows a view from the occlusal side of the left m2; **B**, morphotypes of the m2 cusplets on the metastylid: **1**, metastylid complex is divided into mesial, distal and parietal, located in the middle part of the lingual wall of the metaconid. The number of cusplets present on the metastylid varies between 1 and 7; **2**, metastylid complex has no other cusplets or there are very few. Based on Rabeder (1999: 29, fig. 11, modified). The diagram shows the occlusal view of the left m2.



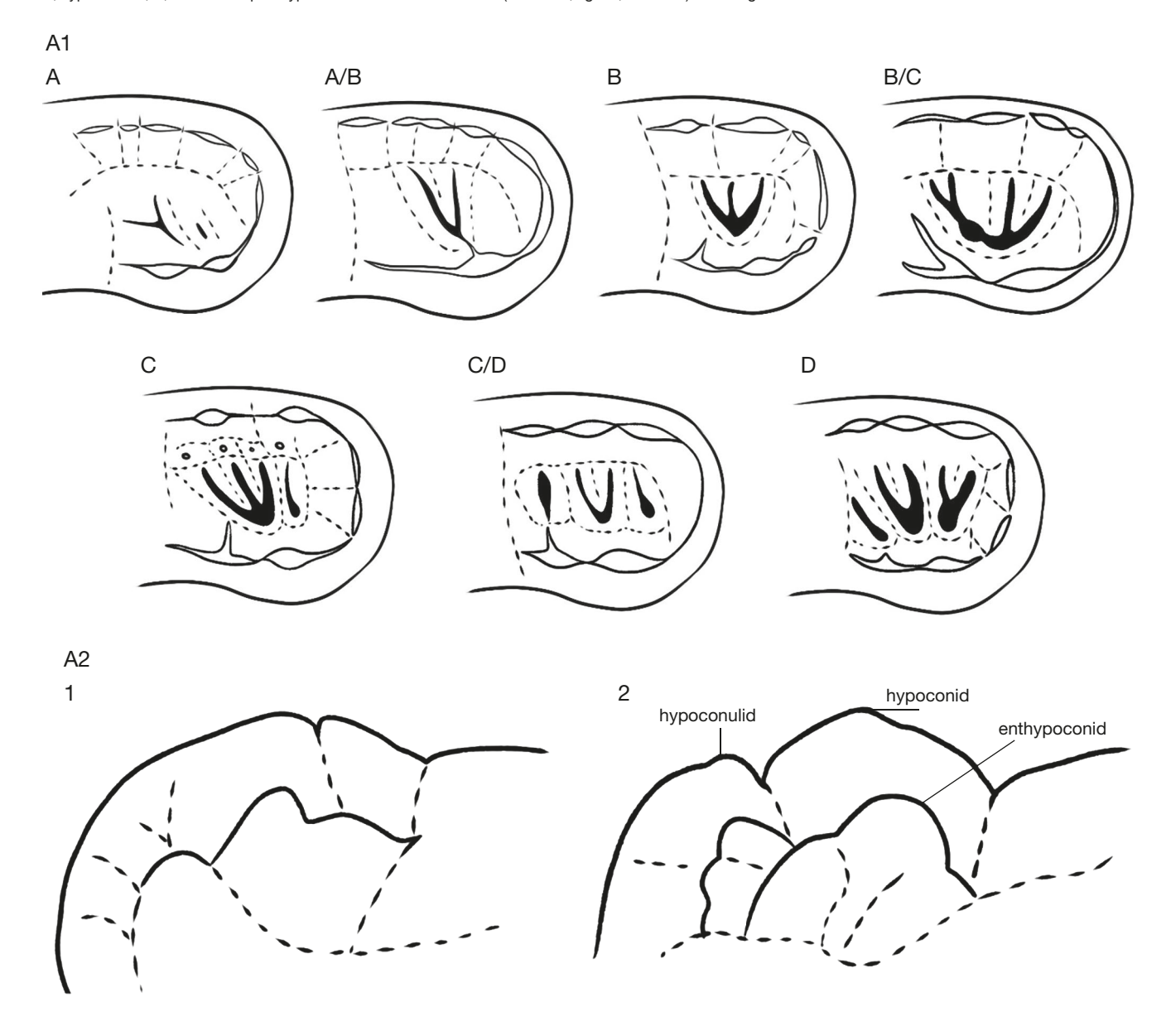
APPENDIX 28. — Morphotypes of the m2 metalophid: based on Rabeder (1999: 29, fig. 9, modified). The diagram shows the occlusal view of the left m2; **A**, develops on the edges of the protoconid (lingual) and metaconid (buccal) creating a high, transverse structure; **A/B**, weakly developed thickening on the lingual edge of the protoconid; **B**, entprotoconid occurs on the lingual edge of the protoconid, which interrupts the continuity of the entire structure. It is formed a three-cusped metalophid, and the edge itself is relatively short and runs from the metaconid only to the entprotoconid. It is usually not located in a straight line between the metaconid and the protoconid, but shifted either more lingually or more buccally; **C**, prominent cusplet is present on the inner edge of the metalophid. The metalophid therefore contains 4 cusplets, which are not connected; **D**, 4 cusplets creating a continuous edge.



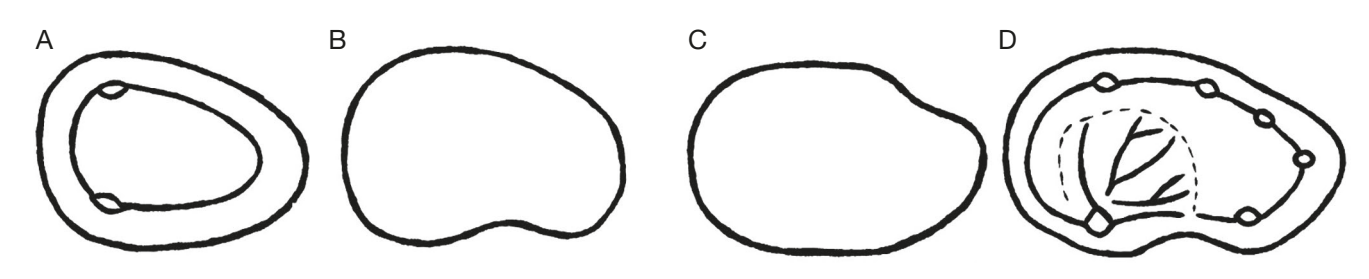
APPENDIX 29. — Morphotypes of the m2 mesolophid: **A**, not fully developed, main mesolophid; **A/B**, mesolophid is more strongly developed, but the connection is not completely closed; **B**, mesolophid is strongly developed and the connection is already fully closed; **B/C**, strong mesolophid; beginnings of the formation of a second, smaller mesolophid; **C**, low and short second mesolophid; another edge running transversely to the inner surface of the crown; **C/D**, higher and stronger second mesolophid; **D**, both mesolophids strongly developed and located most distally, a third, relatively short mesolophid occurs. Based on Rabeder (1999: 30, fig. 12, modified). The diagram shows the occlusal side view of the left m2.



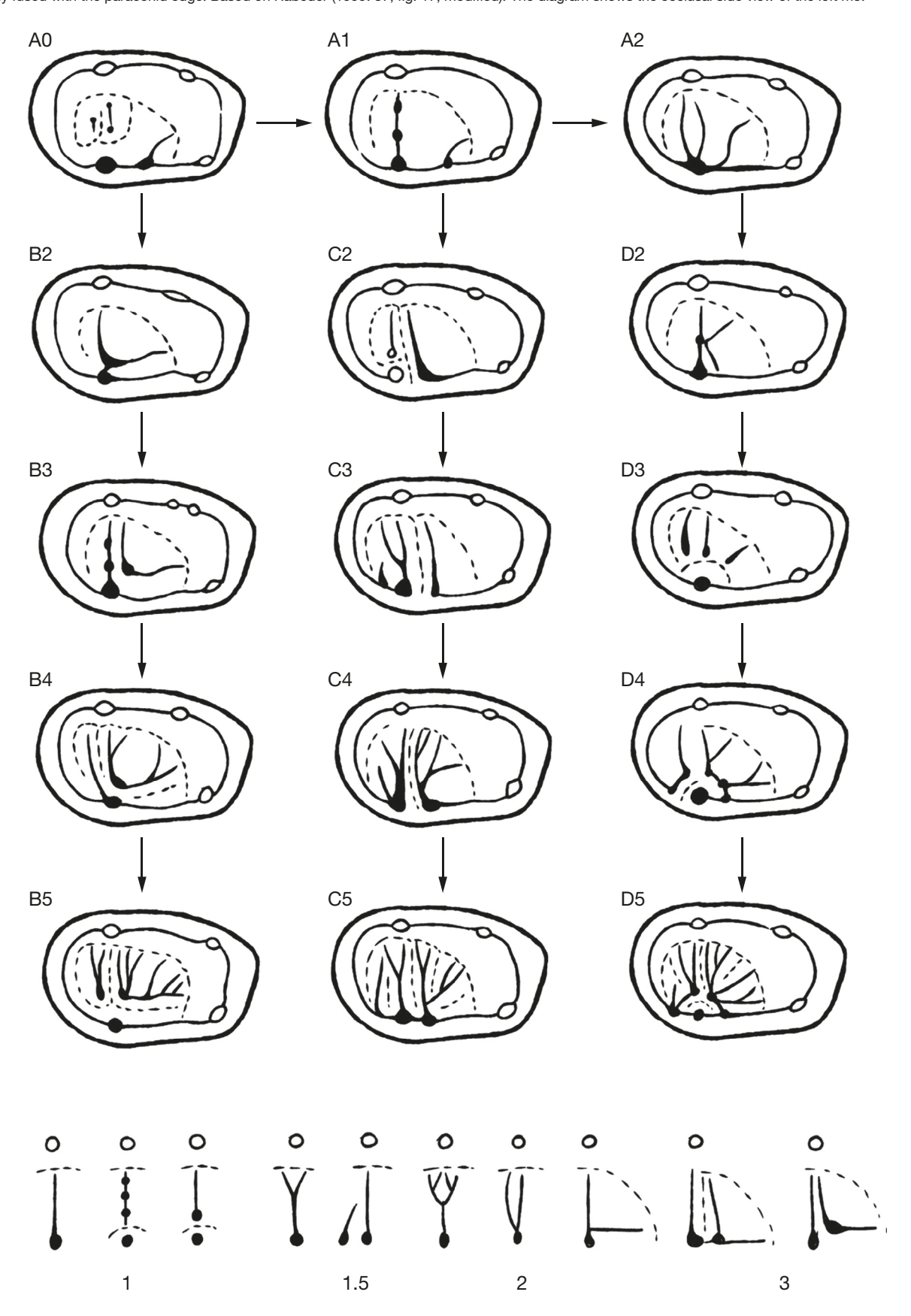
APPENDIX 30. — A1, Morphotypes of the m2 enthypoconid: A, lack of the enthypoconid, only delicate grooves and lines on the inner wall of the hypoconid; A/B, weakly developed enthypoconid, not separated from the hypoconid by a transverse groove; B, well-developed enthypoconid is separated from the hypoconid by a transverse groove; B/C, enthypoconid is not yet fully divided; C, enthypoconid is fully divided into two parts; C/D, present an incompletely developed third cusplet and a rim running from the hypostylid to both enthypoconids; D, enthypoconid is tripartite or there are other, additional forms that complicate its structure. Based on Rabeder (1999: 30, fig. 13, modified). The diagram shows the view from the occlusal side of the left m2. A2, Morphotypes of the m2 hypoconulid: A, hypoconulid; B, well-developed hypoconulid. Based on Rabeder (1999: 31, fig. 14, modified). The diagram shows the view from the occlusal side of the left m2.



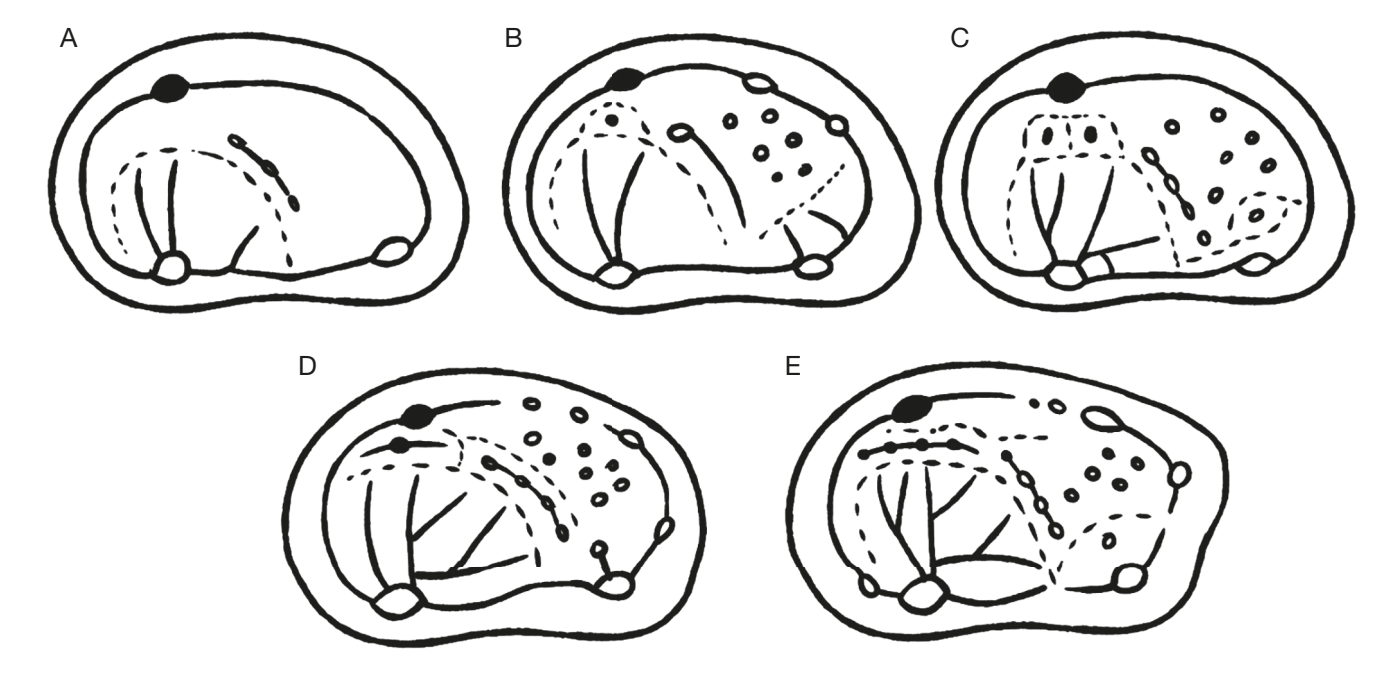
APPENDIX 31. — Third lower molar (m3): morphotypes of the m3 crown shape: **A**, oval or elliptical, without a buccal sinus and an elongated talonid; **B**, well-developed buccal concavity; **C**, considerably elongation of the talonid, the outline reference to an elongated oval; **D**, considerably elongation of the talonid; well-developed buccal concavity. Based on Rabeder (1999: 36, fig. 16, modified). The diagram shows the view from the occlusal side of the left m3.



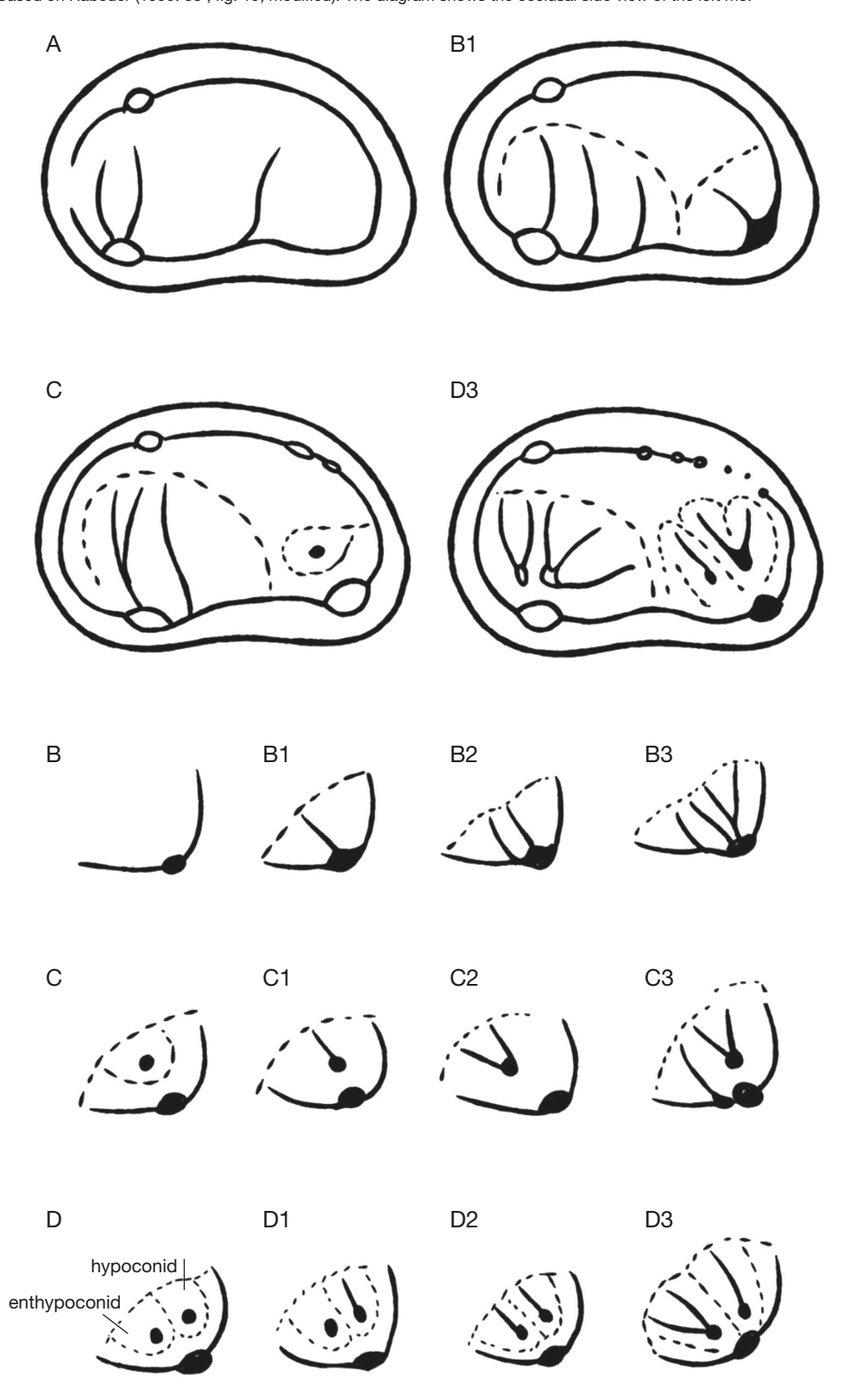
APPENDIX 32. — Morphotypes of the m3 protoconid: **A**, single mesolophid, which arises from the distal ridge of the protoconid and runs diagonally in the distolingual direction; **B**, lack of mesolophid; **C**, mesolophid runs lingually and parallel to the metalophid; **D**, protoconid starting at the apex and develops in the form of an arcuate edge running from the base of the mesolophid, through the entprotoconid to the back of the paraconid. This edge is often weakly developed and strongly fused with the paraconid edge. Based on Rabeder (1999: 37, fig. 17, modified). The diagram shows the occlusal side view of the left m3.



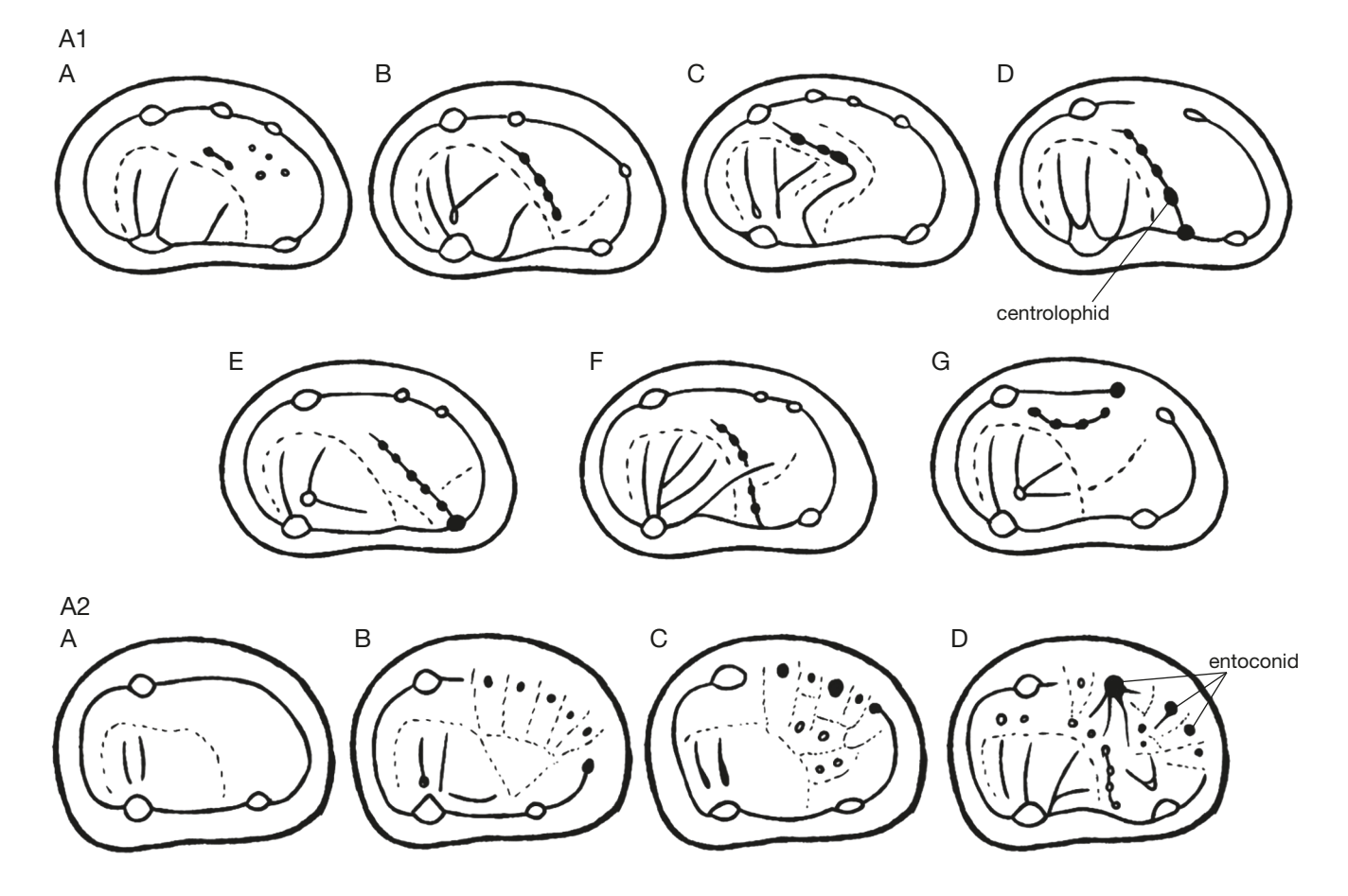
APPENDIX 33. — Morphotypes of the inner wall of the m3 metaconid: **A**, smooth surface; **B**, single cusplet or edge at the base; **C**, present two cusplets or edges located at the base; **D**, elongated ridge located on the buccal base of the metaconid; **E**, three or more cusplets or edges located at the base of the inner wall of the metaconid. Cusplets have elongated and thin edge connected to the centrolophid. Based on Rabeder (1999: 38, fig. 18, modified). The diagram shows the occlusal view of the left m3.



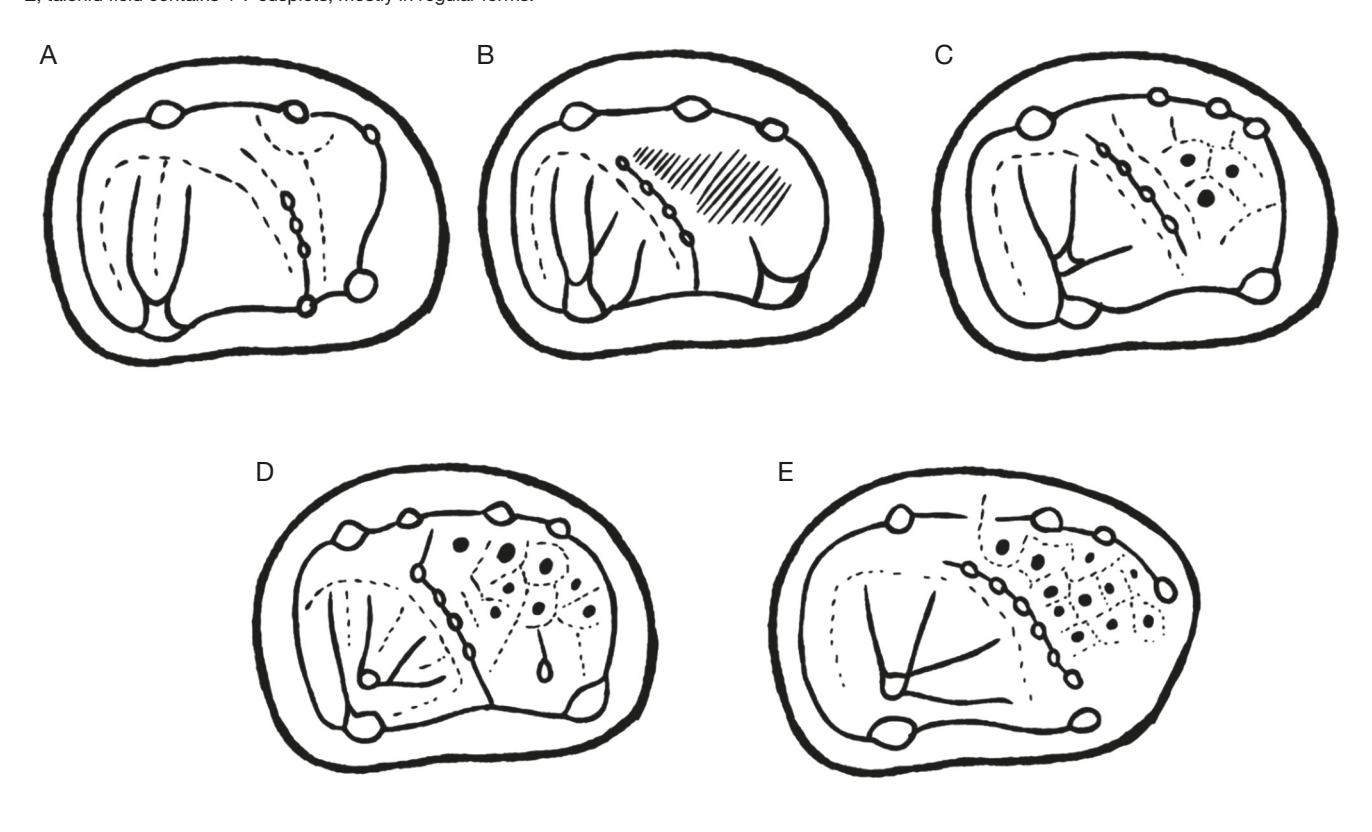
APPENDIX 34. — Morphotypes of the m3 hypoconid: **A**, without hypoconid; **B**, weakly developed hypoconid; **C**, present single enthypoconid; **D**, strong, double or triple enthypoconid. Based on Rabeder (1999: 38, fig. 19, modified). The diagram shows the occlusal side view of the left m3.



APPENDIX 35. — A1, Morphotypes of the m3 centrolophid: A, centrolophid absent; B, weak centrolophid starts from the disto-buccal side of the base of the metaconid and runs obliquely to the base of the buccal edge, from which it is separated by a deep groove; C, moderate centrolophid is connected to the mesolophid or to one of the distally running edges of the protoconid; D, centrolophid is connected to a cusplet on the buccal edge located between the hypoconid and the protoconid; E, direct or enthypoconid-hypoconid connection of the centrolophid; F, cross between the centrolophid and the mesolophid or one of the protoconid edges running distally; G, centrolophid in the form of a slightly curved arch to the base of the entoconid. Based on Rabeder (1999: 38, fig. 20, modified). The diagram shows the occlusal side view of the left m3; A2, morphotypes of the m3 entoconid: A, without entoconid and the lingual edge running behind the metaconid is smooth; B, lingual edge is divided by transverse grooves, which causes the separation of additional cusps; C, enlargement of 1-2 cusps in the tooth row; D, surface of the entoconids is covered with lines and edges; Based on Rabeder (1999: 39, fig. 21, modified). The diagram shows the occlusal side view of the left m3.



APPENDIX 36. — Morphotypes of the talonid m3 field surface: A, lacking the talonid field, and the entoconid and the inner surfaces of the distal edges are separated by deep grooves; B. weakly developed talonid field lacking cusplets on its surface; C. well-developed field with 1-3 cusplets; D. talonid field contains 4-7 cusplets; E, talonid field contains 4-7 cusplets, mostly in regular forms.



APPENDIX 37. — Morphological descriptions of metapodials.

The metacarpal 1 of the proximal articulation surface for the carpale 1 is indented in a saddle-shaped form. In the area of the medial epiphysis, there is a relatively wide fovea. The distal trochlea runs sloping from mesial-distal towards distoproximal direction.

The metacarpal 2 from TW are on average shorter but also bulky as other known metacarpal 2 of *U. deningeri*. The tuberculum mediale is well-developed.

The proximal articulation of the metacarpal 3 is set nearly at right angles to the end of the shaft, the dorsal face expanding considerably more than the distal. It is vertically convex, transversely concave. There is a broad oval surface set on its inner side. These two articular surfaces are divided from each other by a well-marked ridge. On the external side, there are two concave surfaces, which overhang and articulate with the metacarpal 4. They are deeply concave, and are more confluent than those of the metacarpal 2. On the mesial surface, a shallow groove of the proximal epiphysis runs diagonally, and trapezoidal ligament is attached to its upper part. The entire head of the bone is roughened for the reception of the ligaments binding the bone to the carpus and its fellow metacarpals. The shaft presents a triangular section proximally, and it is nearly circular in the middle and distally. A slight palmar ridge is developed behind, at the point where it joins the distal articulation, and it is flattened in front. The distal epiphysis is a bulb-shaped, and divided from the epiphyseal line of the shaft by deep dorsal and lateral depressions. The distal articulation is epiphyseal and symmetrical, having the inner tuberosity larger than the external one. On the palmar or inferior surface, they develop a short ridge in the median line. In general, the distal articulation is almost straight on the inner side and strongly curved on the external side.

Similarly moderately long and robust is the metacarpal 4. The metacarpal 5 is the largest and the most massive among all metapodials from TW. It's proximal epiphysis strongly thickened and flattened. The proximal articulation for the hamatum forms a continuous surface with that of the metacarpal 4, and as it is convex only in vertical direction and covers the entire end of the bone. The inter-metacarpal articulation is flattened, segmental in form, set at right angles to that for the hamatum, and interrupted inferiorly by a large ligamentary notch. In front, it rises an articular surface, which fits into a corresponding hollow in the metacarpal 4. Both proximal articulation facets run gently from mesial to the distal and protract medially. The medial articulation surface (for the metacarpal 4) shows two round lobes. The larger one, lobes anterior, runs down distally into triangular area. Externally, its head presents a large tuberosity, which affords attachment to strong ligaments that bind the bone to the hamatum, cuneiform, and pisiform. In addition, there is a large tuberosity on the palmar surface. The proximal epiphysis is deeply convex and the anterior limit ends with an

acute angle. Laterally, it develops a bulge and forms a semilunar convex surface. The shaft is proportionally shorter and more robust than triangular in section, to be more tapering, and to arch more decidedly in a palmar and outward direction than any other metacarpal bone. The distal epiphysis is strongly convex externally and concave internally, and the outer tuberosity is larger and set lower on the bone than the inner one. The medial part is narrower, while the palmar process is large and well-developed.

The proximal articulation of the metatarsal 2 is formed by a medial concavity that is frontally bulged and distally directed to the medial side. It also narrows pointedly in its distal direction, and has a triangular shape. Laterally, there are two wellmarked surfaces, both concave and joined to the metatarsal 3. The proximal articular surface for the entocuneiform is well pronounced and its median ridge is strongly shifted dorsally, while it is enlarged and curved frontally. Medially, it forms a short constriction and a distal bulge. The articular surfaces for the metatarsal 3 are separated from each other, and distal one is much larger and rounded. The proximal articulation facet for the tarsal 2 is composed by two different areas, clearly separated by large, well-developed, rounded and differ in size incisions. The mesial part is strongly widened and curved, non-isosceles triangle in shape. The distal part is smaller and rectangular in shape. An elongated, smaller indentation shifted towards the medial side and is positioned centrally. The larger indentation is more oval-shaped, situated more laterally and running anterior-medially. Medially, the articular surface is divided into two sides: frontally, the first one is horizontally elongated, stretching out and sloping to the medial plane. Behind, there is a flat and short end of the surface. Frontally, there is one concavity, similar to that described on the previous bone. Medial articulation is divided into two parts, smaller anterior and larger posterior ones. Both areas are separated by semi-circular incision, strongly pleated at the base. The lateral indentation is similarly developed and also splits into two, dimensionally different areas. The medial crest and a medial articulation facet slopes towards the medial side and are quite shallow and elongated. The metatarsal 2 has a massive and curved diaphysis, front-distally flattened and rectangular. Distal articulation is relatively large, rounded, and irregular-shaped. The medial epicondyle is more prominent than the lateral one.

The diaphyseal depth of the metatarsal 3 barely declines from proximal to distal. Two large rounded indentations of different size are notable on the proximal articulation facet for the entocuneiform. The latter is composed of a distal, approximately rectangular shaped part and another part, widening towards anterior, which has the shape of a non-isosceles triangle, the curved basis of which points anteriorly. Both parts are clearly separated in the assumed overlapping area by two incisions spanning from medial to lateral. The medial articulation facet is split into two parts. It is developed into a smaller mesial and a larger distal partial facet, which are separated by an incision that ends posteriorly in a semi-circular shape, and the base of which is strongly pleated. The outline of the proximal articulation facet of metatarsal 4 corresponds to that of *U. deningeri*, only the antero-medial articulation facet is more prominent and rectangularly shaped. The diaphysis is slightly more elongated and built more stoutly. In frontal view, the diaphysis widens strongly towards the proximal epiphysis. Its holds a medial crista and a medial articulation facet which slopes towards the medial side. The lateral epicondyle is more prominent than the medial epicondyle.

Although incomplete, preserved metatarsal 5 from TW also resembles those in other Middle Pleistocene specimens. The medial protuberance is moderately developed on the plantar side of the diaphysis. It widens continually to merge with the distal articulation. The diaphysis tapers off towards distal, and its narrowest point is within the proximal third of the diaphysis. The medio-plantar protuberance in the area of the distal diaphysis is somewhat more strongly developed.